UNIVERSITY OF SÃO PAULO

SCHOOL OF ENGINEERING

Lais Ferrer Amorim

# HYDRODYNAMICS AND WATER QUALITY ASSESSMENT OF LAKES BY THERMAL BEHAVIOUR AND MODELLING

São Paulo

2020

LAIS FERRER AMORIM

# Hydrodynamics and Water Quality Assessment of Lakes by Thermal Behaviour and Modelling

Revised Version

Thesis presented to the School of Engineering of the University of São Paulo to obtain the title of Doctor of Science.

Concentration area: Civil Engineering

Advisor: Prof. Dr. José Rodolfo Scarati Martins

São Paulo

2020

Este exemplar foi revisado e corrigido em relação à versão original, sob responsabilidade única do autor e com a anuência de seu orientador.

São Paulo, ______ de ____________________ de __________

Assinatura do autor: ________________________

Assinatura do orientador: ________________________

Catalogação-na-publicação

Amorim, Lais
HYDRODYNAMICS AND WATER QUALITY ASSESSMENT OF LAKES BY THERMAL BEHAVIOUR AND MODELLING / L. Amorim -- versão corr. -- São Paulo, 2020.
155 p.

Tese (Doutorado) - Escola Politécnica da Universidade de São Paulo. Departamento de Engenharia de Hidráulica e Ambiental.

1.Hidráulica 2.Modelagem Matemática 3.Lagos 4.Qualidade da Água I.Universidade de São Paulo. Escola Politécnica. Departamento de Engenharia de Hidráulica e Ambiental II.t.

# ACKNOWLEDGMENT

I begin by thanking God who presents me with many gifts, in addition to perseverance and strength in building the path, without ever failing. I continue to thank my family, who never tire of emphasizing the value of my achievements and supporting me for whatever the situation may be. Especially my mother Luzia, my father Antônio, my sister Luana, my husband Rafael, my in-laws Sandra and Fernando, my grandparents Rita, Antônio, Áurea, José Cláudio, Maria Helena and Rubens, who follow everything closely.

I am very grateful to my Advisor, José Rodolfo Scarati Martins, who is an example of a teacher, professional and person, always inspiring us to achieve our best. Thank you, Rodolfo, for sharing your knowledge, your time, your dedication and your life with us.

I extend this gratitude to my friends who walk beside me, exchanging experiences, giving support, sharing their time, their dreams and their achievements with me. Among these, I would like to highlight those who accompanied me directly at the Polytechnic School of USP, without whom this work would not have been possible, they are: Ligia, Pedro, Flávia, Fábio F., Fábio P., Maria Cristina, Ariel, Bárbara and Rodrigo.

I take this opportunity to thank all the infrastructure and faculty and staff at the Polytechnic School that provided this work and collaborated along the way. I highlight the collaborators of the Post-Graduation Secretariat, always helpful, the technician Fábio Campos from LabSan, in addition to the entire team of the Hydraulic Technology Centre.

For supporting the research, I would like to thank CAPES / CNPQ, Fundação Centro Tecnológico de Hidráulica – FCTH and colleagues at MOMA-SE.

# LIST OF FIGURES

# LIST OF TABLES

# ACRONYMS

- ANA – National Agency of Water
- EMAE – Metropolitan Water and Energy Company S.A.
- INMET – National Institute of Meteorology
- MOMA - Modelling Program for Strategic Metropolitan Waters as an Input for Water and Territory Management in the Face of Climate Change
- NMAE – Normalized Mean Absolut Error
- RMS – Root Mean Square Error
- MAE – Mean Absolut Error
- CETESB – São Paulo State Environmental Company
- CTH – Hydraulic Technology Centre

## Summary

# *CHAPTER I - Theoretical basis and Contextualization*

# 1. Contextualization

Lakes are lentic environmental with unique hydrodynamic, which depends on the morphology, in and outflows and atmospheric variables. This last driving force has its influence represented, mostly, by radiation and wind.

In this type of environment, is common to have calm surface areas in which the solar radiation enters and transfers the heat to the lakes, causing a heterogeneous distribution across the water column. The upper layers get warmer than the deeper ones, which changes the water density of it and enables vertical stratification.

All the interactions in the water column are harmed when the water column is divided into layers with different density. This condition means no gas or nutrients exchanges, impairing the food channel and oxygen availability across the lake.

When an external energy is transferred to the water surface, coming for example, from wind or advective movements, the vertical stratification can be broken. This transfer provokes the column inversion, mixing the lake and homogenizing the distribution of the constituents.

The development of the populations, industries and human activities that need water increases the necessity to ensure its availability during the year. The reservoirs' construction is encouraged in the effort to provide water guarantees and minimize the effects of drought seasons. Nowadays Brazil has 172,837 reservoirs, which occupy an area of 44,429.00 km² and represent 72.1% of the water body units in the country, according to Brazil’s Conjuncture of Water Resources (ANA, 2018).

Lakes and reservoirs have other uses, besides water supply, such as hydropower generation, irrigation, flood control or landscape component, in many cases, they have multiple uses. Because of its social purpose, the reservoirs are especially found near to the urban and metropolitan areas, which expose them to the anthropic pressures typical of those areas.

In this context, the interest in understanding lakes’ hydrodynamics and its effects on the water quality grew, aiming an appropriated management of the reservoirs and contributing areas. Tracing a timeline to the lakes' water quality in the 21’s century, the first papers highlighted are the ones published by Hodges, Imberger, Laval and Bonnet, Poulin, Devaux in 2000. Those two works explained items like the difficulty of modelling vertical stratification and getting accurate results with a scale smaller than monthly or weekly, the wind role on the hydrodynamics and the importance of a hydrodynamic model as input to the water quality simulations.

Keeping with the modelling timeline, in 2001 Ambrosetti and Barbianti described the physical process on the lake and advanced on the occurrence of the mixing event. 2003 brought the eddy turbulence observed on small scale (WÜEST e LORKE, 2003) and in 2008 it was correlated with Phyto spring bloom by Peeters, Straike, Lorke and Ollinger. Another important contributions on this period was the books from Chapra (2008) and Ji (2008), they present the basis of the theory of water quality modelling.

Since 2010's the research change to another level with the improve of the computation capacity, models are now capable of representing the global warming impacts on the lakes mixing regime (KIRILLIN, 2010). Across the years' indices were created, aiming to describe the power of lakes' stratification, and in 2011 they were compiled and automatically calculated by a numerical code proposed by Read et al.

The lakes' research field keep on improve with the equipment development, reducing the frequency measures and producing even more accurate results (MARTINS, VINÇON-LEITE, *et al.*, 2014) (KIRILLIN e SHATWELL, 2016) (SOULIGNAC, VIÇON-LEITE, *et al.*, 2017) (AMORIM, MARTINS, *et al.*, 2017). Also the attempts to model the effects between the lakes' physical characteristics and process on the water quality are improving with development of coupled systems (CUYPERS, VINCON-LEITE, *et al.*, 2011) (VINÇON-LEITE, LEMAIRE, *et al.*, 2014) (READ, PATIL, *et al.*, 2015) (LIU, BENOIT, *et al.*, 2015) (WANG, LIU, *et al.*, 2016).

An important part of the water quality modelling is to be able to represent the algal role in the ecosystem, this segment still need to model development and improvement. Some researchers have published relevant material, trying to show how to use biomass indicators to measure and model the algal organisms (SADEGHIAN, CHAPRA, *et al.*, 2018), also the role of algal blooms on the public health (BROOKS, LAZORCHAK, *et al.*, 2016).

Another field that needs better development is the interaction between sediments and lakes' hydrodynamics, especially the capacity to measure and modelling its resuspension and the effects on water quality. Important contribution on this research area is found in Luettich Jr., Harleman, Somlyódy (1990), Somlyódy and Koncsos (1991) Bailey and Hamilton (1997) Lou, Schwab, Beletsky and Hawley (2000), Cózar, Gálvez, Hull, García, Loiselle (2005), Jin and Sun (2007) Wu, et al (2013), Jalil, et al. (2017), Matisoff, Watson, Guo, Duewiger, Steely (2017).

Based on the context here discussed some questions were identified. The first one focuses on the reservoir management theme, intending to improve the operator's capacity to forecast situations that can compromise its uses. To do that it needs to investigate the possibility of a functional relationship between the atmospheric forces and the lake thermal status changing. On the mathematical modelling field, emphasis on the three-dimensional modelling, it is possible to use a quasi-3D model to represent the thermal changings and its consequences in the hydrodynamics and the water quality, including vertical transport capacity?

This research aims to answer those questions, and to do that, different lakes were studied. The first step was to count on a time high-resolution monitoring system to collect field data, along with secondary sources, as public agencies. The functional relationship was developed basing on the lakes' hydrodynamic energy balance and the proposition of proxies that can represent it, identifying the atmospherical forces state on the moment of the change of thermal state.

The quasi-3D model was constructed for two lakes (small and medium-size) and tested according to the field measurements in terms of hydrodynamics, water quality and capacity to represent the sediments resuspension. Finally, those two methods were evaluated as forecast tools to represent the climate change effects on lakes' mixing regime.

This research has important contributions to the limnologic, monitoring, water quality management, and modeling areas. Such as a precise, easy and rapidly way to identify and forecast the lakes' thermal state, applications of monitoring techniques and its reflection in the hydrodynamic and water quality models, the relationship of the water column inversion and the bed material resuspension, also the demonstrations by different tools of how the climate change can modify the lakes thermal behavior.

## 1.1. Thesis organization

This thesis is divided into five chapters, which explain the hydrodynamic and environmental modelling theoretical base, the hypotheses investigated in this work, the scientific contributions produced building the thesis and the suggestion to next researches.

The context in which this research was built is described in the first chapter, along with the knowledge gaps and investigated questions. It presents the fundamental base, about lake hydrodynamic, water quality and mathematical modelling.

The investigated hypotheses are described in chapters II and III. In the second one, the methods were applied in four different lakes to build a curve that describes the lake thermal stability, according to the atmospherical driving forces. Then, chapter III presents the quasi-3D model results in hydrodynamics, water quality, and bed material resuspension of two lakes.

Chapter IV evaluates those two management tools in terms of reliability, quickness, types of results and complexity. Climate change simulations were performed in two lakes, aiming to demonstrate the use of those two tools.

The final chapter brings the general discussions, the thesis main scientific contributions, and the directions to the next researches, along with the bibliography used in the work. The whole scheme of the thesis is demonstrated in Figure 1.

**Figure 1. Thesis organization**

***CHAPTER I - Theoretical basis and Contextualization***

- Hydrodynamics Contextualization;
- Lakes and reservoirs ecosystems;
- Environmental Mathematical Modeling.

***CHAPTER II - Hypothesis #1 – Lakes' Thermal Stability Correlation with Atmospheric Driving Forces***

- Methods and Materials;
- Study Cases (Hedberg Lake, Crètèil Lake, Bourget Lake and Billings Reservoir);
- Results and Discussions;
- Conclusions.

***CHAPTER III - Hypothesis #2 – Quasi-3D modeling as a Reservoir's Management Tool***

- Methods and Materials;
- Study Cases (Hedberg Lake and Billings Reservoir);
- Results and Discussions;
- Conclusions.

***CHAPTER IV - Evaluation of Management Tools to Forecast Lakes' Thermal Condition***

- Methods and Materials;
  - Climate changes simulations;
- Study Cases (Hedberg Lake and Billings Reservoir);
- Results and Discussions;
- Conclusions.

***CHAPTER V - Comments and Referrals for Upcoming Papers***

- Scientific contributions;
- Bibliography.

Source: Author.

## 2. Lakes and reservoirs ecosystems behaviours and relationships

Lakes and reservoirs are similar environments. When one is built in a river, has its characteristics changed from a lotic to a lentic environment, behaving like a lake in the regions near to the dam. Lentic systems are characterized by low flow velocities, greater depths and high detention time. Its hydrodynamics is influenced by wind, water density, and vertical stratification (CHAPRA, 2008) (FRANZEN, CYBIS e MERTEN, 2011).

The circulation of the water in the reservoir is the result of the forces of morphometric, meteorological and hydrological conditions. The tension caused by the wind on the water surface moves the water mass in its direction and create a mix water column. This force competes with the solar radiation which tries to stabilize the temperature in the water column and maintain the stratification. Those interactions result in a series of movements in the water mass (IMBERGER, 1998) (BONNET, POULIN e DEVAUX, 2000).

The water body hydro and thermal dynamic is governed mostly by inflows and outflows, morphological and hydrodynamics characteristics, heat balance and transparency of the water (KIRILLIN, 2010). The heat balance involves the surface energy exchanges, also the exchanges in the interface water-soil and light penetration in the water (Figure 2). The most important fluxes occur on the water surface, in this interface the main driving forces are solar radiation and wind, the principal losses are from evaporation, sensible heat and long wave radiation losses and the reflections (HENDERSON-SELLERS, 1986).

In the water column the heat flux is governed by the light penetration, which varies according to the water turbidity, a high concentration of suspend material in the water elevates the turbidity indices and limits the radiation penetration (HENDERSON-SELLERS, 1986). The turbidity is a measure of water clarity or transparency and its effect can be quantified as an extinction coefficient ($\eta$), which is inversely proportional to the Secchi depth ($Z_s$), that is measured in the field with the Secchi disk. Empirical relationship between the Secchi depth and light extinction can be given by equation 1, in which C is a constant with typical values between 1.7 and 1.9 (JI, 2008).

$$K_e = {}^{C}/_{Z_s} \qquad \text{(Eq.1)}$$

**Figure 2. Elements in a lake heat balance**

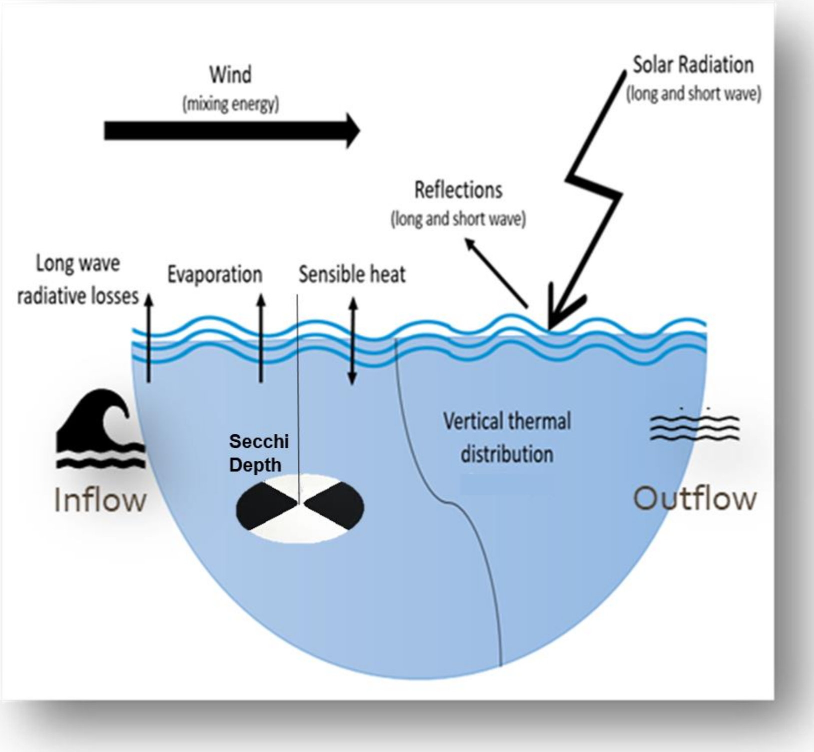


Source: Author.

The net energy available in the water ($\emptyset_N$) is given by Eq.2, which show the energy sources as being the incident short ($\emptyset_S$) and long ($\emptyset_{ri}$) wave radiation and the losses are the reflections (short, $A_s$, and long-wave, $A_L$, Albedo), the long-wave radiative ($\emptyset_{ro}$) and non-radiative ($\emptyset_L$) loss. The last term comprises tree energy exchanges: evaporation loss, precipitation gain and sensible heat transfer, however the precipitation portion is much smaller than the others, consequently the non-radiative losses can be determined only by the sum of the latent heat and the sensible heat (HENDERSON-SELLERS, 1986).

$$\emptyset_N = \emptyset_S(1 - A_s) + \emptyset_{ri}(1 - A_L) - \emptyset_{ro} - \emptyset_L \qquad \text{(Eq.2)}$$

This correlation gives the energy boundary conditions, while in the lake the heat flux is based on Fourier Law and the Thermodynamics first Law, which says that the energy variation in a body can be expressed by the balance between the heat flux and the external workforce. The energy variation in an element can be described by equation 3, and equation 4 represents a three-dimensional form. In which, *DE* in the energy variation in time (*t*), $\tau$ is the workforce, *Q* is the flux, $\hat{u}$ is the element's internal energy, $T$ is the temperature, $k$ is the thermal conductivity, $p$ in the pressure and $V$ is the velocity.

$$\frac{DE}{Dt} = \tau - Q \qquad \text{(Eq. 3)}$$

$$\rho \frac{D\hat{u}}{Dt} = k\nabla^2 T - p\nabla V \qquad \text{(Eq. 4)}$$

## 2.1. External variables

The main energy source in the lake is the solar radiation, it controls the water temperature and the photosynthesis because unlike the others heat flux components, which all occur at the water surface, the solar radiation can penetrate and distribute the heat through the water column (AMBROSETTI e BARBANTI, 2001). This heat provokes significantly effects in the water column stabilizing it by warming upper layers and creating layers with different densities, what will lead to a peculiar hydrodynamic behaviour (BONNET, POULIN e DEVAUX, 2000) (ELC¸I, 2008). The aquactic life is also deppending on this heat source, because it makes the photosinthesys possible, interfering in the whole food chain and being one of the main oxygen sources in the lakes and reservoirs (MARTINS, 2017).

The radiation waves suffer some losses in their way from the atmosphere until the water surface. First by scattering and adsorption, and next, when it reaches the water surface, the losses are by directions changings, absorption, transformations, and dispersions. Because of that, the quantity of solar radiation recevied by a place dependend on its' climate zone. Tropic zones recevies a bigger amount of radiation than the temperate and polar portions of the globe. Another factor that can reduce the amount of incident radiation is the shading from trees and steep riverbanks, resulting in water temperatures much lower than those in unobstructed areas (AMBROSETTI e BARBANTI, 2001) (JI, 2008) (MARTINS, 2017).

Another external factor that is determinant in the lake thermal dynamic is the wind, which varies with time scales, including diurnal variations, time scale of weather systems and the seasonal changes. The stress provoked by the wind on the water surface is one of the factors that can break the stability created by the heat transmitted by solar radiation. Wind stress is the tangential force per unit area due to the wind horizontal movement over the wind surface, what determines it it's the wind speed and direction and factors transforming the wind speed into wind stress. This transformation is estimated by the Eq.5.

$$\tau = \frac{1}{2} C_D \rho_A U^2 \quad \text{(Eq.5)}$$

In this equation, $U$ is the wind speed measured at 10m above the water surface (m $s^{-1}$), $\rho_A$ is the air density (kg $m^{-3}$), $C_D$is the drag coefficient and $\tau$ is the wind stress (N $m^{-2}$) (JI, 2008). The wind drag coefficient may be linearly dependent on the wind speed, reflecting increasing roughness of the water surface with increasing wind speed. The drag coefficient presents three different baselines, represented by the breakpoints in Figure 3, which are a piece-wise linear function of wind drag coefficient and wind speed. Breakpoint A determine the constant wind drag coefficient from zero to the specified wind speed, and the breakpoint C, specify the constant wind drag coefficient from the specified wind speed and higher. Between the breakpoints a linear interpolation applies. A constant wind drag coefficient can be used to model's application, or it can linearly increase being a piece-wise linear function of wind speed (CHIN, 2006).

**Figure 3. Wind drag coefficient variations according to the Wind speed**

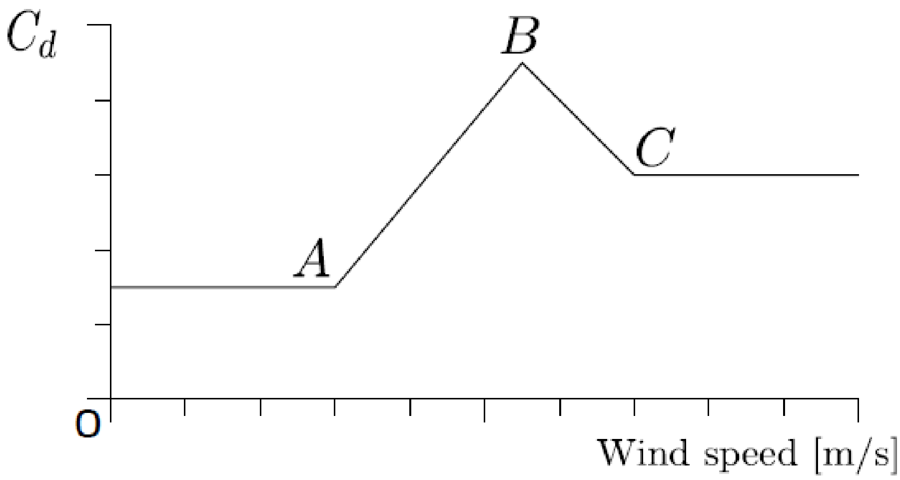


Source: DELTARES (2014).

The wind initiates a tilting motion on the water surface leading to the surges creation, which accelerates the water under the action of the applied force until a reverse pressure force due to the sloping water surface is built up, and turn the layers over (IMBERGER, 1998).

This balance between the energy provided by the solar radiation and the meteorological conditions, especially the wind force, creates a characteristic thermal behaviour for the lakes and reservoirs, which is called the mixing regime. Lakes and reservoirs located in different latitudes can have distinct mixing regime, what leads to a lake regime classification. When the water body mix completely at least one time during the spring and heat season, it is classed as polymictic, a dimitic lake stratifies two times in a year and a monomict only once, even in winter or summer (HENDERSON-SELLERS, 1986) (KIRILLIN e SHATWELL, 2016).

## 2.2. Lakes and reservoirs hydrodynamic

The heat balance and the forces that influence it cause effects in the one of the most important property, the temperature. This physical characteristic is crucial in lake's hydrodynamic and water quality due to a number of reasons like: the vertical profile affects the water column stratification and the vertical mixing; dissolved oxygen solubility is determined by water temperature; many biochemical and physiological processes are governed by temperature, higher temperatures can increase metabolic and reproductive rates throughout the food chain; re-aeration and volatilization are affected by temperature; many aquatic species can tolerate only a limited range of temperatures. Beyond the environmental relations it has particular economic importance, for industrial cooling and the formation of ice in navigable waterways (AMBROSETTI e BARBANTI, 2001) (BONNET, POULIN e DEVAUX, 2000) (JI, 2008).

The influence of the water temperature can be seen in the water density. The point of maximum density is reached around 4°C getting less density with a temperature decrease or increase, but it can also be affected by salinity and turbidity. In the natural environment the solar radiation heats up the water surface making it lighter than the deeper ones creating density differences in the reservoir water column, hence stratified layers with different temperature and density. This density differences between bottom and surface inhibits vertical mixing, unless the wind force is big enough to break the thermal stability created (JI, 2008) (MARTINS, 2017).

Commonly is defined three layers in the stratified hydric boyes: the epilimnion is the superior layer where the temperature is usually stable and vertically uniform, followed by the metalimnion, where occurs the maximum temperature gradient, and the hypolimnion that extends itself until the bottom of the lake. But the circulation creates oscillations in the layers and mix the mass vertically (IMBERGER, 1998) (JI, 2008) (MARTINS, 2017).

**Figure 4. Stratified lake layers**

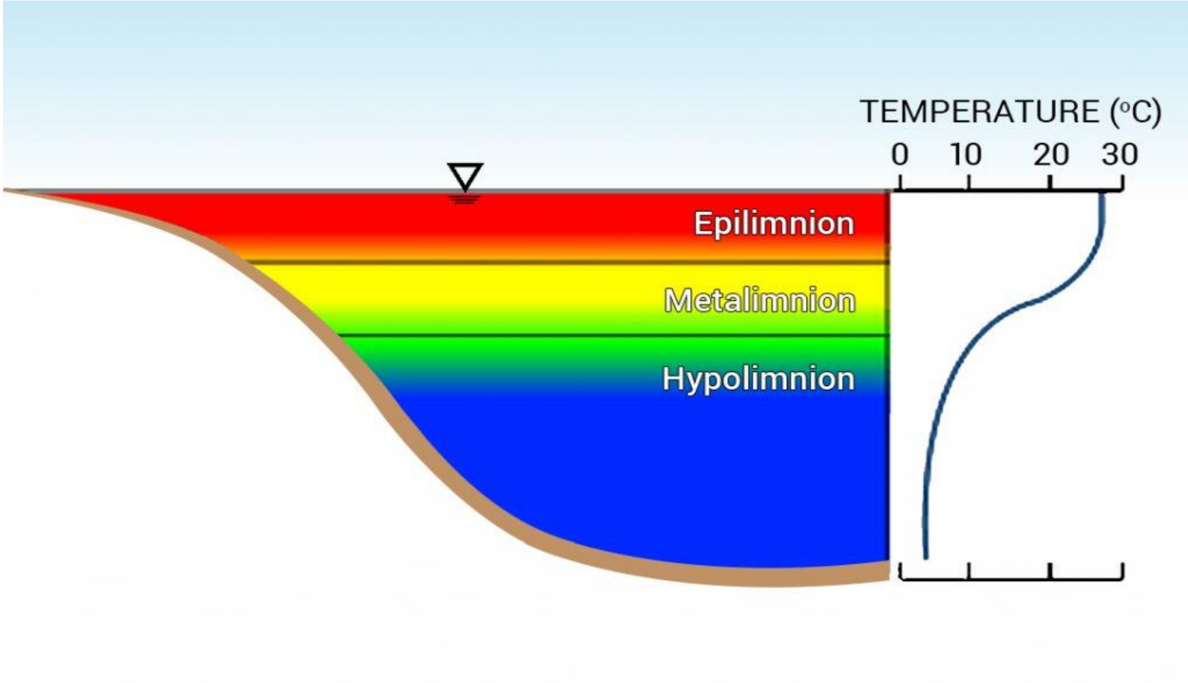


Source: EE Modelling System (2017).

When the energy provided by the wind creates strong vertical oscillations in the isothermal, it breaks the stratification and mixes the water column, re-suspending bed material. Internal movements (seiches) induced by the wind create an oscillation on the vertical velocity component, making it capable of suspend bed materials (AMBROSETTI e BARBANTI, 2001). This phenomenon can have significantly effects on the water quality as will be discussed in the next topic.

The idea of establishing a link between the external conditions and lakes mixing regime has been pursued since the 80's, i.e. Spigel and Imberger (1980); Fee et al., (1996), and Amorim et al., (2017). Lake indices such as Schmidt Stability (Eq.6), Lake number (Eq.7), Wedderburn number (Eq.8) and others have been frequently used to evaluate and predict water body's stratification behaviour taking into account meteorological conditions (READ, HAMILTON, *et al.*, 2011).

$$S_T = \frac{g}{A_s}\int_0^{z_D}(z - z_v)\rho_z A_z \partial_z \qquad \text{(Eq.6)}$$

$$L_N = \frac{S_T(z_e+z_h)}{2\rho_h u_*^2 {A_s}^{1/2} Z_v} \qquad \text{(Eq.7)}$$

$$W = \frac{g' z_e^2}{u_*^2 L_s} \qquad \text{(Eq.8)}$$

In the above equations, g'= g . $\Delta\rho/\rho_h$, $\rho_h$ is the hypolimnion density and g is the gravity acceleration, $z_e$ is the depth of the mix layer, $L_s$ is the lake fetch length, $u_*$ is the water friction velocity due the wind stress, $A_s$ is the lake area at surface, $A_z$ is the area at depth z, $z_D$ is the maximum depth of the lake, $z_v$ is the centre volume depth, computed as the volume weighted depth, $z_e$ and $z_h$ are the depths to the top and bottom of the metalimnion (MACINTYRE e MELACK, 2009) (READ, HAMILTON, *et al.*, 2011).

The first index, Schmidt Stability ($S_T$), reflects the resistance to mechanical mixing due to the potential energy inherent in the stratification of the water column, applying a weighting to reduce the effects of lake volume on the calculation, the formulation result in a mixing energy requirement per unit area (IDSO, 1973) (READ, HAMILTON, *et al.*, 2011).

The Wedderburn Number (W) and the Lake Number ($L_N$) add the wind force to the analysis. Lake Number describes lakes internal mixing induced by wind forcing, while Wedderburn Number presents the likelihood of upwelling events under stratified conditions. Lower values of both indices represent a higher potential for increased diaconal mixing, which increases the vertical flux of mass and energy across the metalimnion through the action of non-linear internal waves, otherwise greater values show a more stable and stratified lake (READ, HAMILTON, *et al.*, 2011) (IMBERGER, 1998).

As the water temperature is influenced by atmospheric forces (wind, air temperature, precipitation, solar radiation) the stratification phenomena behave differently in temperate and tropics zones. Lakes and reservoirs located in cooler areas, with the difference between the weather seasons being greater, usually have a weekly stratification time scale or yet stay stratified for all the warm seasons, mixing only in the winter. However, those climate characteristics are not founded in the tropic zone, where the average temperature is higher and is not necessarily much difference between bottom and surface to water body begins to stratifies (HODGES, IMBERGER, *et al.*, 2000) (MARTINS, VINÇON-LEITE, *et al.*, 2014) (MACKAY, NEALE, *et al.*, 2009).

As mentioned earlier, the greater effect of the stratification is the mass transport limitation across the water column, this includes the nutrients dispersion and the oxygen vertical profile. Due to the interface with the atmosphere and possibility to exchanges, hence the upper layers of a stratified lake have higher dissolved oxygen concentration than the deeper ones, in extreme cases, the bottom layer can have anoxia problems (MARTINS, 2017). The dissolved oxygen is the major parameters in the water quality evaluation so that propriety has a determinant influence in this matter.

**Figure 5. Typical dissolved oxygen and temperature vertical profiles on the Billings reservoir**

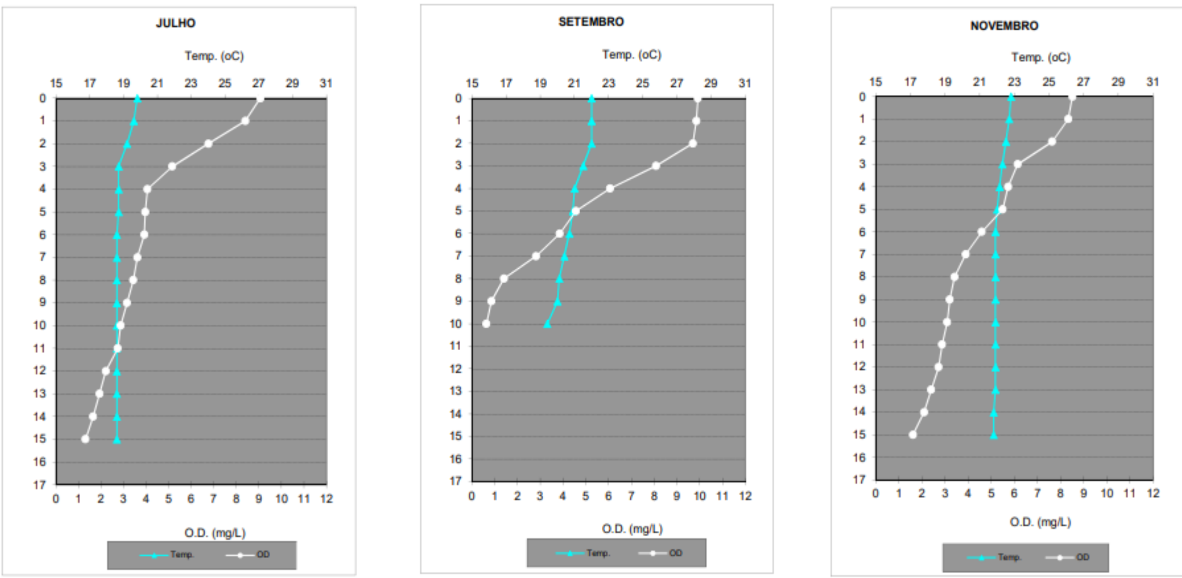


Source: CETESB (2017).

When the energy provided by the wind breaks the stratification and mix the water column a re-suspension from the material at the bottom may occur (KULLEMBERG, 1976) (BAILEY e HAMILTON, 1997) (MACINTYRE e MELACK, 2009).

This phenomenon can perform significantly effects on the water quality, breaking the transport limitation and making available again the substances absorbed into the sediment. In a healthy environmental this would not be a problem, but in polluted urban waters, the unbalanced entrance and exit of nutrients lead to the formation of eutrophics systems (ELÇI, 2008) (CHUNG, BOMBARDELLI e SCHLADOW, 2009) (JALIL, LI, *et al.*, 2017).

## 2.3. Water Quality relationships

Water quality represents the physical, chemical, and biological characteristics, it’s a response of the hydrodynamic processes, which control the transport of algae, nutrients and dissolved oxygen in a water body. Beside the internal process, there are other factors that affect the water quality condition such as meteorological forces, internal processes, inflows and outflow (JI, 2008) (SPERLING, 2007) (PEETERS, STRAILE, *et al.*, 2007).

Shallow inland waters have a faster response to external forces variability than deeper ones. Lake water quality conditions are influenced by the onset, duration, strength and turnover of the water column, which is influenced by the atmospheric conditions, that can make them to be climate changes indicator (ELC¸I, 2008) (MACKAY, NEALE, *et al.*, 2009) (READ, WINSLOW, *et al.*, 2014).

Another important factor in the water condition is the incoming load of pollutants, which has its consequences intensified because of the high detention time that occur is this type of water body. The water's degradation main causes are the entry of wastewater, input of nutrients from the agriculture areas, sediments and organic matter of the catchment, toxic products, organoleptic and pathogenic organisms (PEETERS, STRAILE, *et al.*, 2007).

Several process are affected by the pollution like the nutrients enrichment in the water, the grow and development of the algae and phytoplankton, the concentration and the increase of chemical elements accumulation and the trophic state of the water body, what make harder to keep a good condition of water quality (BROOKS, LAZORCHAK, *et al.*, 2016) (WENGRAT e BICUDO, 2011).

Eutrophication is a process of nutrient over enrichment of a water body, resulting in accelerated biological productivity (growth of algae and weeds). Symptoms of eutrophication include algal blooms, reduced water clarity, and oxygen depletion. In modelling studies, water quality and eutrophication are sometimes used interchangeably to represent the processes of water body enrichment with nutrients (BROOKS, LAZORCHAK, *et al.*, 2016) (CHAPRA, 2008) (PEETERS, STRAILE, *et al.*, 2007). The reservoir trophic state reflects its nutrients quantity, hence the algal growth and the primary production, according to those characteristics can be classified into:

a) Oligotrophic: water body with low biological activity and excellent water quality, since the water is low in nutrients and algae and both primary production and biomass are severely limited.
b) Mesotrophic: water body with medium biological activity and good water quality.
c) Eutrophic: water body with excessive biological activity and poor water quality. The water has abundant nutrients and high rates of primary production, frequently resulting in oxygen depletion in the bottom layer.

A consequence of the pollution is the accelerated eutrophication. The wastewater and diffuse loads input in the lakes and reservoirs increases the nutrients availability, with more food the algal development is faster creating a bloom. In those situations, a superficial film is formed blocking the light entrance in the water column and impairing all the exchanges between the surface layer and the atmosphere, which will lead to serious harmful consequences for the ecosystem. Some eutrophication consequences are the low rate of dissolved oxygen in the deeper layers, dead of aquatic life, added odour, taste and toxicity to the water; impossibility to the public distribution, recreation and fishing (Figure 6) (SPERLING, 2007).

**Figure 6. Algal bloom records in Billings reservoir (SP - Brazil). Photo "C" show the intake blocked by the algae bloom in 2008**

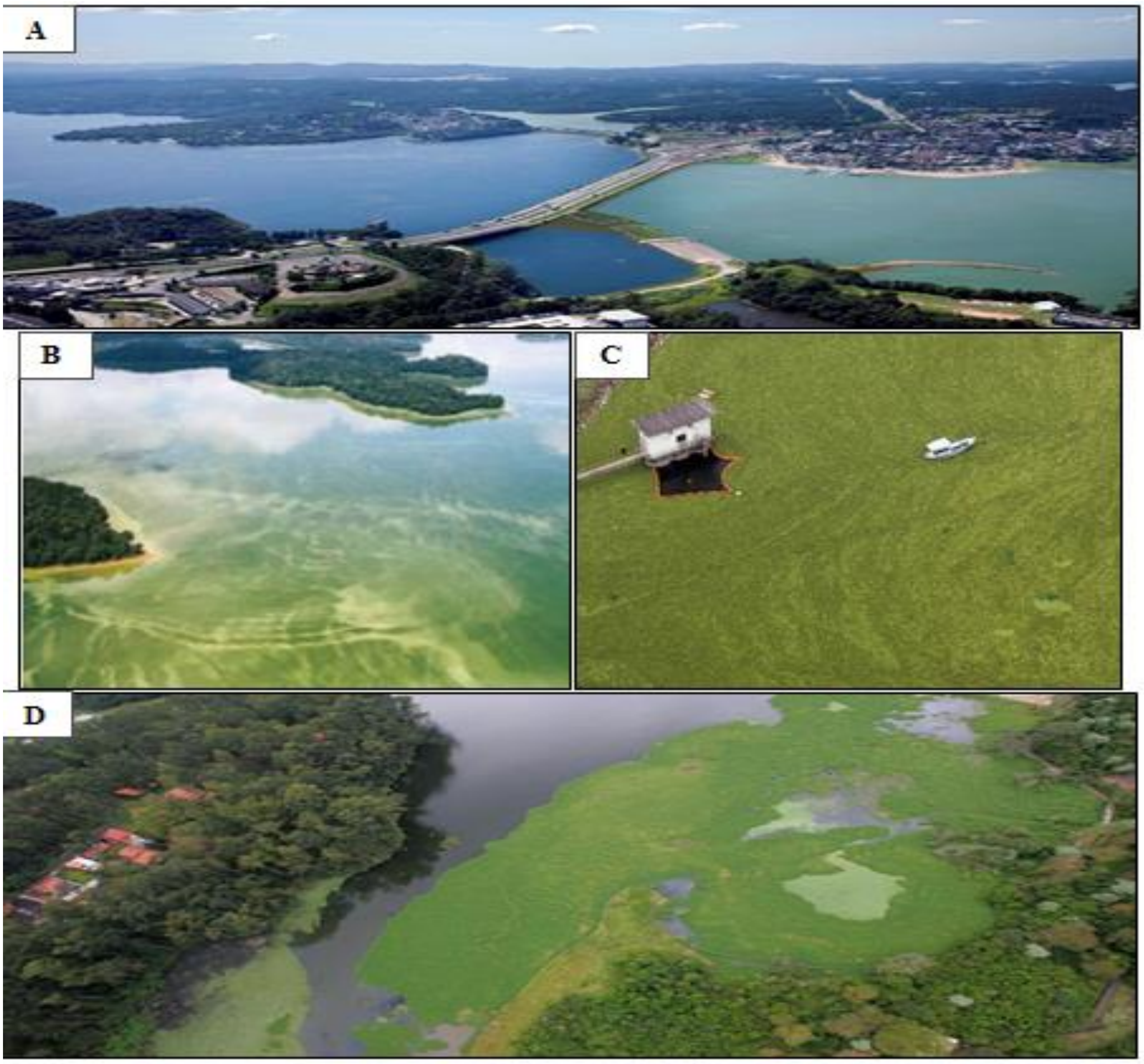


Source: **(ESTADÃO, 2016)**

The algal blooms can also be influenced by the mixing regime on lakes, the nutrients can attach to sediments in water systems and each time the turnover occur, depending on the vertical velocity created, they can be re-suspended in the water column and be once again available to the organisms (SOMLYÓDY e KONCSOS, 1991). Studies of the Billings reservoir (MARTINS, VINÇON-LEITE, et al., 2014), show that this reservoir has a daily mixing regime (Figure 7) and along with the watershed loads contribution, can create a propitious environmental to algae development.

**Figure 7. Temperature records in the surface and bottom water of the Billings reservoir**

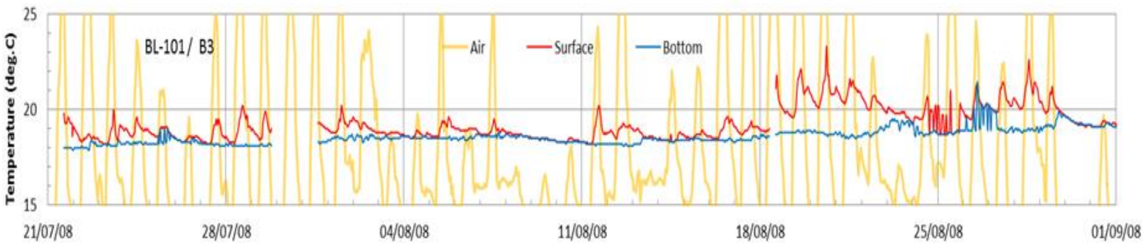


Source: Martins (2017).

Some parameters are used by the legislation and the researches to evaluate the water quality condition, in lakes and reservoirs the most used are the Dissolved Oxygen - DO, Biochemical Oxygen Demand – BOD, Nitrogen in many forms, such as Ammonia – NH4 and Nitrate – NO3, Phosphorus, total and orthophosphate – PO4 and Chlorophyll-a (SPERLING, 2007) (CONAMA, 2005).

The dissolved oxygen, as mentioned before, is the most important variable in the water quality, basically because it suffers influence of all the others, and it reflects if aerobic life in the environmental is possible. The oxygen main sources are the atmosphere exchanges and photosynthesis, however it can also be artificial added to the water. The oxygen is present in most of the phenomenon occurred in lake ecosystem, the bacteria that consume the organic matter use oxygen to breath, both Nitrogen and Phosphorus needs oxygen to transform in other forms that can be utilized by the organisms, consequentially its vital to aquatic life (SPERLING, 2007) (PIVELI e KATO, 2006).

The organic matter present in the surface water is mostly from the wastewater, especially in countries like Brazil where the majority of the cities don't have appropriate wastewater treatment, but there's also a significant contribution from the nonpoint source pollution. This matter will serve as food to the organisms in the water and will be metabolized in sub products, such as carbon dioxide, sulphates, phosphates, ammonia and nitrates. The parameter that measures the oxygen consumption to mineralize the organic matter is the Biochemical Oxygen

Demand – BOD, which is utilized by Brazilian laws as an indicator of the organic matter in the water. A more precise parameter related to the organic matter is the total organic carbon, both are fundamental to control the water pollution (PIVELI e KATO, 2006).

Nitrogen can be founded in four different forms, the organic Nitrogen (Norg), Ammonia ($NH_4$), Nitrate ($NO_3$), Nitrite ($NO_2$) and Nitrogen Gas ($N_2$), as showed in the Figure 8. In the nitrification, the transformation from $NH_4$ to $NO_2$ and then to $NO_3$, rates of oxygen are consumed decreasing the amount of dissolved oxygen available in the water, automatically higher loads of Nitrogen in any form can cause water pollution. Other problems associated with high Nitrogen concentration in the water are the eutrophication, as this is an essential nutrient for plant growth, and the toxicity, since depending on the water pH the Ammonia gas ($NH_3$) appears and it is toxic to fish (CHAPRA, 2008).

**Figure 8. Nitrogen cycling process in an aquatic system**

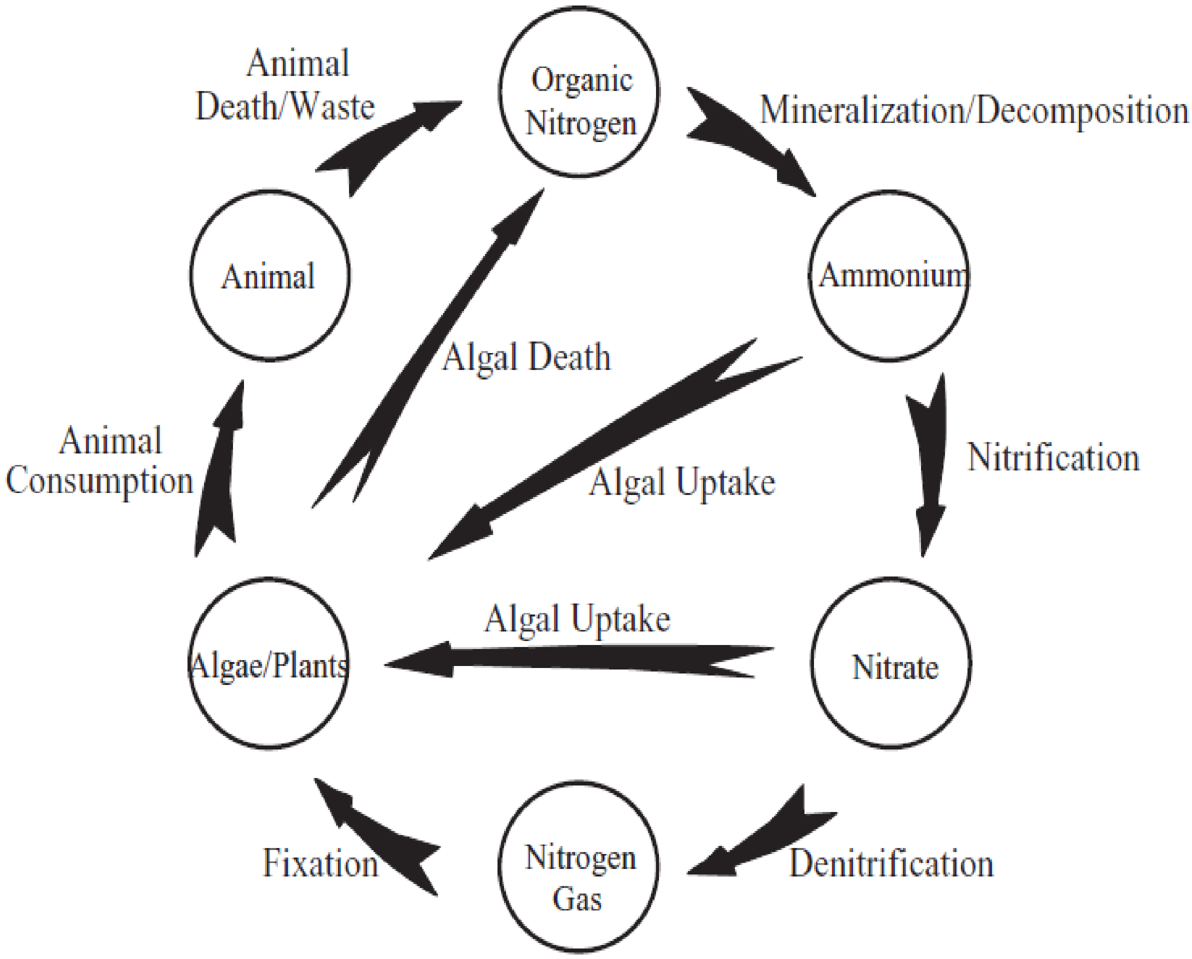


Source: Ji (2008).

Another essential nutrient for algae growth is the phosphorus. In the water it can be founded in organic and inorganic form, but only a portion named orthophosphate is readily available to consumption (Figure 9). Usually this nutrient is in short supply relative to the other macronutrient, however in water bodies which receive waste water or input from agricultural lands can have high phosphorus concentrated loadings prompting to an unbalanced environmental (CHAPRA, 2008).

**Figure 9. Phosphorus cycling process in an aquatic system**

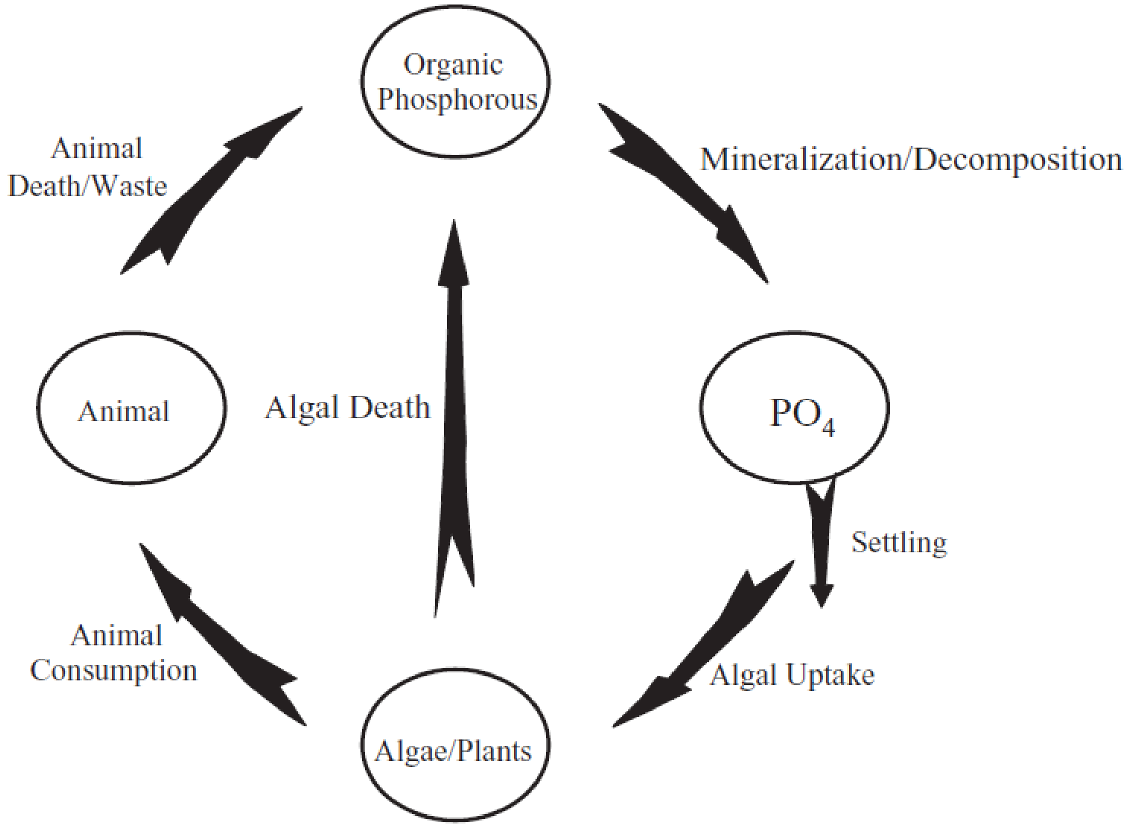


Source: Ji (2008).

When the environmental unbalance happens, the eutrophication appears as consequence, to monitor the algae growth the Chlorophyll-a parameter is used. Chlorophyll-a is considered to be directly proportional to the concentration of algal biomass, is easier to measure and provides a reasonable estimation. The Eq.9 can be used to convert Chlorophyll-a in algal biomass, B represents algal biomass concentration as carbon (C) (mg C/L), Chl is Chlorophyll-a concentration (mg Chl/L), and α is carbon to chlorophyll ratio (mg C/mg Chl), α value varies widely depending on the makeup of the algae population, typically ranging from 15 to 100.

This parameter is also applied to represent lake trophic status and to set up water quality criteria (JI, 2008).

$$B = \alpha Chl \qquad \text{(Eq.9)}$$

Summarizing the previously discussed, the aquatic environmental is a complex combination of food availability, organism development, atmospheric exchanges and external forces, all they connected and with a role to play. Balanced, all the process occur normally, and the ecosystem has a healthy development, as well as the water quality condition, however the loadings introduced by the anthropic activities can distort this condition producing harmful consequences to the environmental, even incapacitating the water use.

The Figure 10 demonstrates the main process in an aquatic ecosystem related to the water quality. The Dissolved Oxygen main sources are the exchanges between the air-water interface and the algae production, while almost all other processes, as the Phosphorus, Nitrogen, and Organic matter transformations, are consumers. The sediment can be a source of the nutrients, but a sink of Oxygen (SOD), just like the atmospheric deposition.

**Figure 10. Lake environment functions and dependences**

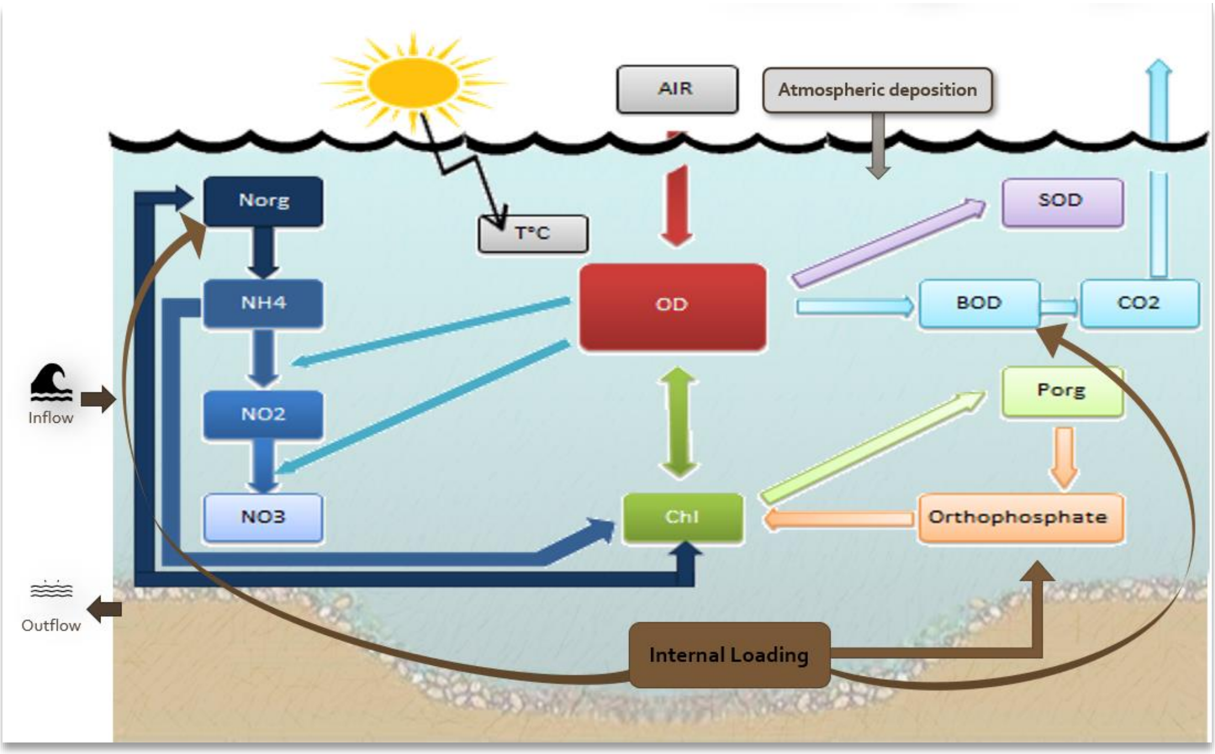


Source: Author.

## 2.4. Environmental measurements in lakes and reservoirs

To be able to study and comprehend environmental phenomenon monitoring data is required. The information provided by the monitoring data base is helpful to define trends, evaluate behaviours, calibrate mathematical models, perform law inspection/surveillance and others.

The scheme of Figure 11 summarizes most of the monitored parameters on the lakes' environment, it includes the geometric parameters (morphometry, depth, length), hydraulics (flow, water level), physical (light penetration, temperature, turbidity), chemical (chemical elements concentration) and biological (algae production). External variables comprise all the climate parameters which interact with the lake, the commonly monitored are radiation, wind, and direction of the speed, air temperature, humidity, and precipitation).

In this research when the study areas are described, the monitoring system applied is defined with them.

**Figure 11. Monitored parameters on the lakes' environment**

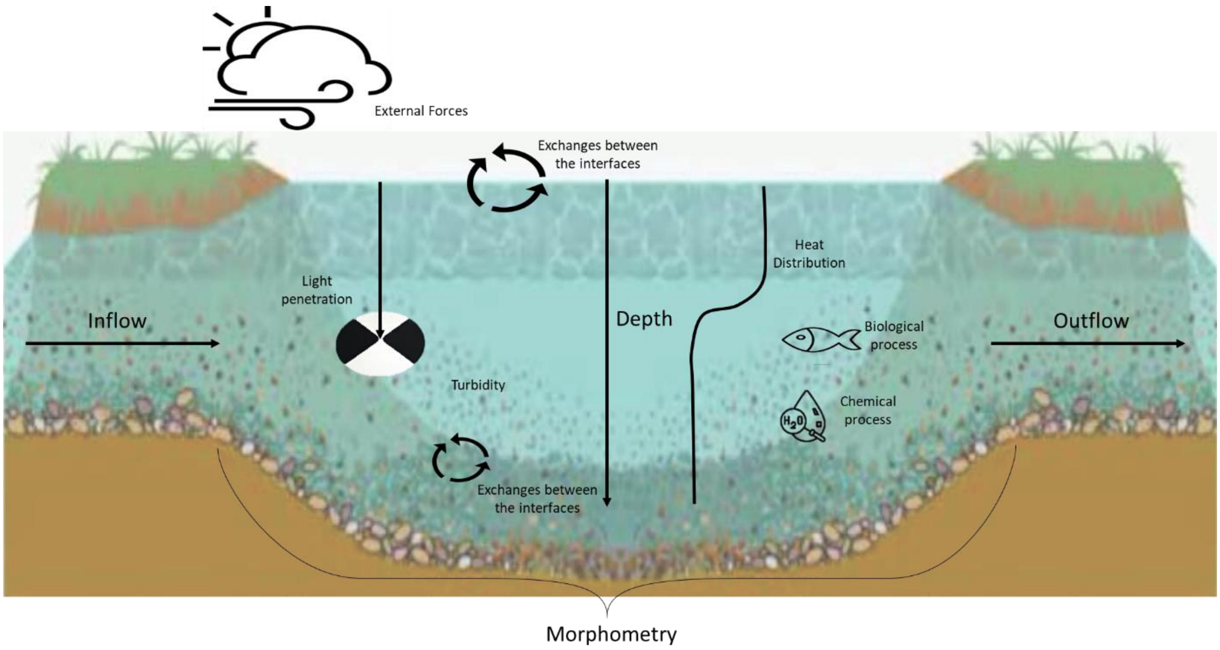


Source: Author.

# 3. Environmental Mathematical Modelling

Hydrodynamic and water quality researches of reservoirs can be made with mathematical models. The modelling of those systems may be realized by a zero-dimensional model, considering total mixing of the water body, one-dimensional, two-dimensional and three-dimensional models, depending on the proposal of the research (MARTINS, VINÇON-LEITE, *et al.*, 2014).

But only the three-dimensional models are able to simulate particles path in the three directions. For that they are an important tool in the water quality evaluation, scenarios creation, and understanding of different answers of the environmental for the external forces (IMBERGER, 1998).

Hydrodynamic process is governed by three conservation laws, the mass conservation, energy conservation and momentum conservation. In models' equation they are frequently manipulated and simplified, but always with the same principle (Eq. 10). The first law states that mass can neither be produced nor destroyed and this balance is represented by the continuity equation, which accounts the mass flux flowing through a defined area to enter or leaving the control volume (JI, 2008).

$$\text{Mass accumulation} = \text{Mass in} - \text{Mass out} + \text{Sources} - \text{Sinks} \qquad \text{(Eq. 10)}$$

To be able to represent those phenomena in a mathematical model, some hypotheses and simplifications are assumed. The next topics will comment more on the methods to simulate water bodies' hydrodynamics and water quality.

## 3.1. Advection and diffusion

The water boy's environmental characteristics are modified when a discharged enters, it could happen in terms of water level, temperature, and chemical elements concentrations. For the last one, the determining factors in the resultant concentration are the hydrodynamic transport and chemical/biological reactions. The system motion can be divided into two categories (CHAPRA, 2008) (JI, 2008):

- Advection: is the transport by mean velocities (i.e. without turbulence), it's the matter motion from one to another position in space.

- Dispersion/Diffusion: is the mass movement due to random motion, this transport reduces the material concentration. On a microscopic scale it can be divided in molecular and turbulent diffusion, molecular results from the random Brownian motion of water molecules and the turbulent is produces by the eddies.

The transport consists in two components the advective and dispersive flux, both are defined as the mass crossing a unit area per unit time. The mass of pollutant transport due to advective flux ($J_a$) is in the same direction as the flow and depends on the concentration (C) and the water velocity ( $\vec{v}$). The dispersive fluxes caused by molecular diffusion moves from high to low concentrated areas and is explained by the Fick's law, which states that the rate of mass movement is inversely proportional to the mass concentration gradient. But the major originator of dispersive motion in terms of transport is the turbulent mixing (JI, 2008) (CHAPRA, 2008).

$$J_a = C \quad \vec{v} \tag{Eq.11}$$

$$-\frac{\partial C}{\partial t} = \frac{\partial}{\partial x}\left(D\frac{\partial C}{\partial x}\right) + \frac{\partial}{\partial y}\left(D\frac{\partial C}{\partial y}\right) + \frac{\partial}{\partial z}\left(D\frac{\partial C}{\partial z}\right) \tag{Eq.12}$$

In above equations $J_a$ represents the advective flux, D is a diffusion coefficient, x, y, z are the directions of the flux (JI, 2008) (CHAPRA, 2008) (MARTINS, 2017).

## 3.2. Models types

Natural systems are always three dimensional, but some phenomena can be more significant in one direction than the others, this allows modelers to simplify it to other spatial resolutions depending on how the variations occur. The hydrodynamic and water quality have spatial variations over length, width, and depth, but in some cases simplification in the governing equations are allowed. The reduction in dimensionality should result in reductions on time simulation and computational processing. A numerical model developed for a water body should only include the dimension(s) where the variations affects its water quality, the models can be (CASULLI e STELLING, 1998) (MARTINS, 2017) (CHAPRA, 2008):

- Zero-dimensional (0D): assume a well-mix water body with no spatial variation. This type of model calculates water quality variables based on mass conservation, they might be used as a preliminary analysis in lake studies.

- One-dimensional (1D): simulate the spatial change over a single dimension, usually used in rivers simulations. Can also be used in lakes, when the major variation is across the water column.
- Two-dimension (2D): consider lateral and longitudinal variations (2DH) or in another arrangement lateral and vertical change (2DV).
- Three-dimensional (3D): describes the changes in all three spatial dimensions and provide the most detailed pollutant distribution assessment.

To choose which model type use in the numerical simulation the mains points are the transport behaviour and the study objectives.

## 3.3. Hydrodynamic modelling

The principal features in hydrodynamic modelling change three-dimensionally, are time-dependent, have a complete thermodynamic process, a vertical turbulence mixing, and a free surface. This is the case of lakes, like the ones here studied, making it particularly important to well represent the hydrodynamic of the environment allowing to link the external forces with the lake's behaviour, and water quality effects. Some points need special attention, like: (CASULLI e STELLING, 1998) (CHAPRA, 2008) (MARTINS, 2017):

- External forces should cover the entire modelling period;
- Meteorological forcing units (data collected x models request);
- The time step needs to ensure computation stability (Courant number);
- Unless the model uses a wetting-drying scheme, the water depths cannot be too small;
- Choose the corrected coordinate model to what should be represented (sigma or z-model coordination).

### 3.3.1. Models governing equations

In 3D simulation cases, due to its complexity, it is necessary to have a numerical scheme that can minimize problems with stability, due to the time step dependence from the spatial discretization, wave velocity, or the Courant number (CASULLI e STELLING, 1998).

The solution proposed for Leendertse (1967) and Stelling (1983) is a way of factorization the barotropic pressure and the continuity equation. It was extended to the 3D models by using the

Reynolds Average Navier-Stokes equations (RANS) continuity (11) and momentum (12) equation. In this model, the hydrostatic and the hydrodynamic components of the pressure are considered separately.

$$\frac{\partial \rho}{\partial t} + \frac{\partial \rho v_i}{\partial x_i} = 0 \qquad \text{(Eq.13)}$$

$$\frac{\partial \rho \overline{u_i}}{\partial t} + \frac{\partial \rho \overline{u_j}\,\overline{u_i}}{\partial x_j} = -\frac{\partial \overline{p}}{\partial x_i} + \rho g_i + \frac{\partial}{\partial x_j}\left[\mu\left(\frac{\partial \overline{u_i}}{\partial x_j} + \frac{\partial \overline{u_j}}{\partial x_i}\right) - \frac{2}{3}\mu\left(\frac{\partial \overline{u_k}}{\partial x_k}\right)\delta_{ij}\right] + \frac{\partial(-\rho \overline{u_i' u_j'})}{\partial x_j} \qquad \text{(Eq.14)}$$

On the above equations, $x_i$ is the position at coordinates axes *i,j*, and *k*, $\rho$ is the temperature dependent water density, $\overline{u_i}$ is the time averaged velocity component at direction *i*, $\overline{p}$ is the hydrostatic pressure, $\mu$ is the water dynamic viscosity, $\delta_{ij}$ is the *Kronecker Delta* and $\overline{u_i' u_j'}$ is the Reynolds stress (TENNEKES, 1984).

In order to simplify the 3D simulation, a hydrostatic assumption was created to shallow water models. In this, the vertical acceleration and diffusion are so small that, the motion equation in the vertical direction can be simplified as shown in (15). The models which applied this assumption can be called a quasi-3D model (CASULLI e CHENG, 1992).

$$\frac{\partial p}{\partial x_k} + \rho g = 0 \qquad \text{(Eq.15)}$$

Several numerical solutions for this aproach are availabe as the ones proposed by Casulli et al (1992, 1998) and Ji (2008) and consider using a staggerd grid as shown in

Figure 12. A reference water elevation h is considered and η is the depth above the reference. The Reynolds strees terms require closure equations to be determined and different models can be employed.

All this formulations and dedutions are important for the closure model, which need to be applied in the models to represent the tensions around each element.

**Figure 12. General grid Solution forquasi-3D problem**

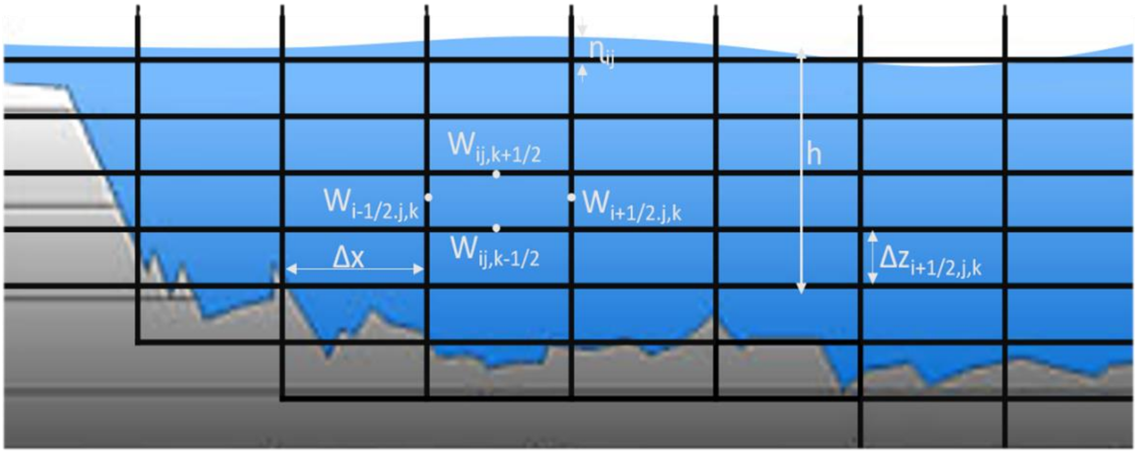


Source: Data from CASULLI; CHENG (1992).

Water temperature and salinity concentration influence directly on the water density, those alterations can be represented by a transport equation (14). Which describe the variations (c) in the Temperature or the Salinity depending on the time, velocity components (u,v,w) and the eddy diffusivity coefficients (horizontal $v_c^h$ and vertical $v_c^v$) (CASULLI e STELLING, 1998) (CASULLI e CHENG, 1992).

$$\frac{\partial c}{\partial t} + u\frac{\partial c}{\partial x} + v\frac{\partial c}{\partial y} + w\frac{\partial c}{\partial z} = v_c^h\left(\frac{\partial^2 c}{\partial x^2} + \frac{\partial^2 c}{\partial y^2}\right) + \frac{\partial}{\partial z}\left(v_c^v\frac{\partial c}{\partial z}\right) \qquad \text{(Eq.16)}$$

### 3.3.2. Vertical mixing and turbulence models

Vertical and horizontal mixing is influenced by eddies circular motions, once it is random and circular. However, this research explored the *quasi-3D* models' capacity to represent especially the vertical component, therefore this item is focused on it.

The turbulence flow can be imagined as an irregular random particle velocity fluctuation that can transfer mass through the mixing of turbulent eddies. In lakes and reservoirs environmental vertical mixing is generally caused by the wind, as discussed before, and the amount of vertical mixing is controlled by the density stratification, once that strong vertical stratification inhibits the mixing. To represent this phenomenon by numerical models vertical and horizontal turbulent dispersion are used, through the Vertical Eddy Viscosity (VEV) and Vertical Eddy Diffusivity (VED) (JI, 2008) (CHAPRA, 2008) (MARTINS, 2017).

The turbulence process plays a critical role in vertical mixing and in water bodies it can be generated at the bottom or surface. To calculate the vertical turbulent mixing coefficients in the momentum and mass transport equations a turbulence model is necessary, these are two-equation turbulence closure models with turbulence variables, such as turbulence kinetic energy and diffusivity (*k-ε model)* or turbulence kinetics energy and turbulence length scale (*k-l*).

The turbulence closure scheme calculates vertical turbulent momentum diffusion ($A_v$) and mass diffusion ($A_b$) coefficients, the models correlated them with the vertical turbulence intensity ($q$), turbulence length scale ($l$) and Richardson number ($R_q$). This allows an enclosure to the turbulence models, by giving them boundary conditions as a way of layers interaction (JI, 2008) (CHAPRA, 2008) (MARTINS, 2017).

$$A_v = \frac{(1+8R_q)ql}{(1+36R_q)(1+6R_q)} \quad \text{(Eq.17)}$$

$$A_b = \frac{0.5ql}{(1+36R_q)} \quad \text{(Eq.18)}$$

$$R_q = -\frac{gH\frac{\partial b}{\partial \sigma}}{q^2}\left(\frac{l^2}{H^2}\right) \quad \text{(Eq.19)}$$

## 3.4. Water quality modelling

A water quality model is based on the mass balance equation. The base information (water depth, currents, turbulence mixing, temperature, and sediment concentration) is provided by the hydrodynamic and sediment models. That information is also used to characterize the laws governing chemical, biochemical and biological processes, boundary and initial conditions (JI, 2008) (DELTARES, 2014) (CHAPRA, 2008) (MARTINS, 2017).

Water quality in water bodies depends on physical processes (Figure 13), earlier described by the hydrodynamic model. The hydrodynamic transport determine how nutrients are advected and dispersed within the water column and transported in and out the system, the atmospheric exchanges can add or remove nutrients and gaseous (reaeration) from the water body, nutrients sorption and desorption can be approximately represented by the equilibrium partitioning process and is affected by the total suspended solids concentration and the partition coefficient (JI, 2008) (DELTARES, 2014) (CHAPRA, 2008).

Also the biochemical reactions transform nutrients and algal uptake reduces the concentration of dissolved nutrients, the exchanges on the bed – water Interface contributes on the dissolved nutrients balance via the diffusion process and particulate nutrients can settle on (or be re-suspended from) the bed, depending on hydrodynamic conditions. And to finish, the sediment diagenesis or decay is a significant factor for determining the nutrient cycling and oxygen balance in the water column (JI, 2008).

**Figure 13. Processes affecting the water quality in an aquatic system**

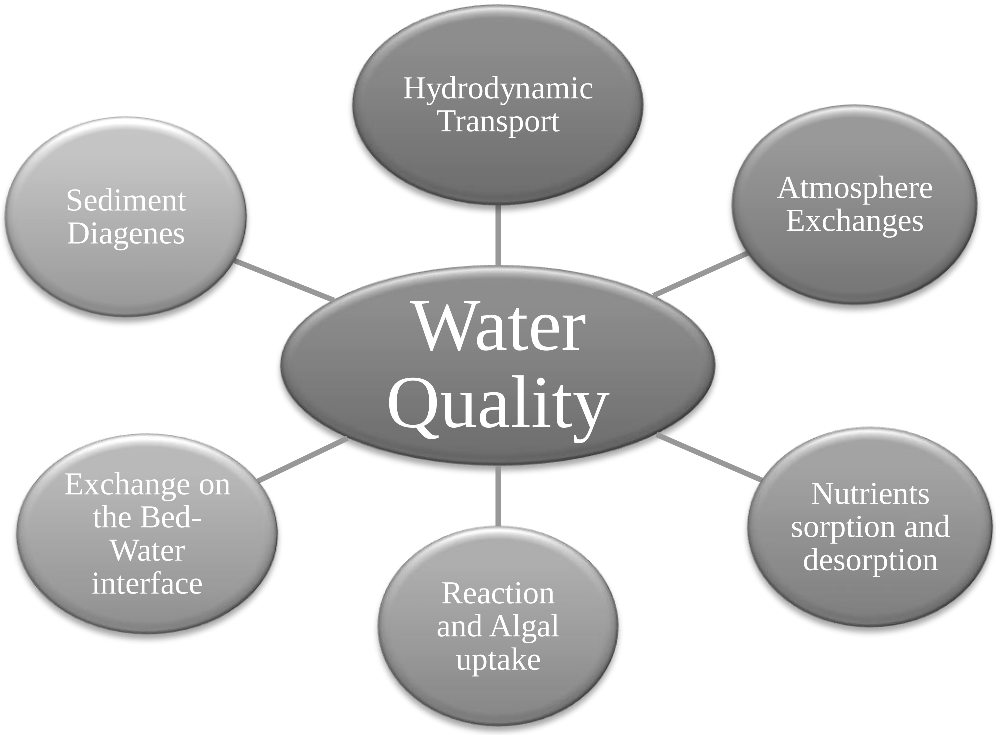


Source: Author.

### 3.4.1. Governing equations

The concentration alterations are determined with the mass balance equation (Eq. 14). The main processes in pollutant interactions with the environment are the advection and dispersion term. The first one considers the inputs and outputs and the pollutant downstream movement, while the dispersion term describes how the pollutant spreads in the water.

The reactivity term refers to the chemical and/or biological processes, and the loading term describes the influence of external forces. Other involved processes are the bed particle deposition and resuspension, represented by the settling term. (JI, 2008) (CHAPRA, 2008) (MARTINS, 2017).

To mathematically represent the water quality variables a set of coupled mass conservation equations are used, hence all of them have a similar form (Eq. 14). They describe the material entering or leaving the water body, the horizontal and vertical transport, and all physical, biological and chemical transformations. Numerical models that use this type of expression represent the concentration variation in time, in the three directions, the velocities, due to the turbulent diffusivities, and sources-sinks per unit volume (JI, 2008) (DELTARES, 2014) (CHAPRA, 2008) (MARTINS, 2017).

A kinetic equation is used to express the kinetic processes and external loadings $\partial C/\partial t = S_c$, which refers to the mathematical description of the time dependency of any dynamic process. If it's a first-order kinetics process the linearizing equation is:

$$\frac{\partial C}{\partial t} = kC + R \qquad \text{(Eq.20)}$$

where $k$ is kinetic rate ($\text{time}^{-1}$) and $R$ is the source/sink term due to external loadings and/or internal reactions (mass/volume/time) (MARTINS, 2017).

The described variables difficult to determine and are influence by many aspects, like hydrodynamic conditions, temperature gradient, and nutrient concentrations, so a better description of them implies in a more realistic model (JI, 2008) (DELTARES, 2014) (CHAPRA, 2008).

## 3.5. Delft 3D Model and Software

In this study the software chosen to model the described phenomena in water was the Delft3D, which is a mathematic model based on the resolution of the Navier-Stokes equations, using the finite difference method. The main reasons for this choice were the model capacity of quasi tri-dimensional modelling, which applies to the research objective, the widespread and knowing reliability of the software and for being an open-source system. Still, there are also some disadvantages to using the Delft3D model, among then the major is the processing time (DELTARES, 2014).

The Delft3D has a set of modules covering a range of aspects (Figure 14), each module can be executed independently or in combination with other modules. All of them are dynamically interfaced to exchange data and results when the simulated process requires. The information exchanged between modules is provided automatically, each module writes its results in a communication file, and reads from it the required information (DELTARES, 2014).

**Figure 14. Delft3D system architecture**

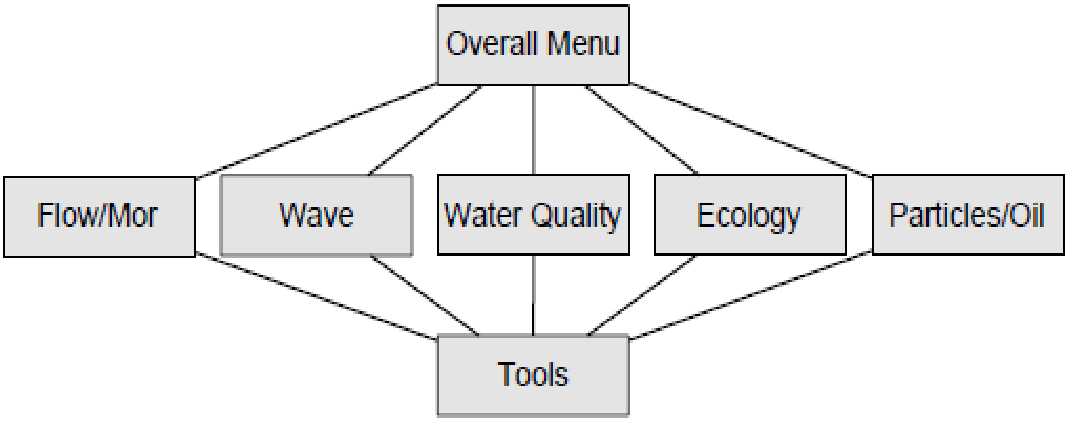


Source: DELTARES (2014).

In this research, the modules used are FLOW and Water Quality. The first represents the lake's hydrodynamic, while the second focuses on the ecosystem relationships evaluations. Both module count with ways of introduce the initial and boundary conditions, physical, numerical and process parameters, the domain representation, time frame, external operations; i.e.: in/out discharges, and provide depth variant results, in defined control points, and spatial variant result, as study area maps in each specific simulated time.

### 3.5.1. FLOW

The hydrodynamic module, Delft3D-FLOW, is a multi-dimensional hydrodynamic simulation program that calculates non-steady flow and transport phenomena resulting from tidal and meteorological forcing on a curvilinear, boundary-fitted grid (DELTARES, 2014).

The environmental representation is made through an orthogonal, curvilinear grids of variable grid size, where morphological information, such as bathymetry can be attached. The vertical representation can be made by using to different schemes: z-model and the commonly used σ-coordinate system. In the σ-coordinate system the number of layers over the entire horizontal computational area is constant, irrespective of the local water depth, and the distribution of the relative layer thickness is usually non-uniform. This allows for more resolution in the zones of interest such as the near surface area and the near bed area but will not always have enough resolution around the pycnocline, giving significant errors in the approximation of strictly horizontal density gradients in areas with steep bottom topography (DELTARES, 2014).

The Cartesian Z co-ordinate system has horizontal co-ordinate lines, which are (nearly) parallel with density interfaces in regions with steep bottom slopes, it is important to reduce artificial mixing of scalar properties such as salinity and temperature. The Z-model is not boundary-fitted in the vertical, the number of grid cells in the vertical varies for each horizontal grid point. The both co-ordinates models can be summarized by Figure 15 (DELTARES, 2014).

**Figure 15. Vertical computational grid z-model (left) and σ-model (right)**

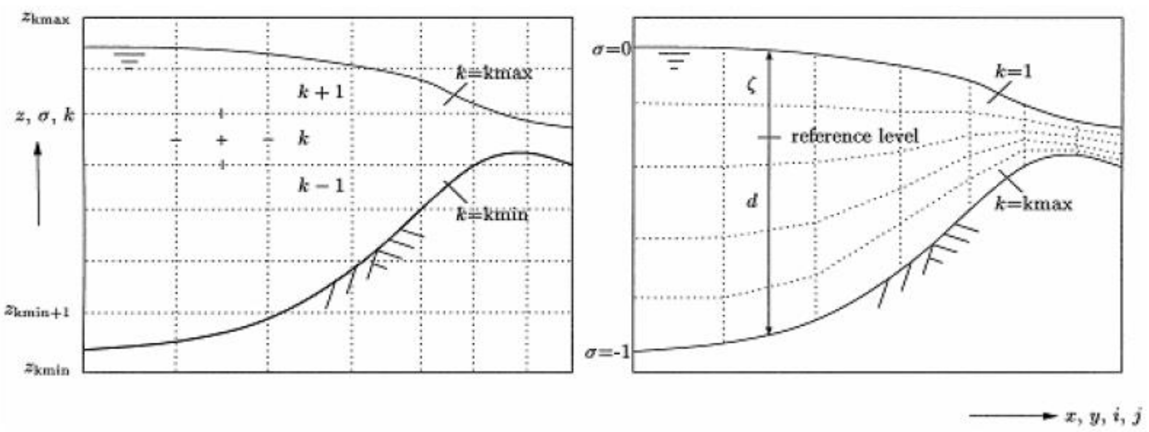


Source: DELTARES (2014).

To create a scenario, a represented domain using a numerical grid with morphologic data is needed, then the number and thickness of the layers can be chosen, as well as the simulation time frame. In this module is possible to simulate four types of constituents: salinity, temperature, pollutants/tracers and sediments, and also two physical process, wind and wave (DELTARES, 2014).

Initial and boundary conditions have a wide diversity of input data that can be selected depending on the monitoring data collected. The initial conditions specify the water body state at the simulation beginning, so the model can have a faster stabilization and proximity to reality. Boundary conditions represent the system in and out flow, those data will not be calculated by the model but have a lot of influence in its results (DELTARES, 2014).

The constants and coefficients that affect hydrodynamic process, resulting from the external forces, bottom roughness, water viscosity and turbulence, discussed in the previous items, are characterized in the physical parameters. They are:

- Gravity;
- Water and air density;
- Salinity;
- Wind drag coefficient;

- Bottom roughness;
- Horizontal and Vertical Velocity;
- Horizontal and Vertical Diffusivity;
- Model for 3D turbulence;
- Secchi depth;
- Evaporative heat flux (Dalton number);
- Heat convection (Stanton number);
- Temperature monitored data (Air temperature, relativity humidity, cloud cover and radiation);
- Wind monitored data (speed and direction).

Delft3D have also pre-determined options to model the exchange of heat through the free surface. There're six options, each one with apply to different situation, as showed in Table 1. Once again, the selection depends on the available data and the calibration process (DELTARES, 2014).

There are also some possibilities in numerical parameters about advection scheme for momentum and transport, filters and parameters to consider a cell dry or flooded.

**Table 1. Deft3D heat flux options**

| Option | Specifications |
|---|---|
| No flux | The background temperature is used throughout the model area. |
| Absolute flux, total solar radiation. | The absolute temperature is computed. The relative humidity, air temperature and the solar radiation for a clear sky have to be prescribed. The net atmospheric radiation and the heat losses due to evaporation and convection are computed by the model. |
| Absolute flux, net solar radiation | The absolute temperature is computed. The relative humidity, air temperature and the combined net solar and net atmospheric radiation have to be prescribed. The terms related to heat losses due to evaporation and convection are computed by the model. |
| Excess temperature | The heat exchange flux at the air-water interface is computed; only the background temperature is required. |
| Murakami | The relative humidity, air temperature and the net solar radiation have to be prescribed. The effective back radiation, and the heat losses due to evaporation and convection are computed by the model. The incoming |

| Option | Specifications |
|---|---|
| | radiation is absorbed as a function of depth. The evaporative heat flux is calibrated for Japanese waters. |
| Ocean | The relative humidity, air temperature and the fraction of the sky covered by clouds is prescribed (in %). The effective back radiation and the heat losses due to evaporation and convection are computed by the model. Additionally, when air and water conditions are such that free convection occurs, free convection of latent and sensible heat is computed by the model and added to the forced convection. |

Source: DELTARES (2014).

The main results derived from simulations performed with FLOW module are water depth, water level, horizontal and vertical velocity, water temperature, water density and turbulent energy. They all can be represented in spatial and punctual graphs.

### 3.5.2. Water quality

In the Water Quality model (D- WAQ), the transport of substances in surface and ground water is represented by the advection-diffusion equation. D-WAQ can be applied on 0D, 1DV, 1DH, 2DV, 2DH and 3D schematizations of a water body. D-WAQ includes the complete natural cycles of C, N, P, Si and O2, as well as cohesive sediments, bacteria, salinity, temperature, heavy metals and organic micro-pollutants (DELTARES, 2014).

D-WAQ solves a simplified representation of the advection-diffusion-reaction equation for each computational cell and for each state variable. The mass balance has the components to describe: the mass at the beginning of a time step, the mass at the end of a time step, changes by advective and dispersive transport, changes by physical and (bio)chemical or biological processes and changes by sources. D-WAQ is capable of describing any combination of constituents and is not limited with respect to the number and complexity of the water quality processes (DELTARES, 2014).

Water quality processes are described by linear or non-linear functions of selected state variables and model parameters, these formulations are available in the form of a library. All the hydrodynamic characteristics can be imported by the FLOW module (DELTARES, 2014).

This module also provides results in space and punctual, for all the variables simulated such as DO, BOD, Algae, Orto-phosphate, Nitrate and Ammonia.

# *CHAPTER II - Lakes' Thermal Stability Correlation with Atmospheric Driving Forces*

# 1. Methods and Materials

Prior to investigating the first hypothesis, a conceptual model should be discussed. Stratification can be postulated as an energy balance considering the energy incident from solar radiation and the kinetic energy transferred by the wind in terms of the surface wind-drag force.

A stratified lake has well-defined isothermals distributed across the water column that depends on the stability of the atmospheric conditions. According to this assumption, a constant wind velocity along the time creates a turbulence pattern that generates a slightly deformed water surface, where the flux is well established inside the mixed layer or epilimnion. In other words, the stratification has inertia energy, which comes mainly from heat provided by the incident radiation. This is called here as the stratification energy.

The lake's thermal conditions can be affected when an instability factor is inserted in the system. The wind's speed fluctuation produces the instability that transfers an amount of energy to the water column, provoking oscillations on the isothermals or internal waves (IMBERGER, 1998) (KULLEMBERG, 1976) (MARTINS, 2017).

It is generally accepted that depending on the accumulated energy initially in the water column and the wind energy fluctuations, these oscillations can amplify the internal waves until the stratification breaks and mix the lake. This oscillating energy is called here as the mixing energy.

Thus, the initial idea proposed, is that the lake's thermal condition results from the energy balance that can be put in terms of a direct correlation between these two impulses (stratification and mixing energy), both atmospheric driving forces.

This relation can be a more precise tool to forecast the water column's thermal condition based only on wind speed, radiation, and water temperature data. To investigate this hypothesis, the first step was to develop a way to compute the mentioned driving forces effectively acting in the episodes of the lake transitions, ‘onset’ or ‘mixing’, and then correlate them.

## 1.1 Relationship Between Atmospheric Variable and Lake Mixing Regime

Field data were used to characterize the exact status of the atmospheric variables (water temperature, wind speed, and radiation) on mix and stratification moments. The lake was considered mixed when there was less than 1 °C difference between surface and bottom temperature. This value was adopted by analysing the monitoring data.

The lakes' thermal response was observed considering four different atmospheric forces combinations, they were: Episodes of Radiation reduction and Wind Speed increase; Increase of Radiation and Wind Speed; Reduction of Radiation and Wind Speed; and Radiation increase and Wind Speed reduction. These analyses aimed to determine the role of each force in the lakes' thermal condition (stratified or mixed).

### 1.1.1 *Accouting the Energies on the Balance*

After presenting each forces' role in the mixing regime, the next step was to account for the energies on this balance. The energies were classified into three portions: initial condition, the stratification energy, and the mixing energy.

To be able to represent the lakes specific characteristics, including boundary conditions, morphometry, in and outflows influence and the lakes' capacity to absorb the incoming energy. If the instantaneous specific incident energy flux if known, the energy effectively transferred to the water column can be computed considering the first order light attenuation coefficient $K_e$ along the depth H.

Considering practical situations, light penetration on the water is also a complex phenomenon due to several factors like turbidity, algae and so. Also, the other processes involving energy transport must be considered making this analytical determination of the stratification energy difficult.

The Schmidt Number was chosen to reproduce the water column's thermal condition, because it reflects the resistance to mechanical mixing due to the potential energy inherent in the stratification of the water column (J $m^{-2}$) (READ, HAMILTON, *et al.*, 2011). The Schmidt Number in the only index, from the previous explained, which has this capacity, and also is simpler to calculate, once it depends only on water temperature and morphometry data, representing the net energy present on the water to sustain the stratification, including all components as advective transport, light attenuation, biomass, etc. Another advantage is that monitoring water temperature is easy and inexpensive.

The stratification energy is derived from the heat transferred by the radiation in a specific time window. The net amount of transferred energy can be calculated by the sum of the incident radiation (W $m^{-2}$) during the photoperiod. Theoretically, the total daily incident solar energy $R_0$ at the water surface in a clear sky can be obtained by integrating the instantaneous radiation specific flux R(t) along the photoperiod duration D, according to equations from Eq. 21 to Eq. 23.

The incident specific radiation flux amplitude $R_d$ (J/s.m²) amplitude can computed by equation 24. Photoperiod duration (D) is computed trough astronomic equations considering local latitude and angular solar inclination (SHERRY e JUSTUS, 1983).

$$R_0 = \int_{12-\frac{D}{2}}^{12+\frac{D}{2}} R(t)\, dt \qquad \text{(Eq.21)}$$

$$R(t) = f(t)\, R_d \qquad \text{(Eq.22)}$$

$$f(t) = \left( cos\, \frac{2\pi}{24} t - cos\, \frac{\pi}{24} D \right) \qquad \text{(Eq.23)}$$

*with (12-D/2 < t < 12+D/2)*

$$R_d = \frac{R_0}{\int_{-D/2}^{D/2} f(t) dt} = \frac{R_0}{\left(\frac{24}{\pi} sin\frac{\pi D}{24} - D\, cos\frac{\pi D}{24}\right)} \qquad \text{(Eq.24)}$$

The gross incident energy $R_0$ is easily estimated by astronomical equations for the local latitude but, for real conditions, the value of R(t) is influenced by meteorological and orographic conditions as cloud cover and mountain shadows, making this evaluation extremely depending on meteorological conditions.

On the other hand, incident radiation can be observed by simple instruments that uses the photovoltaic principle, as presented early, to evaluate instantaneously the amount of incident heat. Thus, considering different time windows (last 24 h, 12 h, and 6 h), the sum of the radiation multiplied by photoperiod, in the chosen time window, gives the specific stratification energy provided (J $m^{-2}$). In this work, experimental data pointed thar the 24h period prior to the episodes of on set or mixing can well represent this variable.

The mixing energy is a more complex concept. It's magnitude derived from the fluctuation of the wind speed, once that a constant velocity only affects the lake’s surface, while the movement induced by its variations changes the way the energy is transferred to the water, causing a tilt in the water column (KULLEMBERG, 1976) (IMBERGER, 1998).

The previous index (LN and Wedderburn) used mean wind velocity to describe mixing episodes, although after an extensively analysis of the monitored lakes' data, using wind data of 5 min resolution, the pattern observed was that the mean wind velocity, did not well represent the instability moments before mixing. Using the gust data, that were also available, was possible to the determine that the wind's speed variance is the form to represent the energy transferred in the instability moments.

The mixing specific energy (J m$^{-2}$) was proposed as de energy associated with the fluctuation of the wind velocity. According to the research of Kullember (1976), the wind can be divided into two portions, one that is constant and characteristic for each place, represented by the mean wind's velocity (W), and another that are the fluctuations (W') around this mean, which can be measured by gusts. The results of each portion in the water column are different, constant wind velocity creates a turbulence pattern provoking slightly deformed water surface, while the fluctuation creates perturbations in the currents, which depending on the inherent power of stratification (Schmidt Number) can mix the water column.(Figure 16) (KULLEMBERG, 1976).

After this assumption, the energy associated to the instantaneous part can be determined by the mean of the wind's speed variance in a time window (m s$^{-1}$), multiplied by the air density (kg m$^{-3}$) and the lake's depth (m). Once again, different time windows must be tested (10 min, 1 h, 6 h, and 24 h), in order to better represent work done to destabilize the water column. In this work the period comprising the last 24h was chosen, because of better results and to match the scale of the stratification energy.

**Figure 16. Isothermals in a lake considering the described inertia energy (left) and mixing energy (right), according to the wind operation (W) and the friction stress produced by it (ζ)**

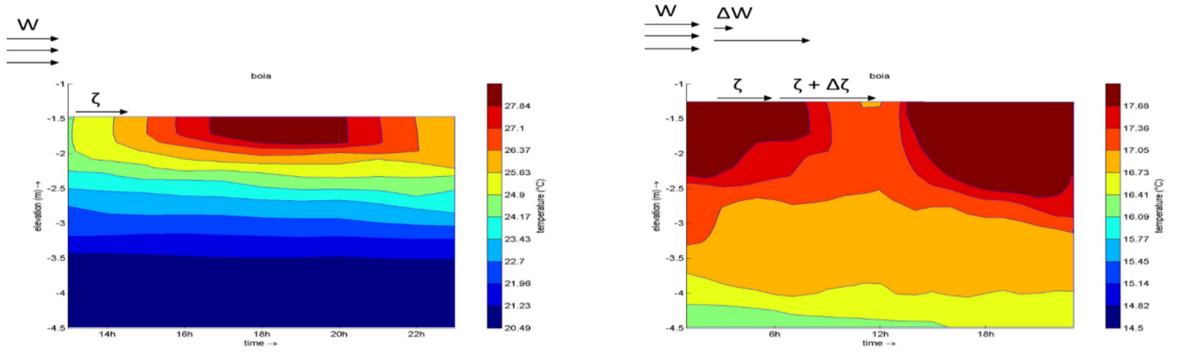

### *1.1.2 Proxy Definition*

From the results of the application of the classical indexes the intervening variables on the lake mixing regime were identified, to improve the demonstration of its interaction the presented energy balance was applied. The role of each intervening variable was represented by a proxy, namely:

- ***Rad***: total amount of the incident radiation on the last 24h (J $m^{-2}$);

To represent all the energy provided by the sun into the lake the total amount of the incident radiation in a window of 24h was calculated. The incident radiation data collected in the field can be transformed in the stratification energy considering the following formulation. In which $Rad_{inc}$ is the incident Radiation $\left(\frac{J}{sm^2}\right)$ and *Tp* is the photoperiod in the time window (s)

$$\boldsymbol{Rad = Rad_{inc} * Tp} \qquad \text{(Eq.25)}$$

- ***W****: mean of the wind's speed variance in a time window($\Delta$U) (m $s^{-1}$), multiplied by the air density ($\rho_{air}$) (kg $m^{-3}$) and the lake's depth ($\Delta$z) (m) (J $m^{-2}$);

The steps to transform the wind's tension ($\tau$) into the mixing energy, from the wind speed (U) measured data, is demonstrated by the following equations. It starts from the wind stress equation (Eq.5), and the variations are represented by the Eq. 26. After simplification (Eq. 27) its multiplied by the water column depth ($\Delta$z), in which this energy is distributed, resulting in the proxies formulation (Eq.28).

$$\boldsymbol{\tau \left(\frac{N}{m^2}\right) = \frac{1}{2} C_D \rho_{air} \left(\frac{Kg}{m^3}\right) U^2 \left(\frac{m}{s}\right)} \qquad \text{(Eq.5)}$$

$$\boldsymbol{\Delta\tau \left(\frac{N}{m^2}\right) = C_D \rho_{air} g \left(\frac{Kg}{m^3}\right) \frac{\Delta U^2}{2g} \left(\frac{m^2}{s^2}\right)} \qquad \text{(Eq.26)}$$

$$\boldsymbol{\Delta\tau \left(\frac{N}{m^2}\right) = C_D \rho_{air} \left(\frac{Kg}{m^3}\right) \Delta U^2 \left(\frac{m^2}{s^2}\right)} \qquad \text{(Eq.27)}$$

$$\boldsymbol{W^* \left(\frac{J}{m^2}\right) = C_D \rho_{air} \left(\frac{Kg}{m^3}\right) \Delta U^2 \left(\frac{m^2}{s^2}\right) \Delta z\ (m)} \qquad \text{(Eq.28)}$$

- ***S****: Schmidt Number mean of the last 24h [J $m^{-2}$].

As explained earlier, the Schmidt Number is applied here because it can include morphometric aspects and the potential energy of the lakes. This proxy reflects the exact state of the lakes' thermal structure, reflecting any other influence that was not directly counted in this balance, such as, disturb derived from in or outflows, or a particulate load of sediments coming from the watershed, which could interfere in the water turbidity. Also, it has advantages related to performing the calculation, only demand data of water temperature, and it is a classic index, with many application cases, enabling comparison (MACINTYRE e MELACK, 2009) (READ, HAMILTON, *et al.*, 2011).

$$S_T = \frac{g}{A_S}\int_0^{Z_D}(z - z_v)\rho_z A_z \partial z \qquad \text{(Eq.6)}$$

Assuming that the thermal condition of the lake is a result of which is the ruling energy of the balance, the proxies were correlated using dimensionless ratios $\boldsymbol{S^{*}\,Rad^{-1}}$ and $\boldsymbol{W^{*}\,S^{*-1}}$. Those proxies reflect the effectiveness of energy transfer from the atmospheric force to the water column, and so, which is the ruling force on balance at the moment. The efficacy of those proxies was evaluated by crossing its results with the lake's water temperature data.

## 1.2 Water Column Stratification Condition

To apply the proxies and create a correlation curve, first, the water column was classified as mixed or stratified. To stablished a classification threshold the monitored data from four lakes were analysed, as described in the next topic, the temperature profile for all of them agreed that when the temperature gradient between water surface and bottom, was minor or equal 1 °C, the water column was mixed (READ, HAMILTON, *et al.*, 2011) (AMORIM et al., 2017).

The calculated proxies were plotted against each other, creating a curve that relates the status of the driving forces to the lakes' thermal response. This curve reflects the stability limit of a stratified profile and can be used to forecast the water column status of a general lake.

# 2. Study Cases

## 2.1 Sites description

Four lakes were considered to perform this research, two small, one medium and one large. The first one is the Hedberg Reservoir, located 10 km from the City of Sorocaba, Sao Paulo State, Brazil (SMITH, BIAGIONI e HALCSIK, 2013). The second is Lake Crètèil situated in Crètèil, Paris (SOULIGNAC, VIÇON-LEITE, *et al.*, 2017). They are both, small, shallow, polymictic lakes, however, one is located in a temperate zone and the other in a tropical zone.

The medium-sized lake is the Billings reservoir, also located in São Paulo, Brazil. It has a total surface area of 127 km² and a perimeter of 90 km (WENGRAT e BICUDO, 2011) (JESUS, 2006). The fourth lake is Lake Bourget, which is a large, deep, monomictic alpine lake in France (CUYPERS, VIÇON-LEITE, *et al.*, 2011) (VINÇON-LEITE, LEMAIRE, *et al.*, 2014).

The Hedberg Reservoir is situated over the preserved area of Ipanema National Forest, enclosing a catchment area of 235 km² (Figure 17). The main river is the Ipanema River and land use includes urban and rural areas. It is in a tropical zone, with a temperature range between 18 and 22 °C (IBAMA, 2012) (ICMBIO, 2008). The lake has a surface area of 0.26 km², a mean depth of 4.5 m and a polymictic behaviour, with several stratifications and mixing events throughout the year. Water quality evaluation showed problems with an excess of nutrients, especially phosphorus C (IBAMA, 2012) (ICMBIO, 2008) (SMITH, BIAGIONI e HALCSIK, 2013).

**Figure 17. Hedberg lake location**

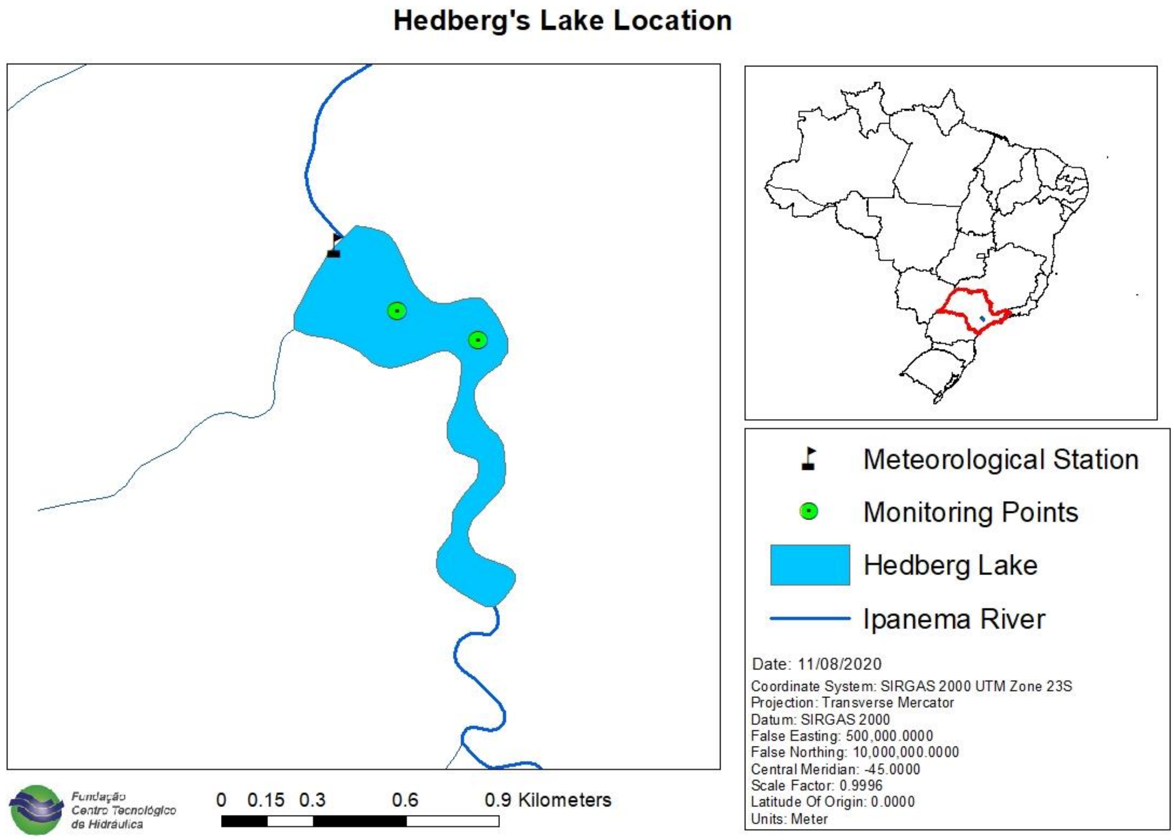


Source: Author.

Lake Crètèil (Figure 18) was the result of a quarry of gravel and gypsum extraction between 1940 and 1976. It was converted to a lake in the mid-1970s. It is surrounded by urban areas (north and east) and a recreation park—Île-de-France (west) (SOULIGNAC, VIÇON-LEITE, *et al.*, 2017). It is located in a temperate zone with a temperature range between -5 and 37 °C. Lake Crètèil has a surface area of 0.4 km² and a mean depth of 4.5 m; the main water contribution comes from the groundwater of the Marne River. This lake is polymictic. It stays mixed in winter and shows several relatively long stratification periods in summer (SOULIGNAC, VIÇON-LEITE, *et al.*, 2017).

**Figure 18. Crètèil Lake localization and surroundings areas**

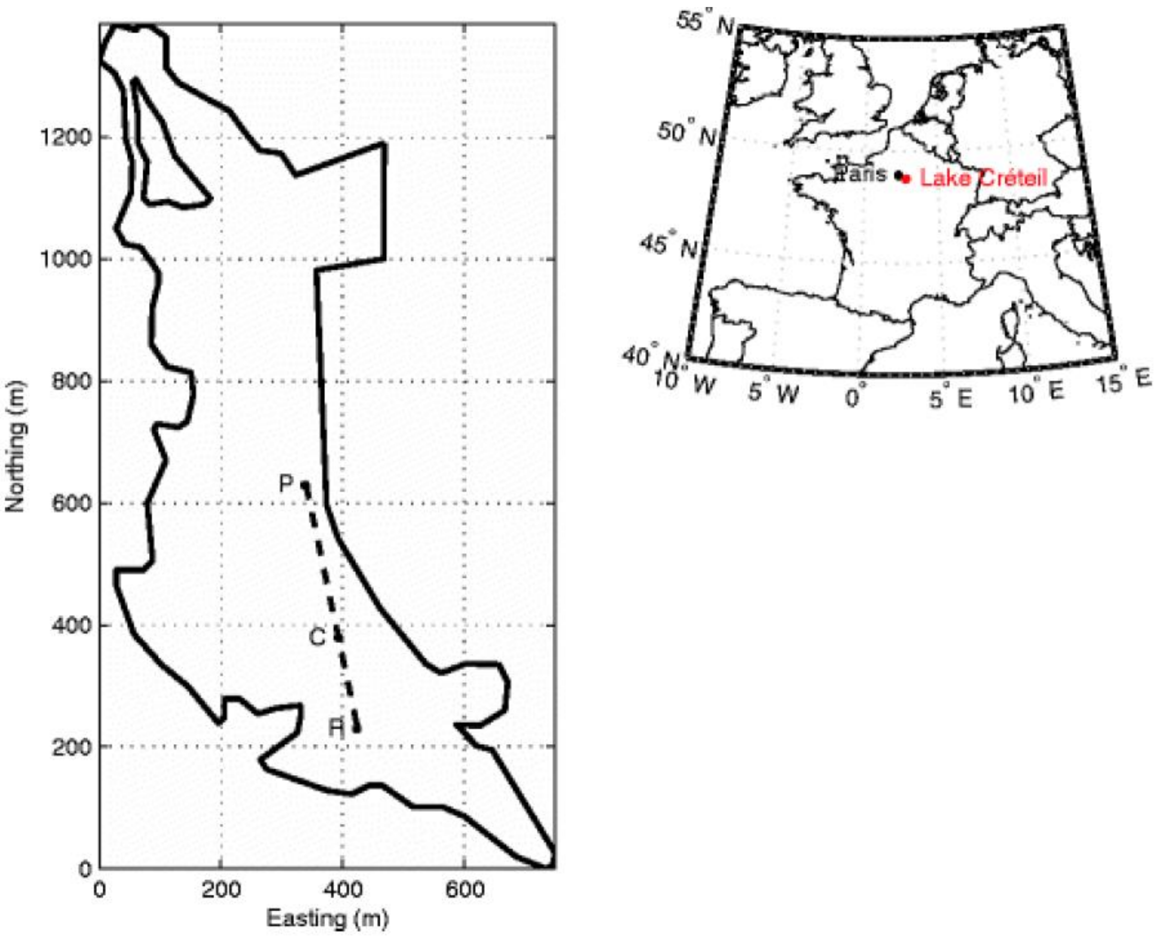


Source: Soulignac, Viçon-Leite, et al (2017).

Billings reservoir is located in São Paulo, Brazil, situated in the Serra do Mar region (23°47' S 46°40' W), 747 m above sea level (Figure 19). This area has a humid tropical climate with irregular topographic, lowland areas and valley bottoms (MARTINS, VINÇON-LEITE, *et al.*, 2014) (WENGRAT e BICUDO, 2011).

The reservoir is situated at the Upper Tietê River basin, which begins between the cities of Salesópolis and Paraibuna and ends in the Rasgão Dam. The flow direction is from east to west draining 5,775 km² and involving 40 municipalities. This is the most urbanised area in Brazil, occupied by 10% of the country's population (FUSP, 2009).

The Billings system is the biggest in the São Paulo metropolitan region, the total capacity is 1.2 billion liters of water. It has a central body with many branches that drain an area of 560 km² with a maximum depth of 18 m and a detention time of 392 days (WENGRAT e BICUDO, 2011) (JESUS, 2006).

**Figure 19. Billings reservoir localization and surroundings areas**

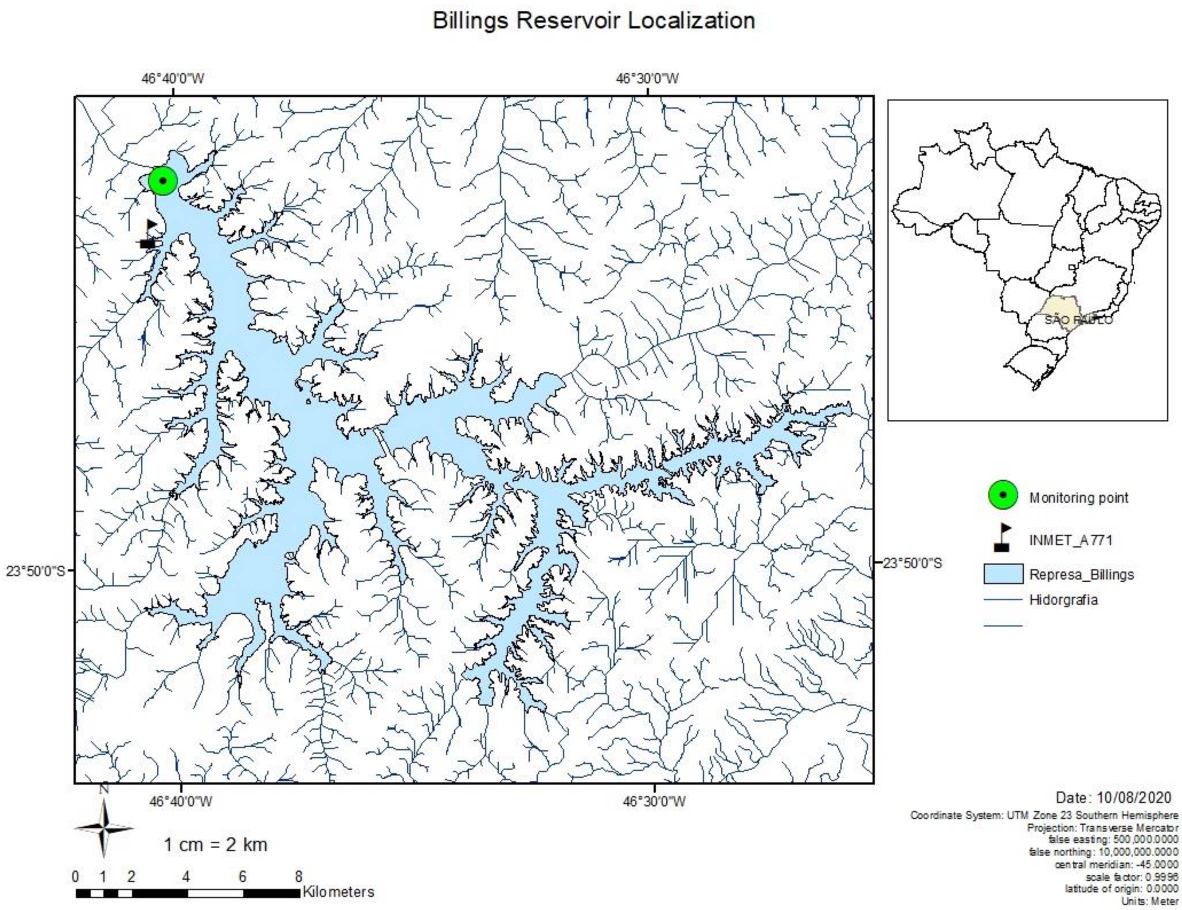


Source: Author.

Lake Bourget is a fjord-type foreland lake located in the borders of the French NW Alps (45°44′ N, 05°51′ W), within the Molasse Basin (560 km²) between the Subalpine and Jura ranges (Figure 20). It is situated in a flood area surrounded by swamps, under the influence of upstream rivers that typify the hydrographic and sedimentary activity in the lake. This is the largest natural lake in France. It is elongated and oriented north-south (length: 18 km; width: 3.5 km; area: 42.3 m²; maximum depth: 145 m; mean depth: 80 m; residence time: 10 years). It is monomict and is influenced by strong winds (CUYPERS, VIÇON-LEITE, *et al.*, 2011) (VINÇON-LEITE, LEMAIRE, *et al.*, 2014).

**Figure 20. Bourget lake localization and surroundings areas**

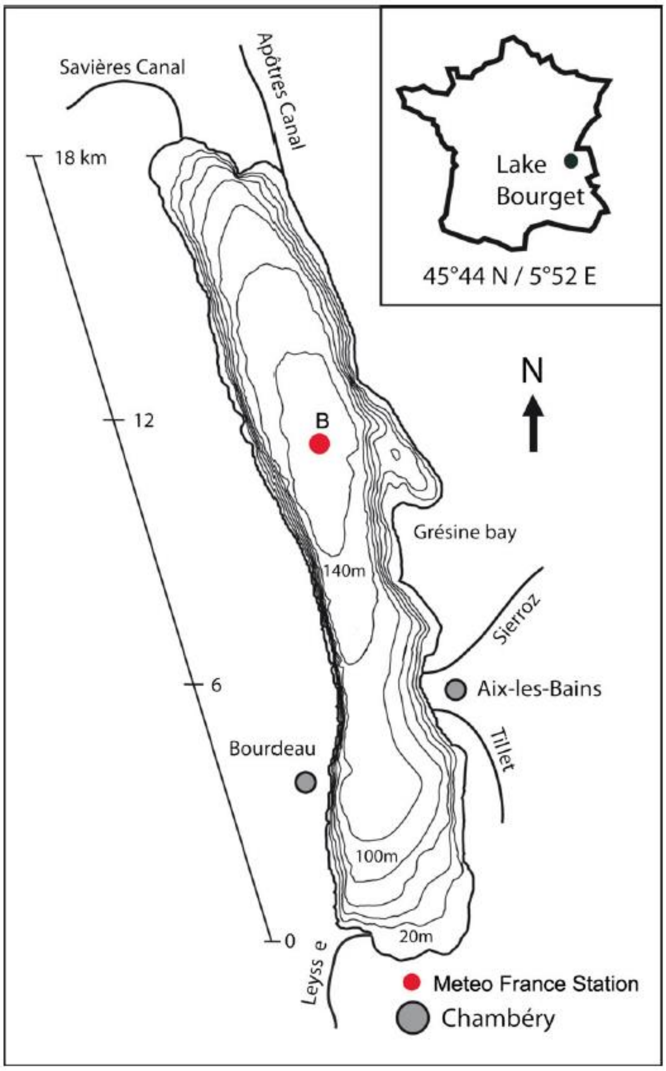


Source: VIÇON-LEITE, et al., (2014).

The water bodies were monitored by teams from University of São Paulo (USP) and Laboratoire d'Eau Environement et Systèmes Urbains École des Ponts ParisTech (LEESU) through the comon project MOMA-SE, founded by CAPES and ANA. Hedberg and Crètèil in the year 2016, Billings in 2018 and Bourget in 2002, using high time-resolution meteorological variables and water temperature instruments.

Figure 21 shows the typical temperature profiles on the four lakes monitoring points, in which it is possible to see that the difference between the temperature range in a stratification condition. Hedberg and Crètèil lakes are similar, with temperatures varying from 18 to 24 °C, Billings reservoir has a minor amplitude (19.5 - 21°C), while Bourget lake has the greater one (5.5 - 22°C).

**Figure 21. Lakes' typical temperature profiles. In which: A – Hedberg lake; B – Crètèil lake; C – Billings reservoir; D – Bourget lake**

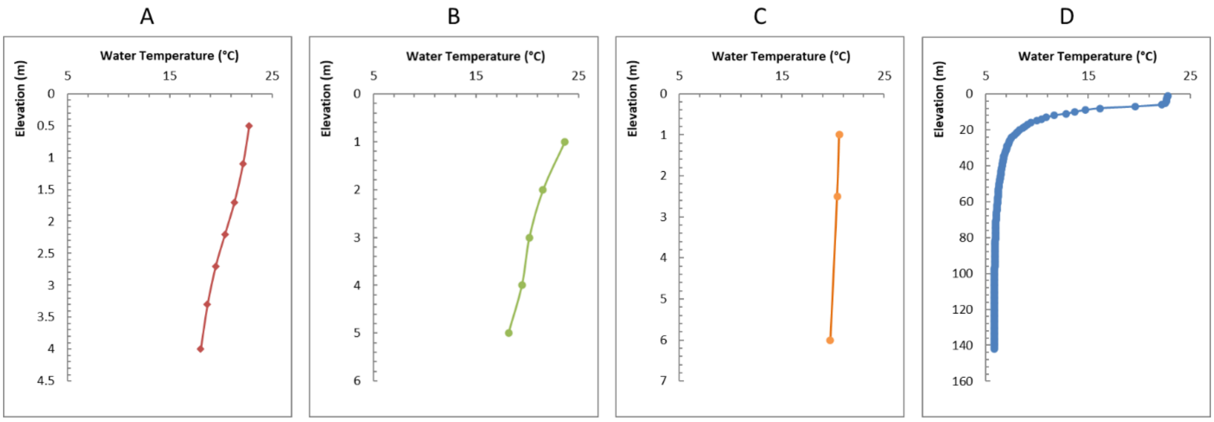


Source: Data from VIÇON-LEITE, et al., (2014); Soulignac, Viçon-Leite, et al (2017) ; Authors data.

## 2.2 Monitoring System

The monitoring system included a set of thermistors (Figure 22) and a meteorological station (Figure 23). This last one was placed on the banks in Hedberg and Billings reservoirs and on the water surface in Bourget and Crètèil lake. The variables recorded were the air temperature, solar radiation, wind's velocity and direction (10m heigh in Hedberg and Billings, 2m heigh in Crètèil and Bourget), atmospheric pressure, relative humidity, and precipitation. The measurement frequency was every 10 minutes for all variables, except for radiation, which was measured within a 5 min interval.

The set of thermistors had probes fixed to a rope and plummet, with a float in the upper end, they were distributed as showed in

Table 2. The time between measurement was the 30s (Crètèil) and 1 min (Hedberg and Billings). The absolute accuracy of the equipment is ±0.2°C and the relative accuracy, verified in the laboratory, is of 0.17 °C. In Bourget, a portable probe was used to register the measures across the water column, with an acquisition frequency of the 30s.

In all of the lakes the chosen measurment point was the deepest point of it, execpt from the Billings reservoir, which has its measures a point near to the dam, due to the interest in this region and the logistic difficults of acess other areas. The thermistors were positioned in a space step that could reproduce the temperature profile along the water column, and well characterize the moments of stratification and mixing.

**Table 2. Specifications of the thermistors**

| Lake | Thermistors Quantity | Depth |
|---|---|---|
| Hedberg | 04 | First at 0.5 m underwater and the rest positioned with 1m spaced. |
| Crétéil | 05 | First at 0.5 m underwater and the rest positioned with 1m spaced. |
| Billings | 06 | First at 0.5 m underwater and the rest positioned with 1m spaced. |
| Bourget | Measured with a probe | First at 1 m underwater and the rest measured with 1m spaced along the 140m. |

**Figure 22. Set of thermistors used on the temperature profile monitoring**

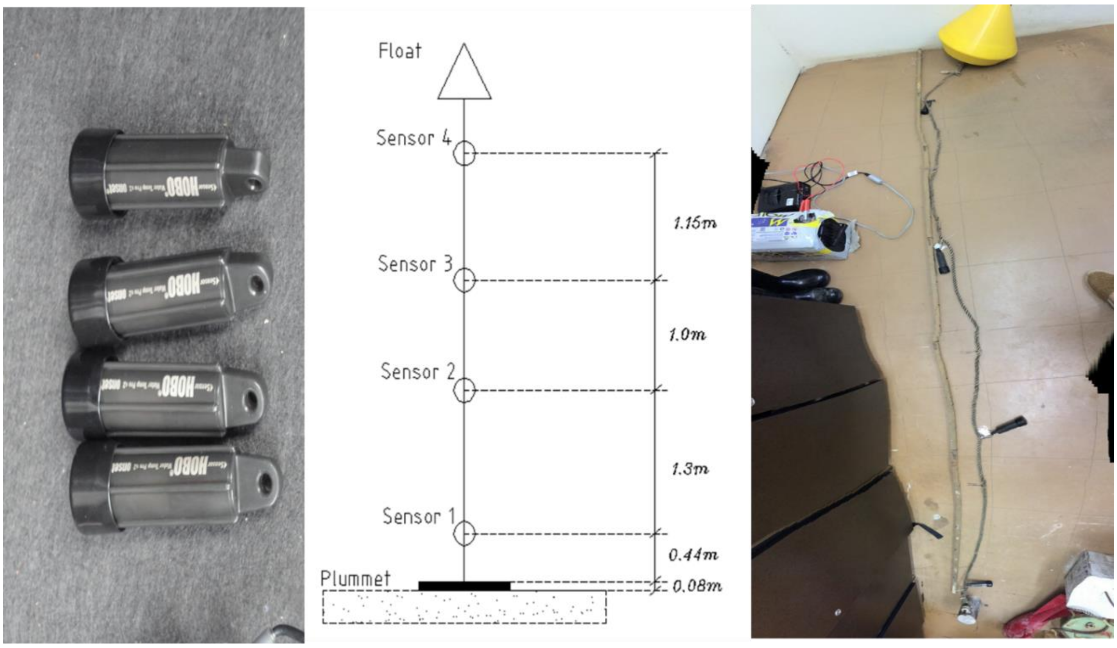


Source: Author.

**Figure 23. Meteorological station**

Source: Author.

# 3. Results and Discussions

## 3.1 Analysis of the Monitored Data

The main energies (wind, radiation and water temperature) on the energetic balance were monitored on the four lakes with high-resolution equipment. The goal was to characterise their behaviour during stratification and mixing events. The period of measurements considered has a six-month duration, which represents winter and spring seasons in both climate zones. In the temperate zone, the lakes were monitored from January to June of 2016 for Lake Crètèil and 2002 for Lake Bourget. In the tropical zone, the monitoring period was from June through December of 2016 for Hedberg lake, and from September to November of 2018 for Billings reservoir.

The monitored data was analysed by plotting measurements in graphs, checking its consistency by looking for outliers and possible errors. Periods with no data or with eventual measurement errors were removed from the time series.

The first thing that stands out when the data is analysed is the difference between tropical and temperate zones. The cool season in both zones shows high wind energy and low incident solar radiation, while in the warm season it is the opposite (Figure 24, Figure 25, Figure 26, Figure 27). The difference is in the amplitude of the variations, which is greater in the temperate zone than it is in the tropical zone.

Another main difference between the two climate zones is the incident solar radiation, which is greater in the tropical zone. The amount of sun energy provided to tropical lakes in winter is similar to the energy provided in the summer to temperate lakes, which leads to more stable water column stratification.

The high-resolution data made it possible to characterise the status of the driving forces at the moment of change in the stability condition. The monitoring revealed what is required to produce a mixing event, i.e., this will only happen if a period of low radiation is followed by the occurrence of gusts of wind. This is a valid condition for both zones, the difference occurs in winter when the temperate lakes tend to stay mixed due to low incoming radiation and high wind speed (Figure 24, Figure 25, Figure 26, Figure 27).

In all cases, the Schmidt Stability Number (***S****) was sufficient to represent each lake's water column behaviour. As shown in the figures below, high ***S**** values correspond to stratified periods, while low ***S**** values are related to mixing episodes. As the classification suggests, several mixing events were found in polymictic lakes, while monomict lakes only mix in the winter.

**Figure 24. Data from the monitoring system for the Hedberg lake**

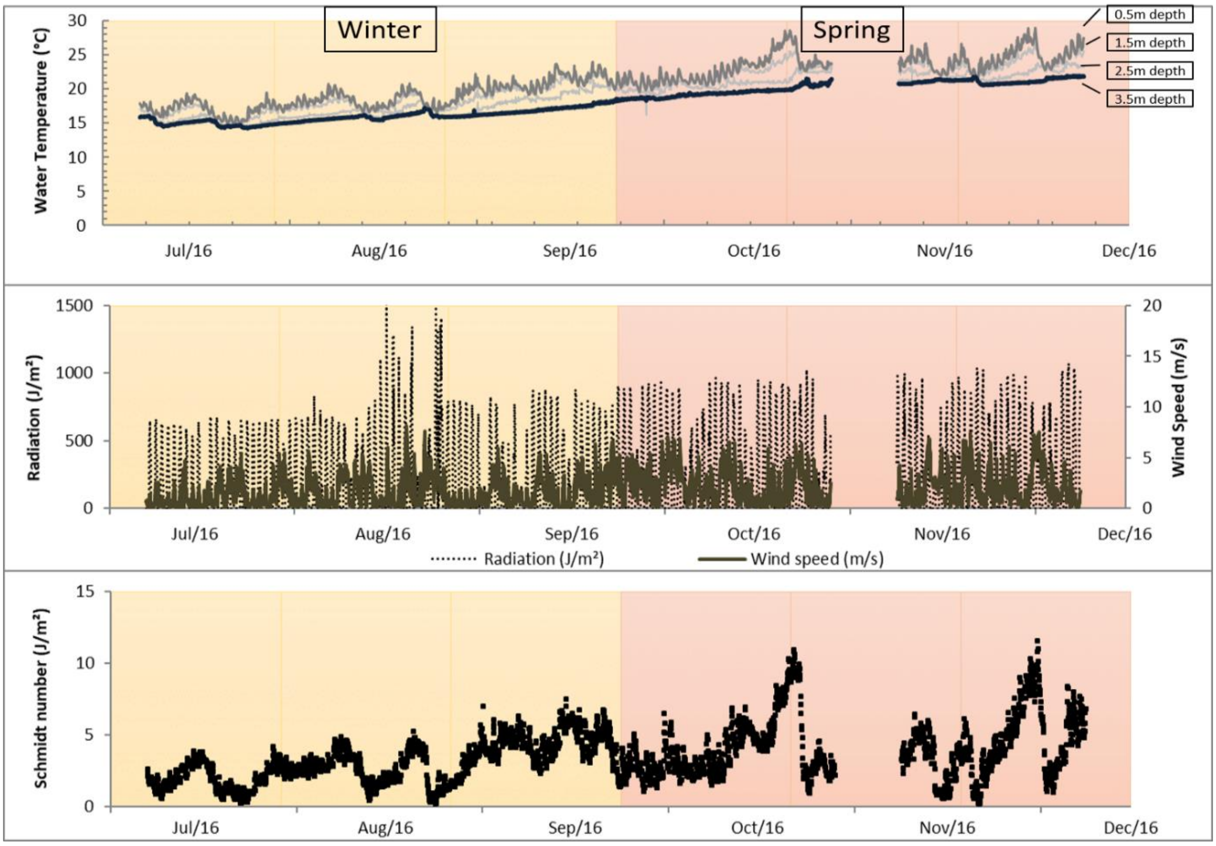


Source: Author.

**Figure 25. Data from the monitoring system for the Crètèil lake**

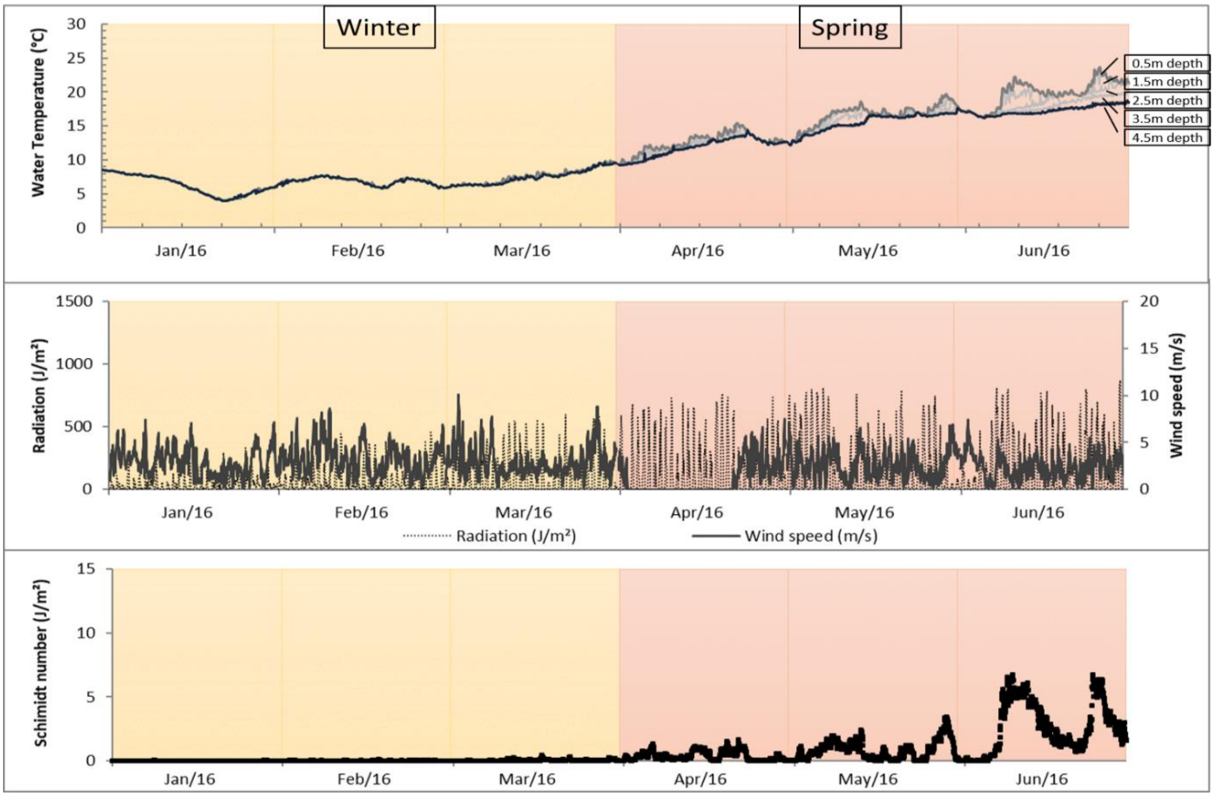


Source: Data from Soulignac, Viçon-Leite, et al (2017).

**Figure 26. Data from the monitoring system for the Billings lake**

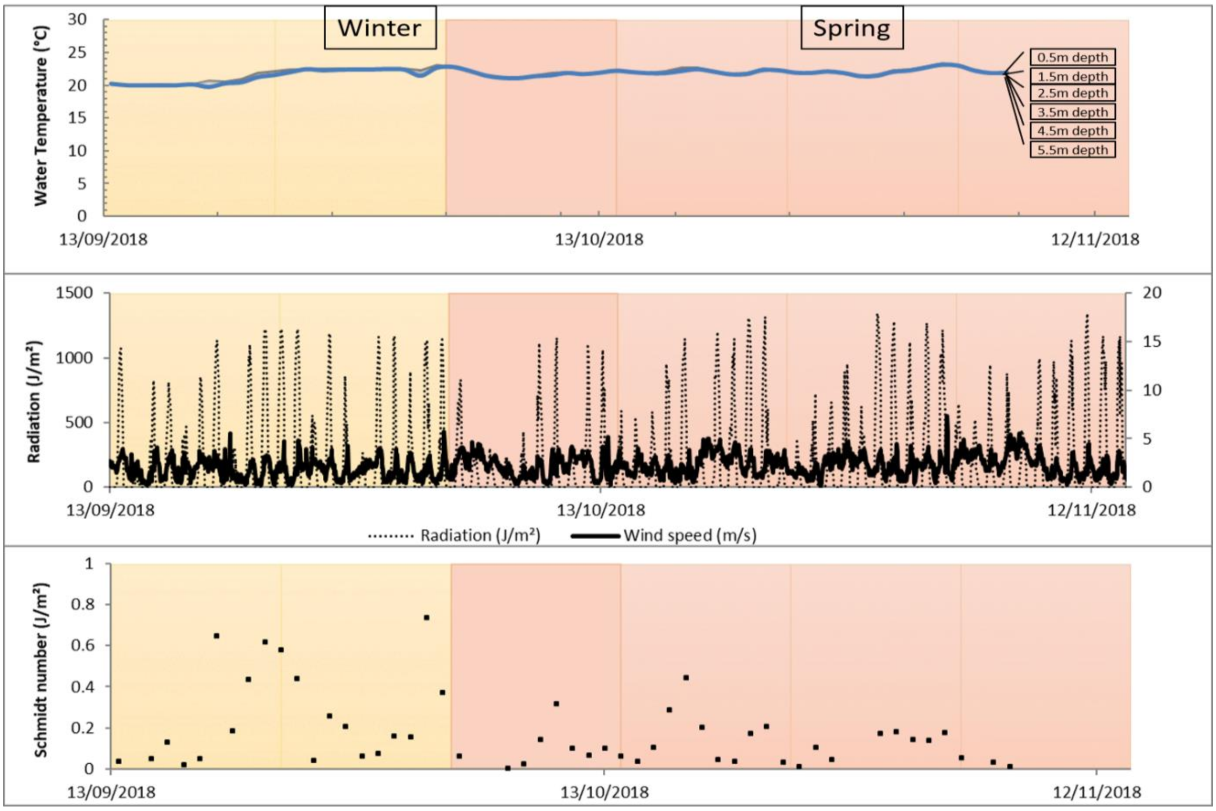


Source: Author.

**Figure 27. Data from the monitoring system for the Bourget lake**

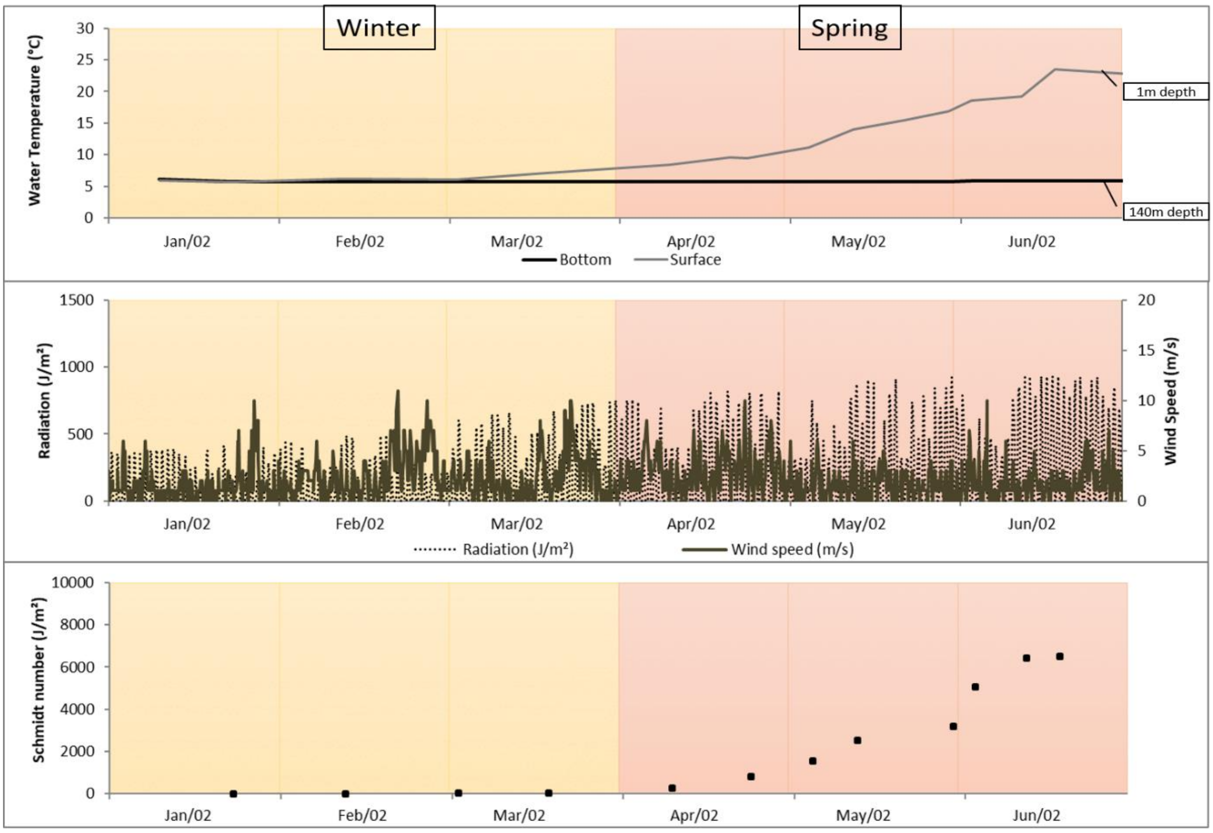


Source: Data from VIÇON-LEITE, et al., (2014).

Continuing with the objective of correlating the lakes' thermal responses to atmospheric driving forces, four situations were selected to study: (1) Lower Radiation and High Wind Speed, (2) Higher Radiation and High Wind Speed, (3) Lower Radiation and Low Wind Speed and (4) Higher Radiation and Low Wind Speed. The variables were considered higher or lower when compared to the mean of each one.

A time series illustrating those situations in each of the lakes is shown in Figure 28. In most of these situations, the water column stays stratified. This evaluation confirms the previous observation, concluding that the radiation is the ruling force on the balance, and a mixing event only occurs when there is a radiation lack combined with wind acceleration.

**Figure 28. Influence of the driving forces conditions on the lake thermal response (Hedberg (A), Crètèil (B), Bourget (C) and Billings (D)). In which: blue blocks mean periods of High Radiation and Low Wind Speed; oranges High Radiation and High Wind Speed; yellows Low Radiation and Low Wind Speed; and greens Low Radiation and High Wind Speed**

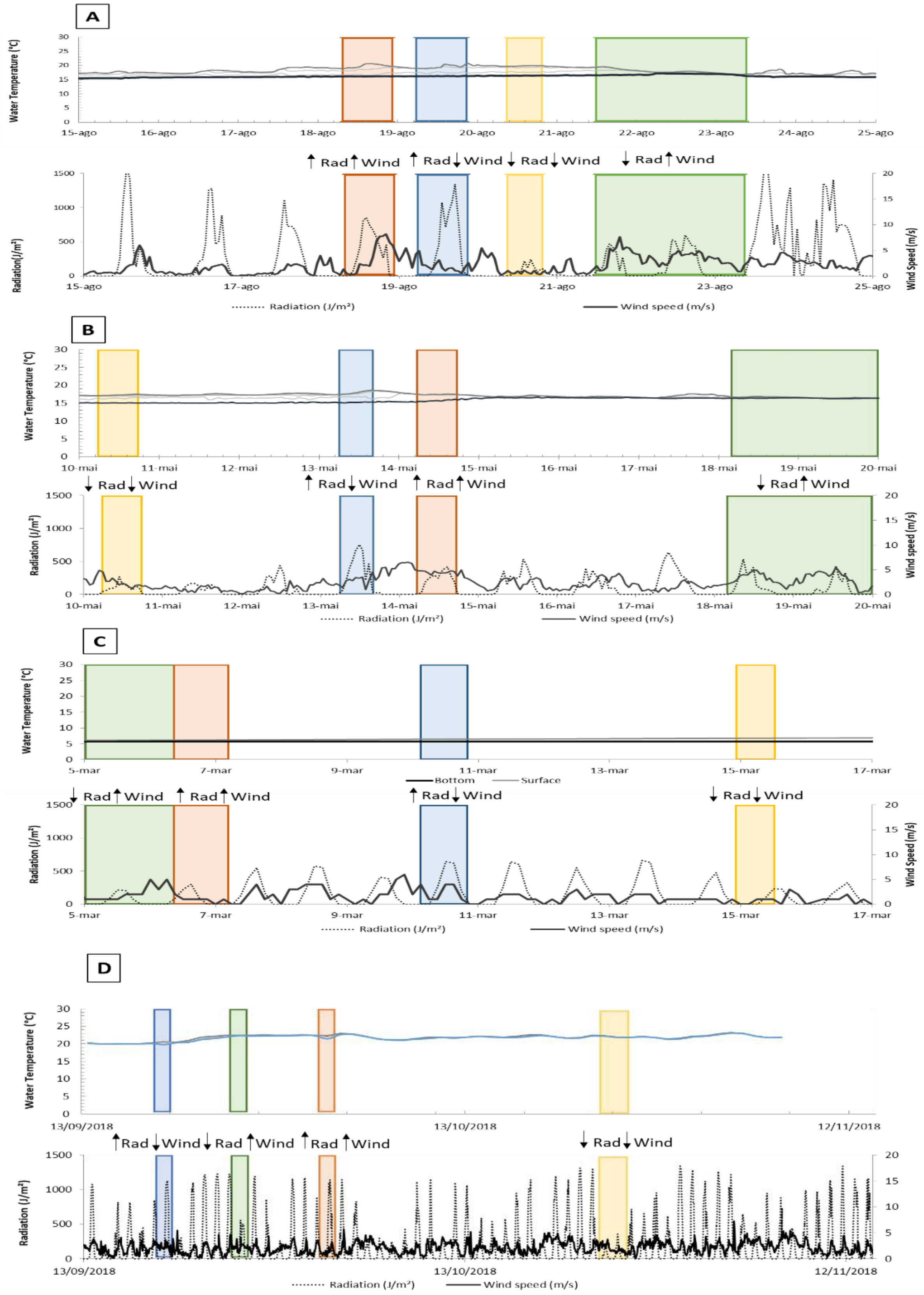


Source: Author; Data from VIÇON-LEITE, et al., (2014); Soulignac, Viçon-Leite, et al (2017).

## 3.3 The Proxies Representing the Water Column Mixing Regime

The graphs from Figure 29 to Figure 32 show the proposed proxies' behaviours over the period analysed. These proxies were used to demonstrate the influence of energy balance on the lakes' mixing regimes. The temperature profile was used to evaluate their efficacy and reliability.

As was expected, for all four lakes the mixing energy proxy (***W*/S****) has higher values in mixing events, while the stratification proxy (***S*/Rad***) shows higher values in stratification peaks. This analysis confirms that the proxies follow alterations in the lakes' mixing regimes and can be used to demonstrate them.

**Figure 29. Mixing and Stratification energy proxies related to water temperature for Hedberg lake**

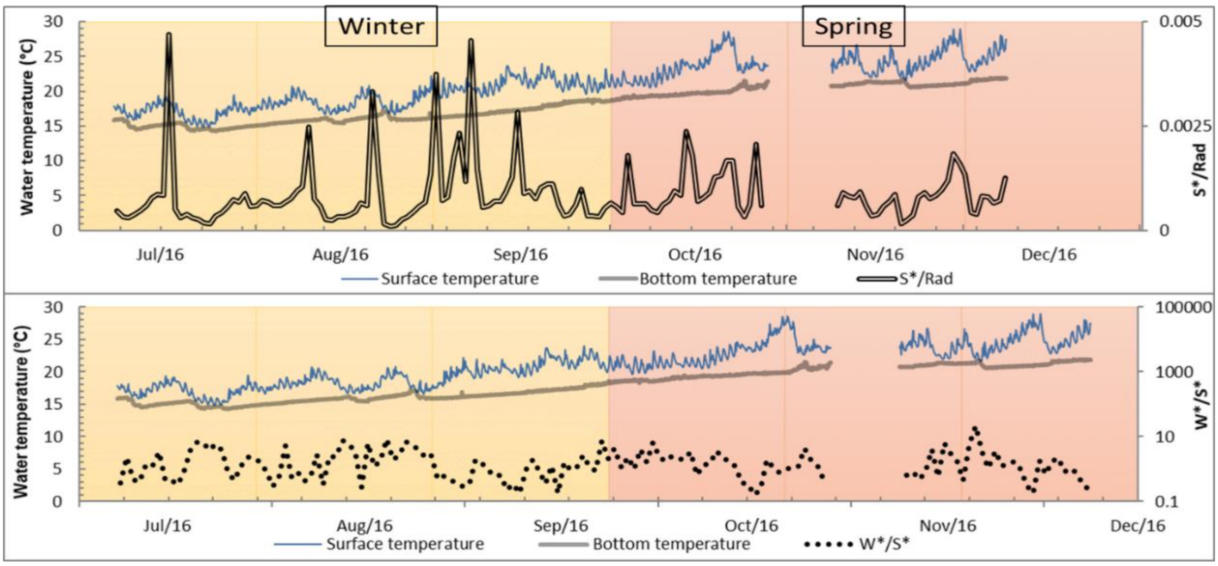


Source: Author.

**Figure 30. Mixing and Stratification energy proxies related to water temperature for Crètèil lake**

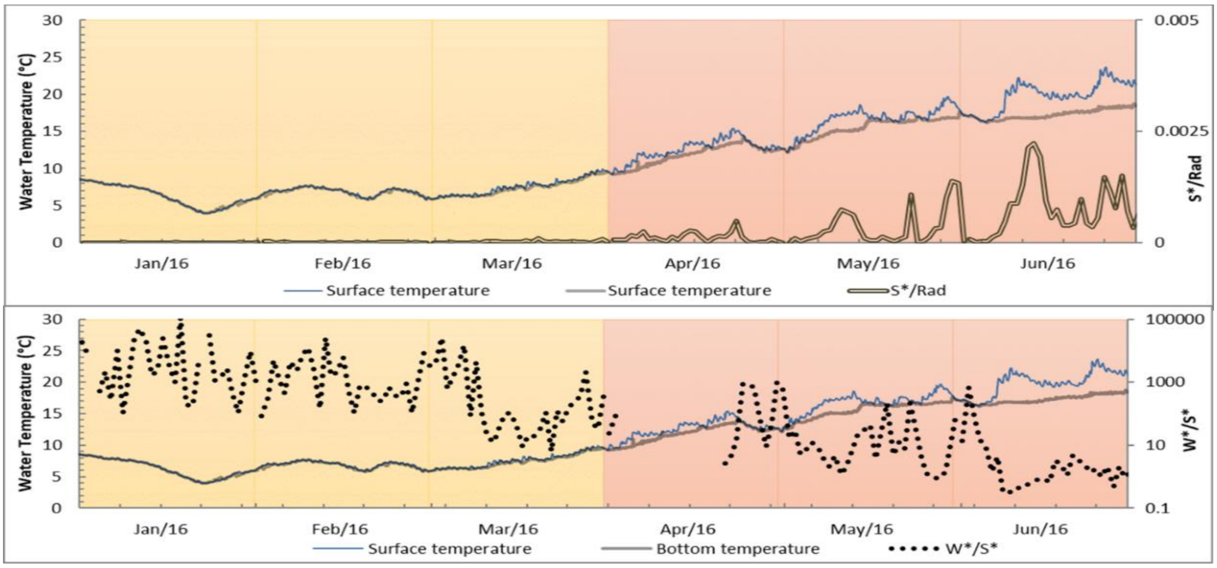


Source: Data from Soulignac, Viçon-Leite, et al (2017).

**Figure 31. Mixing and Stratification energy proxies related to water temperature for Billings lake**

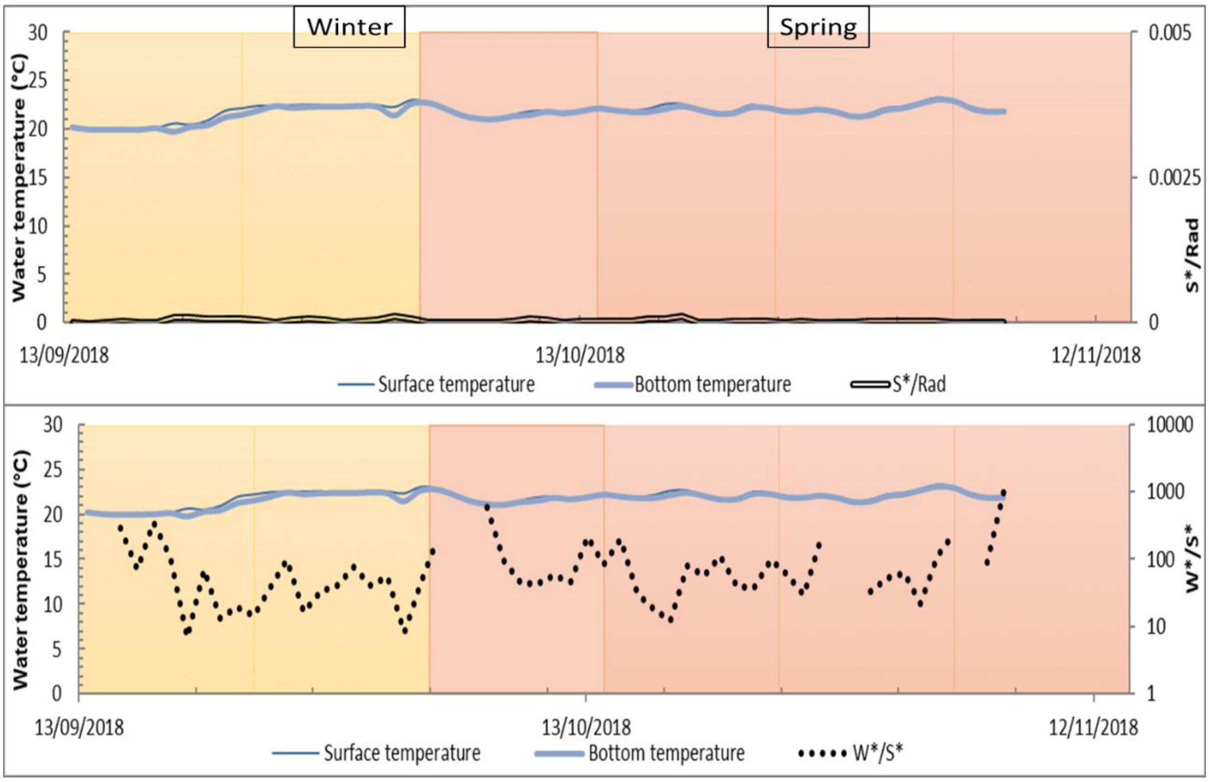


Source: Author.

**Figure 32. Mixing and Stratification energy proxies related to water temperature for Bourget lake**

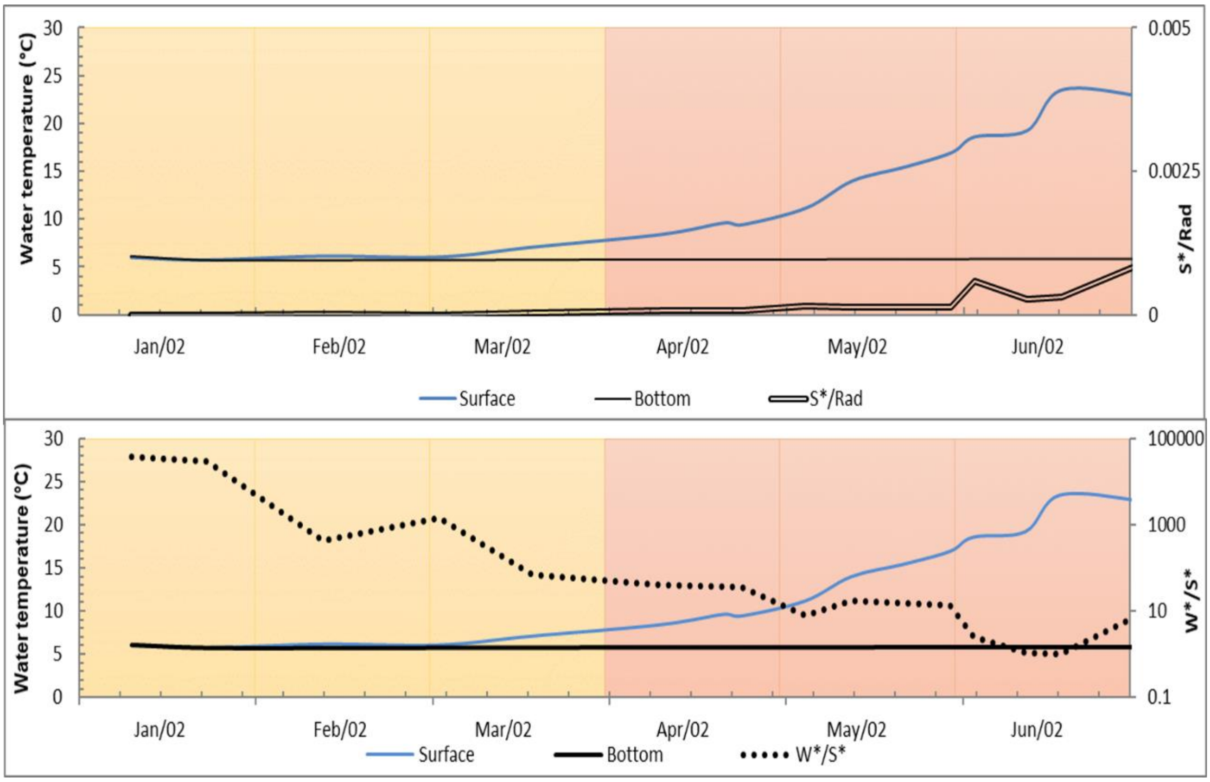


Source: Data from VIÇON-LEITE, et al., (2014).

The next step was to demonstrate the lakes' mixing regimes using only the proxies. Those results are shown from Figure 33 to Figure 36, comparing with the water temperature profile graph to facilitate the interpretation. Again, application of the proxies showed good efficacy in reflecting the mixing regime; if the maximum peaks of ***S*/Rad*** occur at the same time as the minimum peaks of ***W*/S****, the opposite is true.

This evaluation shows which atmospheric force is winning the energy balance and how the water column condition responds to each external alteration. In temperate lakes, the division is more abrupt with the changing of the season; as the weather starts to heat and incoming radiation increases, the proxies' lines invert and stratification begins.

**Figure 33. Mixing and Stratification energy proxies counterbalance evaluation for Hedberg lake**

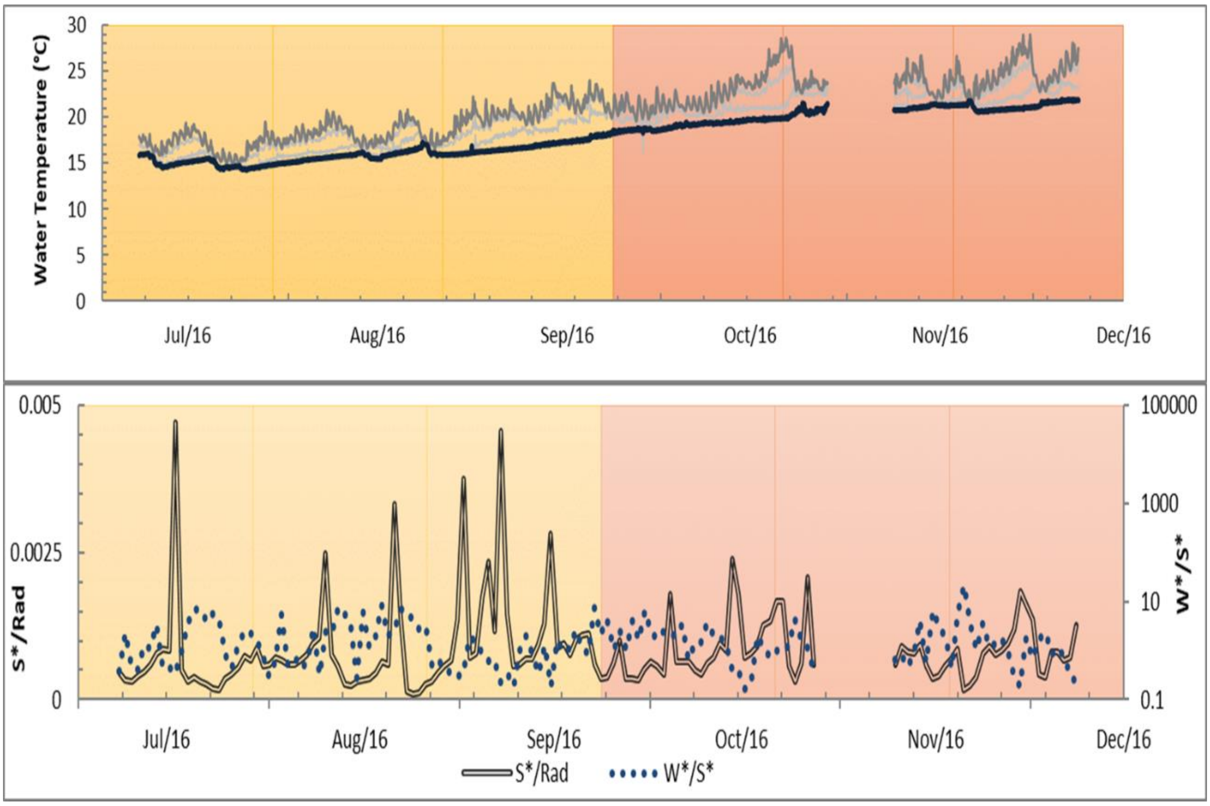


Source: Author.

**Figure 34. Mixing and Stratification energy proxies counterbalance evaluation for Crètèil lake**

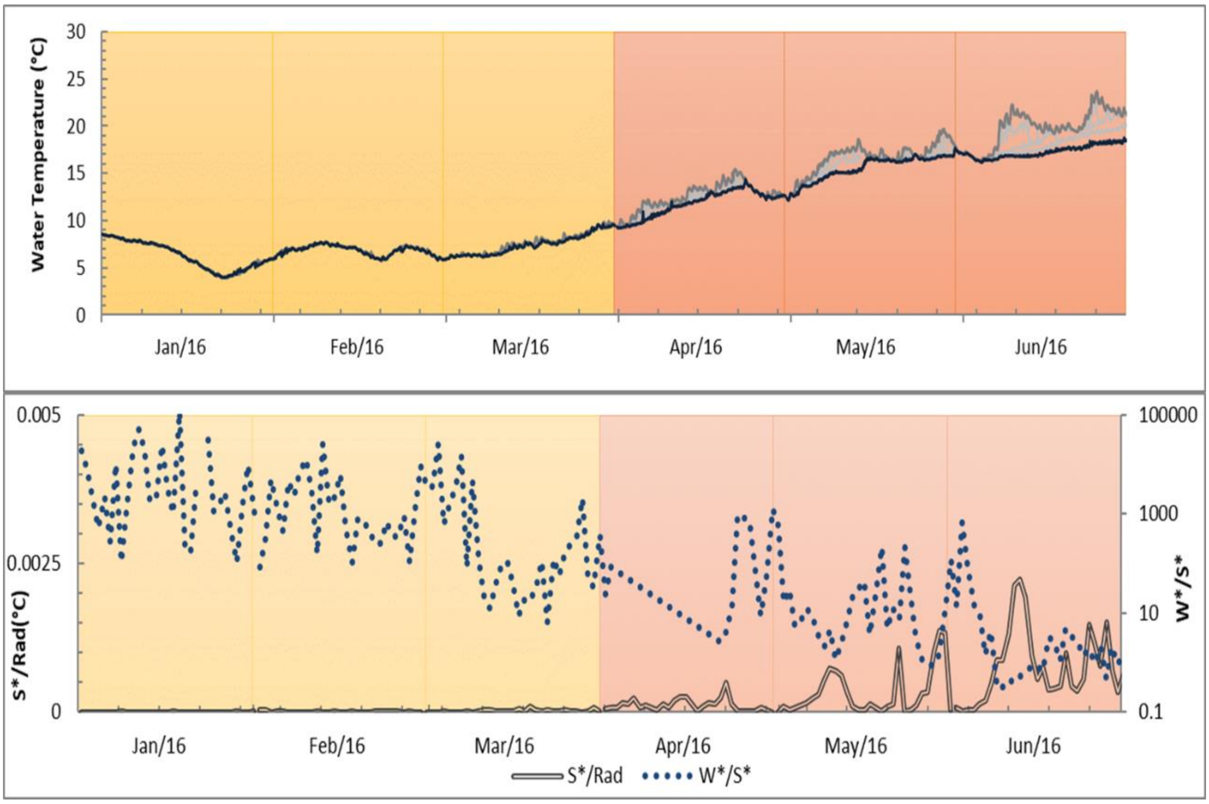


Source: Data from Soulignac, Viçon-Leite, et al (2017).

**Figure 35. Mixing and Stratification energy proxies counterbalance evaluation for Billings lake**

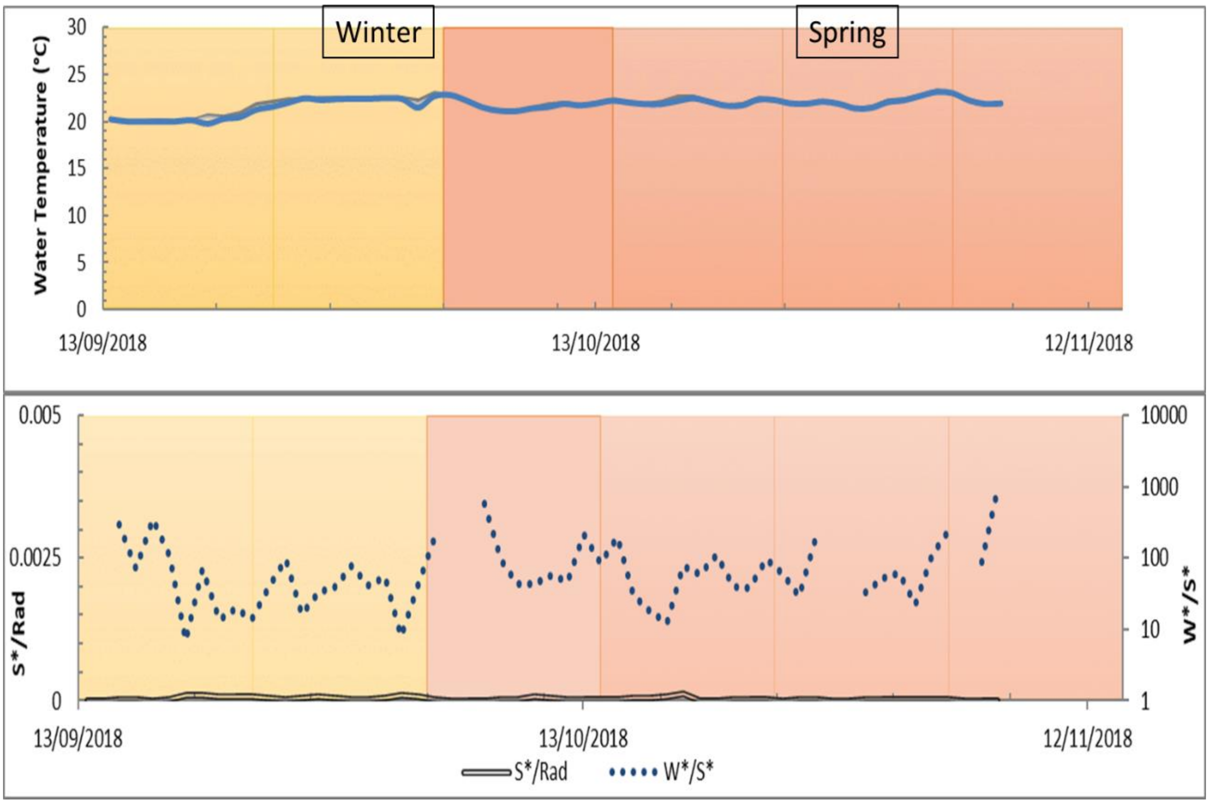


Source: Author.

**Figure 36. Mixing and Stratification energy proxies counterbalance evaluation for Bourget lake**

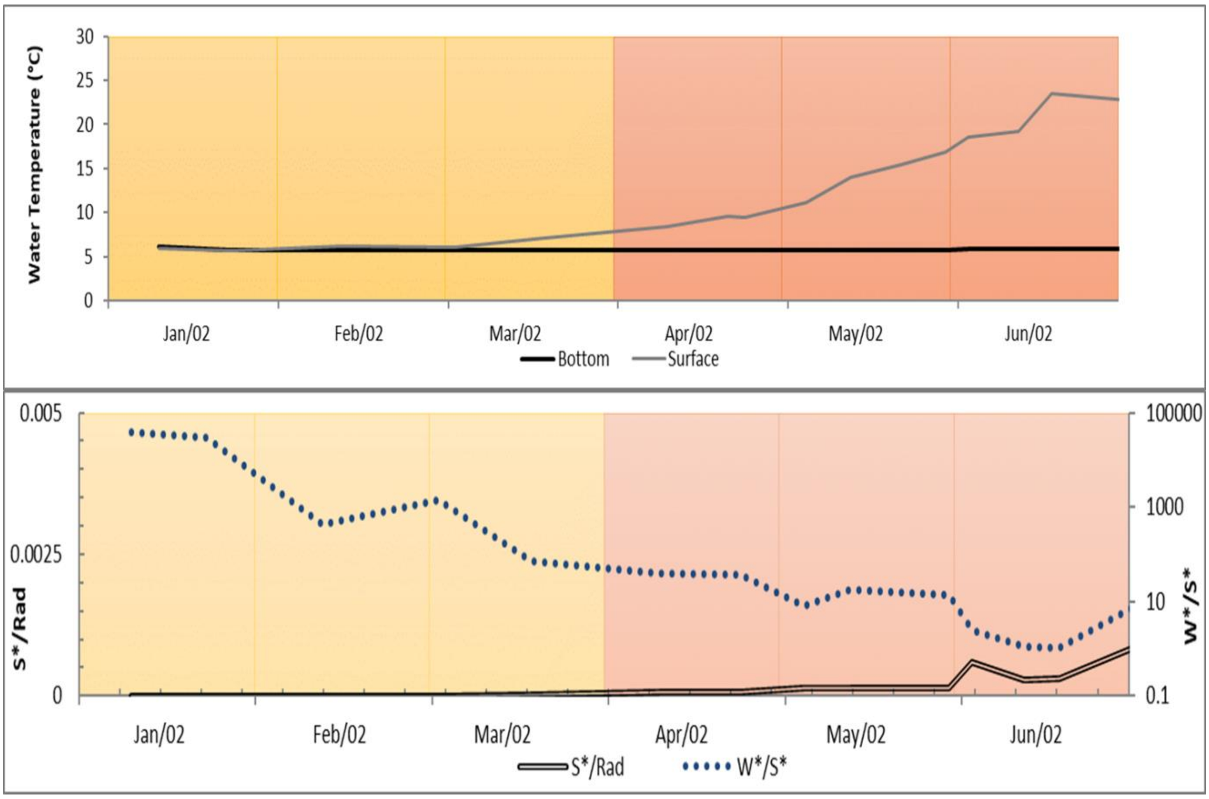


Source: Data from VIÇON-LEITE, et al., (2014).

### 3.4 Water Column Stratification Analysis

With the collected and analysed data of the four lakes, the thermal stability limit curve was established by plotting the stratification and mixing proxies against each other (Figure 37).

Analysing the curve, when the proxies are in a range between ***log*** **W*/S*** >-1.8 and ***log*** **S*/Rad** <-3.8, the wind stress energy is greater than the incident radiation and the water column becomes a mixed mass. On the other hand, when radiation is the force ruling the energy balance, the proxies have values between ***log*** **W*/S*** <-1.9 and ***log*** **S*/Rad** >-3.7, reflecting onset events. Thus, this function expresses water moments of column instability (onset and turnover), any values inside of the cloud represent events of thermal structure alterations. Points that are located far from the curve reflect a stable water column, being stratified (***log*** **W*/S*** <-1.9 and ***log*** **S*/Rad** >-3.7) or mixed (***log*** **W*/S*** >-1.8 and ***log*** **S*/Rad** <-3.8).

The thermal stability limit condition can be expressed by equation 34, with a correlation coefficient of 0.89, considering points in the 95% confidence interval (Figure 38). The application of this equation means that only with data from water temperature, wind speed, and radiation the limits of the thermal condition of any lake can be identified, enable the reservoir's operator to know which conditions can lead to stratification or mixing events.

One of the main gains of the application of this curve is the capacity to know, with fewer data and in a short period, the status of atmospheric forces which can turn the water column unstable. Another point is that the reservoir’s operators can prevent harmful episodes, as algal blooms, by using weather forecasts data. It is also relevant that the proposed proxies can be used to compare different lakes, once it’s dimensionless, unlike lakes’ indices described on the theory.

$$Log\ (S^*/_{Rad}) = -1.1885.\log\ (W^*/_{S^*}) - 6.5341 \qquad \text{(Eq.29)}$$

**Figure 37. Thermal stability limit curve with events’ classification**

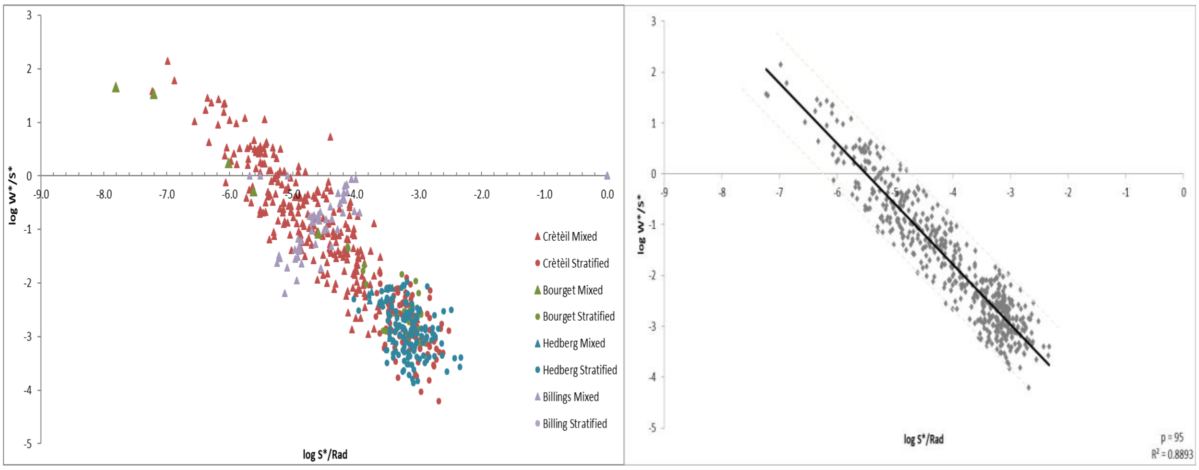


Source: Author; Data from VIÇON-LEITE, et al., (2014); Soulignac, Viçon-Leite, et al (2017).

**Figure 38. Thermal stability limit curve limit curve diagram with the position of areas that explains the water column thermal**

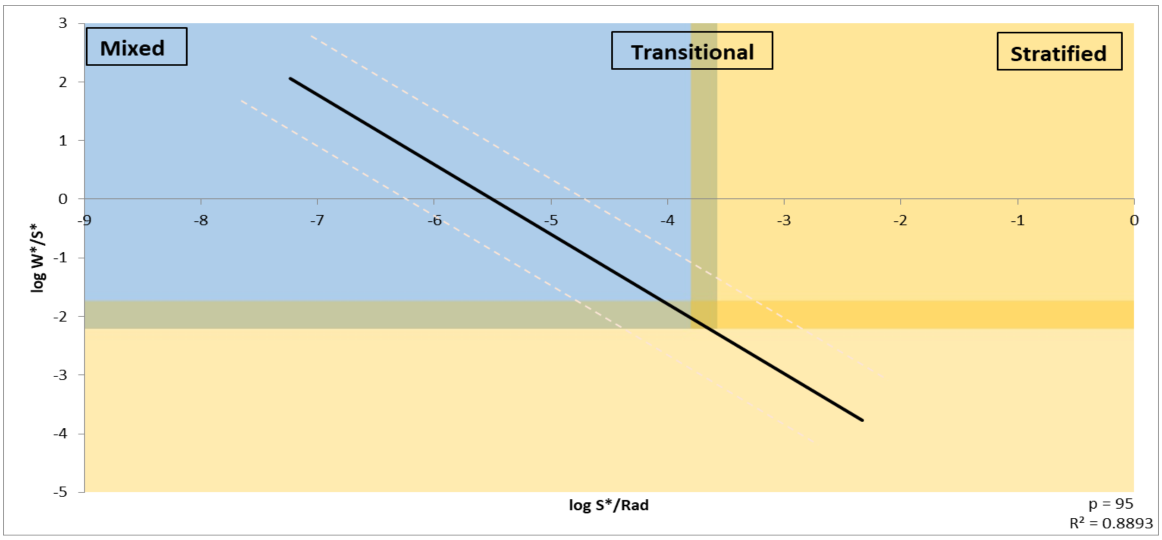


Source: Author.

## 3.5 Evaluation of Proxies performance

To better evaluate the proposed proxies' performance in represent lakes' mixing regime, the thermal condition of the lake was calculated for the complete time series available (2016 – Crètèil; 2002 – Bourget; jun to dec 2016 – Hedberg; sep to nov 2018 - Billings)of the four lakes, using data from wind speed, radiation, and water temperature profile. For the same period was calculated the Lake Number (LN) and the Wedderburn Number (W), using the Lake Analyzer tool and the suggested values (ROBERTSON e IMBERGER, 1994) for the wing drag coefficient (1.3 $10^{-3}$), and the results were compared.

The threshold of 1 was used for both Wedderburn and Lake number as an indication of the water column thermal condition, as described in the bibliography, being >1 tendency to a stratified lake and <1 mixed (ROBERTSON e IMBERGER, 1994) (READ, HAMILTON, *et al.*, 2011). From the graphics of Figure 39 its noticed that the LN and W respond to the alterations on the mixing regime, also that for the most of the lakes the value of 1 for threshold is relevant, although in the Bourget lake, the one with the most powerful stratification, it was not true.

Still on the graphs from Figure 39 is possible to visualize that the W values are almost always greater than the LN. The maximum values of those indices vary trough the lakes, and cannot be correlated with the size of them or used to compare them with each other, for example, the lake with the greatest LN value is Hedberg Lake (30,6389.8), while the Crètèil Lake, which is very similar to the Hedgerg Lake has a maximum value almost 100 times smaller, and the Bourget Lake, the deepest one and with the greater difference between the water temperature from the surface and the bottom, has a maximum value of 0.0004. This analysis shows the earlier commented inaccuracy of the 1treshold and the impossibility to compare the LN magnitudes values between lakes, in a way to determine which one has greater stability.

In the other hand, the proxies proposed in this article are very sensible to the alterations in the mixing regime and represent very well the lakes' thermal condition along the period. For example, in the Crètèil Lake between July and September the LN and W shows values of a mixed water column, while it's in the stratifications pics, along with August in the Hedberg Lake, both indices shows mixing events, while the proxies stay with values in the area of the stratification condition .

To corroborate with the graphics analysis a quantitative method was applied. Using a difference of 1°C between the surface and the bottom from the temperature profile field measurements to establish the actual lakes' thermal condition, the number of the mixed and stratified days were calculated. Also, with the indices, using the value of as 1 threshold, and the determined range ( stratified ***log*** **$W^*/S^*$** <-2.21 and ***log*** **$S^*$/Rad** >-3.81; mixed ***log*** **$W^*/S^*$** >-2.2 and ***log*** **$S^*$/Rad** <-3.8) for the proxies, the same numbers was calculated.

Table 3 shows the results of this analysis, confirming that the proposed proxies has a better performance to establish the water column thermal condition than LN and W. Can be noticed that the LN tends to maximize the numbers of mixed days, once that when the water column first layers mixes, this indices value drops, indicating a mixing event (Figure 39). Calculating the percentual error the proxies performance can show its consistency being always the index with a minor error, looking into the Crètèil Lake, which was the Lake that LN has the better performance, the proxies error was still lower (-7.73% for LN; 30.04 for W and 7.30 for proxies). In the stratification days, the LN better performance was in the Hedberg Lake, but the proxies had the same numbers (2.17% for LN; 5.80 % for W; 2.17 % for proxies).

**Table 3. Proxies performance analysis.**

| Lake | Calculated with Observed Data | | Calculated with LN | | Calculated with W | | Calculated with proxies | |
|---|---|---|---|---|---|---|---|---|
| Number of days in a year | Mixed | Stratified | Mixed | Stratified | Mixed | Stratified | Mixed | Stratified |
| Crètèil | 233 | 130 | 251 | 94 | 163 | 182 | 216 | 99 |
| Hedberg | 4 | 138 | 7 | 135 | 12 | 130 | 4 | 135 |
| Bourget | 4 | 26 | 30 | 0 | - | - | 4 | 26 |
| Billings | 47 | 0 | 47 | 0 | 47 | 0 | 47 | 0 |

**Differences between total measured days and calculated by the indices, are the days with the values stated in the transitional zone of classification, or were not measured.*

**Figure 39. Proxies performance evaluation.**

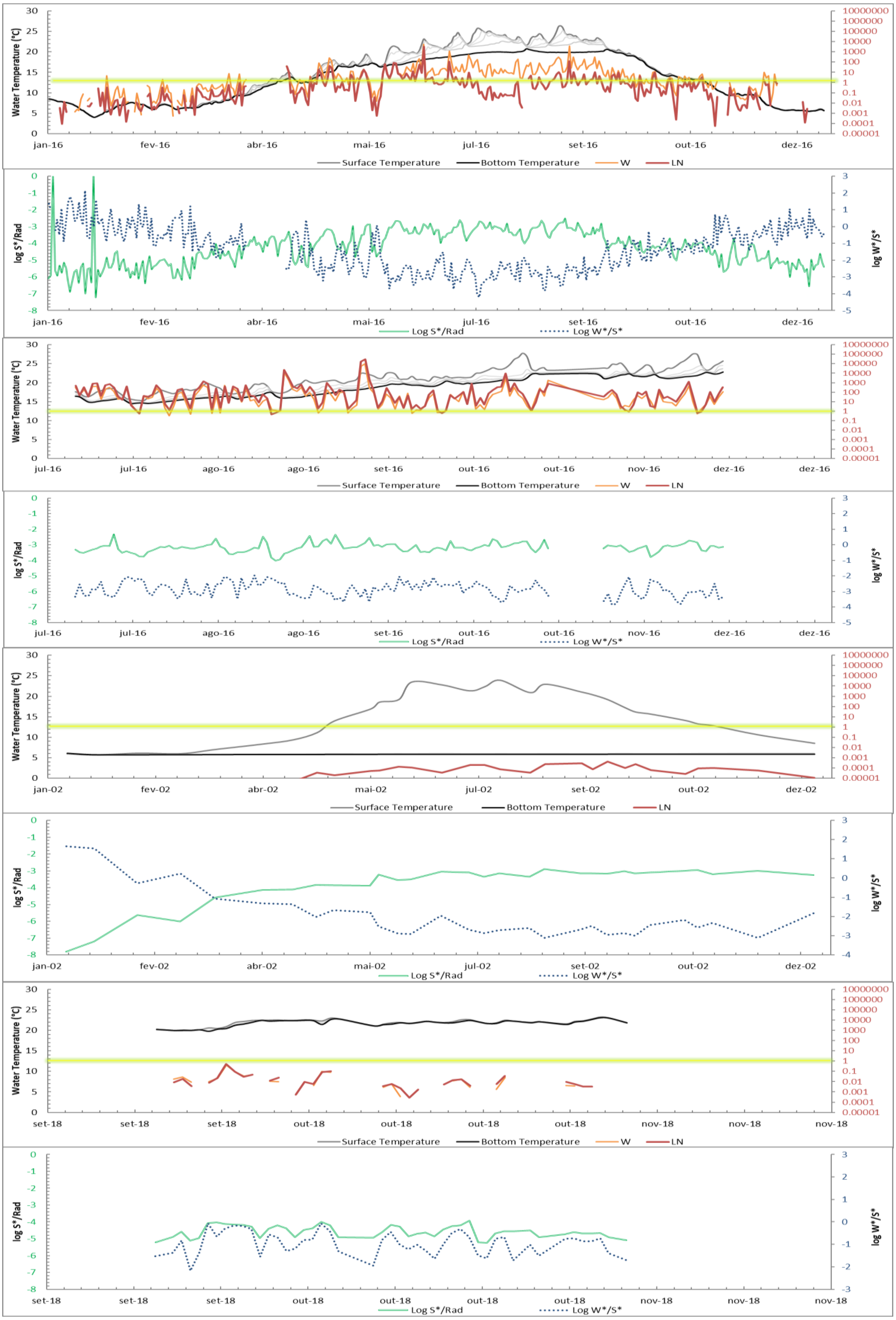

## 4. Conclusion

Aiming to improve the reservoirs management tools, this chapter established a correlation between atmospheric driving forces and the responses on the water mixing regime, represented by the thermal stability curve.

The water temperature and high-frequency monitoring of meteorological data makes possible to account the energies acting in the mixing regime balance and their characteristics on mixing and stratification events.

Boundary conditions, such as lakes' morphometry, the influence of in and outflow, the wind's fetch on the water surface, water turbidity and meteorological and climate conditions were all considered by the two non-dimensional proxies ($\boldsymbol{S^*/Rad}$ and $\boldsymbol{W^*/S^*}$) to represent the lake limit stability condition.

The thermal stability curve shows the ratio between mixing and stratifying energies at the ultimate condition directly from the observed wind and incident solar radiation, integrating all above-mentioned variables. The results are more effective than the other indices presented in literature and unite in the same scale lakes with different morphometry (depth and size) and different climate zones. Additionally, it demands few and easy data from monitoring, to forecast mixing or stratification events, once climate forecast data are applied.

The knowledge and ability to forecast these moments are very important in reservoirs' operation and water quality management. In reservoir operation planning by short-period analysis, it can be useful to prevent mixing events that lead to nutrients water column feedback by resuspension and subsequent algal bloom. In long-term studies, such as global climate change, it can be used in lake modelling research and to evaluate alterations in a lake's mixing regime limit.

From the above explained, it can be noted that the Thermal Stability Curve makes an important contribution to the field of limnology. The further study hopes to expand this correlation to even more lakes with different characteristics, such as morphometrics or specific hydrodynamic conditions.

# *CHAPTER III - Quasi-3D modelling as a Reservoir's Management Tool*

# 1. Methods and Materials

To test the second hypothesis and improve the knowledge of tropical lakes hydrodynamics behaviour, this work performed the steps of getting high-frequency monitoring data, lake representation in a quasi-3D model, including its calibration and validation, and the results accuracy evaluation. The specification of each phase is explained bellow.

## 1.1 Software of 3D Modelling

As explained earlier in Chapter I the software chosen for this research was the Delft3D, which has a set of modules covering a range of aspects, each module can be executed independently or in combination with other modules (DELTARES, 2014).

In this research, the modules used are FLOW and Water Quality. The first represents the lake's hydrodynamic while the second focuses on the ecosystem relationships evaluations. Both modules count with ways of introduce the initial and boundary conditions, physical, numerical and process parameters, the domain representation, time frame, external in/out discharges through an user interface.

## 1.2 Accuracy evaluation

The model's calibration and validation were made by comparing the modelled results with the field measures, especially the temperature profile. This comparison is the first indication that the model represents a hydrodynamic and water quality system. Traditionally, the correlation coefficient and standard error of estimate have been used to measure the efficiency of the model calibration. The most common indices to analyse time-dependent variables are the Mean Absolute Error – MAE (Eq.30); Nash Sutcliffe (Eq.31), Root Mean Square Error – RMSE (Eq.32) and Normalized Mean Absolute Error – NMAE (Eq.33) (CHAI e DRAXLER, 2014) (MCCUEN, KNIGHT e CUTTER, 2006).

$$MAE = \frac{1}{n}\sum_{i=1}^{n}|e_i| \qquad \text{(Eq.30)}$$

$$E_f = 1 - \frac{\sum^{n}(\hat{Y}_i - Y_i)^2}{\sum\ (Y_i - \bar{Y}_i)^2} \qquad \text{(Eq.31)}$$

$$RMSE = \sqrt{\frac{1}{n}\sum_{i=1}^{n} e_i^2} \qquad \text{(Eq.32)}$$

$$\mathrm{NMAE} = \frac{\sum_{i=1}^{n} |(\hat{Y}_i - Y_i)/Y_i|}{n} \qquad \text{(Eq.33)}$$

For above equations, n points to the sample size, $e$ is the error, $\hat{Y}_i$ is the predicted value of the criterion, $Y_i$ is the measured value of the criterion and $\bar{Y}_i$ is the mean of the measured values.

The root-mean-square error (RMSE) has been used as a standard statistical metric to measure model performance in meteorology, air quality, and climate research studies. Another useful and widely used coefficient in model evaluations is the MAE. The difference between them is that the MAE gives the same weight to all errors, while the RMSE penalizes variance, giving to errors with larger absolute values more weight than errors with smaller absolute values. When both metrics are calculated, the RMSE is never smaller than the MAE (CHAI e DRAXLER, 2014).

Researches about the use of metric indices conclude that RMSE is more appropriate to use than the MAE when model errors follow a normal distribution. The sensitivity of the RMSE to outliers is the most common concern, in practice; it might be justifiable to throw out the outliers that are several orders larger than the other samples, especially if the number of samples is limited. Finally, NMAE is normalized to the mean, enabling like comparisons between variables and is absolute so that under and over estimations do not cancel each other out (BRUCE, FRASSL, *et al.*, 2018).

An important aspect of the error metrics used for model evaluations is their capability to discriminate it among model results. The more discriminating measure that produces higher variations in its model performance metric among different sets of model results is often the more desirable. In this regard, the MAE might be affected by a large amount of average error values without adequately reflecting some large errors. Giving higher weighting to the unfavourable conditions, the RMSE usually is better at revealing model performance differences (CHAI e DRAXLER, 2014).

Recognizing the limitations of the correlation coefficients, Nash and Sutcliffe (1971) proposed an alternative goodness-of-fit index, which is often referred to as the efficiency index ($E_f$). The advantage of the Nash–Sutcliffe index is that it can be applied to a variety of model types, for linear models the efficiency index will lay in the interval from 0 to +1. For biased models, the efficiency index may actually be algebraically negative. Nonlinear models, which most hydrologic models are, negative efficiencies can result even when the model is unbiased (MCCUEN, KNIGHT e CUTTER, 2006).

As well as RMSE and MAE, Nash–Sutcliffe can be a useful index however, it can be sensitive to a number of factors, including sample size, outliers, magnitude bias, and time-offset bias. So it's better to use a combination of index to assess model (BRUCE, FRASSL, *et al.*, 2018) (CHAI e DRAXLER, 2014) (MCCUEN, KNIGHT e CUTTER, 2006).

## 2. Study Cases

From the four lakes of Chapter II, two were chosen to apply the mathematical model and test hypothesis #2. They differ much from each other, once that the first is a small and shallow lake, with a simple hydrodynamic, with only one point of input and other for output. While the second area is a larger reservoir, which has multiple uses, as well as many tributaries and unique hydraulic dynamics.

### 2.1 Hedberg lake

Hedberg lake is a result from a dam built in 1811 in the Ipanema River and was used to provided water for a small village and a steel and metallurgic industry. The old constructions and equipment, still present nowadays, are symbols of the colonial heritage in the area and the reservoir is still used as a water supply source, besides flow regulation, recreation, and landscape element. The former village and part of the catchment area are now part of Ipanema National Forest, as described in the previous chapter (Figure 40) (IBAMA, 2012).

The monitoring point is located at centre of the lake, with a mean depth of 4 m and the especifications of the monitoring system are described in the next item.

**Figure 40. The catchment from Hedberg lake**

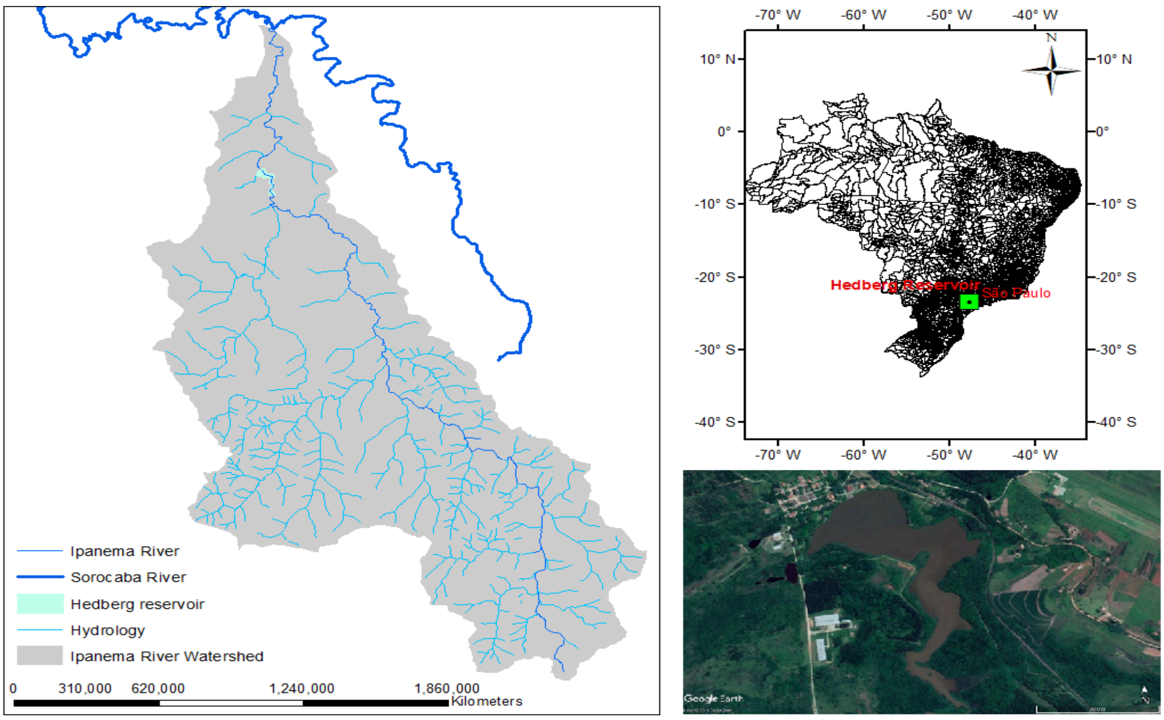


Source: Author.

## 2.2 Billings reservoir

Beyond the morphological characteristics described in the previous chapter, it is important to expose the context of the Billings reservoir formation. It was constructed in the first quarter of the 20th century to provide water for a hydropower plant, but some urban problems such as lack of available water to human supply and floods that became more common in the Tietê basin commanded changes in the original purposes. Aiming to minimize flood problems in 1928 Tietê river' waters started to be reverted to Billings reservoir, what compromise its water quality. With the lack of water due to population growth the reservoir started to be used as water supply. Nowadays it is divided in two parts: Pedreira and Rio Grande, the first one is used in flood control and the second to save water for the public distribution (FCTH, 2008).

The water quality and the preservation of the aquatic life in this basin suffer with the accelerated urbanization consequences, showing low values in water quality index. The investments in the management of wastewater were not enough for a long time, but now exist some programs trying to increase reservoir water quality, they are: Tietê Project Protection and Recuperation; Protection and Recuperation of valley bottoms; Clean River and the Remediation of Pinheiros River (CBH-AT, 2014).

In the search of a better use of the reservoir and the improvement of the water management several studies were realized, the first was the Construction Guide Lines in the 60's. In 1993 the Hidroplan consortium made a studied which the objective was to plan the water uses in a more widely form. Than the principal papers were the one from Jesus (JESUS, 2006) and Castro (2010), which focused in 3D and 2D mathematical modelling with monitoring data. The studied from Castro used an extensive monitoring realized between the years of 2007 to 2009 for the try-out of a prototype of a Pinheiros' River flotation system water, which are diverted for the Billings reservoir. Finally, Martins et All (2014) using the 3D modelling showed the correlation between the segregation and daily moisture and its potential effect in the nutrients' re-suspension.

In this study the monitoring point was located at begging of the reservoir (Figure 41), with a mean depth of 6 m and the monitoring system's especifications are described in the next item.

**Figure 41. Monitoring point in Billings reservoir**

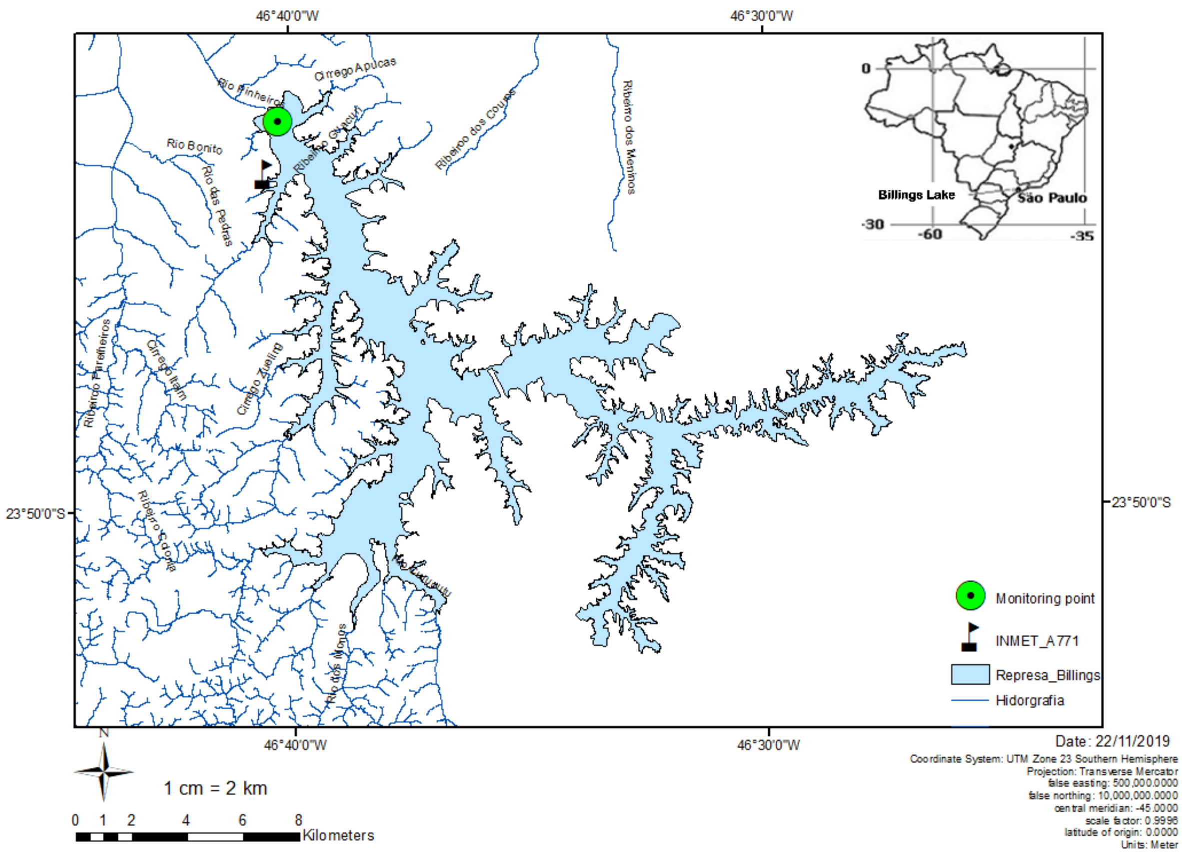


Source: Author.

## 2.3 The monitoring system

Good modelling results lie on good input data and to achieve this goal, a high-frequency monitoring system was built for both study areas. Besides the morphological data, required from the reservoirs' operator, there were four types of monitored data, being: Meteorological Data, Hydrodynamics Data, Water Quality Data, and Vertical Velocity Data. The following item explains how they were made and its specifications.

### *2.3.1 Meteorological data*

In Brazil the main source of the meteorological data is the INMET, their stations distributed across the country provide data from climate parameters. Both areas counted with an INMET meteorological station, in the Hedberg lake it was positioned 1km far from the lake, situated at private airport inside Flonas' area. For the Billings reservoir, the station is in one of its tributaries, close to the reservoir's begging (Figure 41).

The INMET automatic stations provided hourly data from many variables, but the ones used in the model input data were:

- Air Temperature;
- Humidity;
- Wind Speed and Direction;
- Radiation;
- Precipitation;
- Evaporation.

The monitoring system in Hedberg lake still counted with a meteorological station placed at the banks, installed to measure variables with a frequency greater than the INMET station. Air temperature, solar radiation, water level, wind's velocity and direction, atmospheric pressure, relative humidity, and precipitation were measured each 10 min. Solar radiation was taken in a 5 min interval to provide an accurate representation of incident energy.

To ensure the consistency of the measured data, they were compared with the data from the INMET station. Collected data showed good agreement and enabled the use of the station. The registers of the monitored data for the simulations period are showed in the Figure 42 and Figure 43.

**Figure 42. Meteorological data used as input on the Hedberg lake hydrodynamic model**

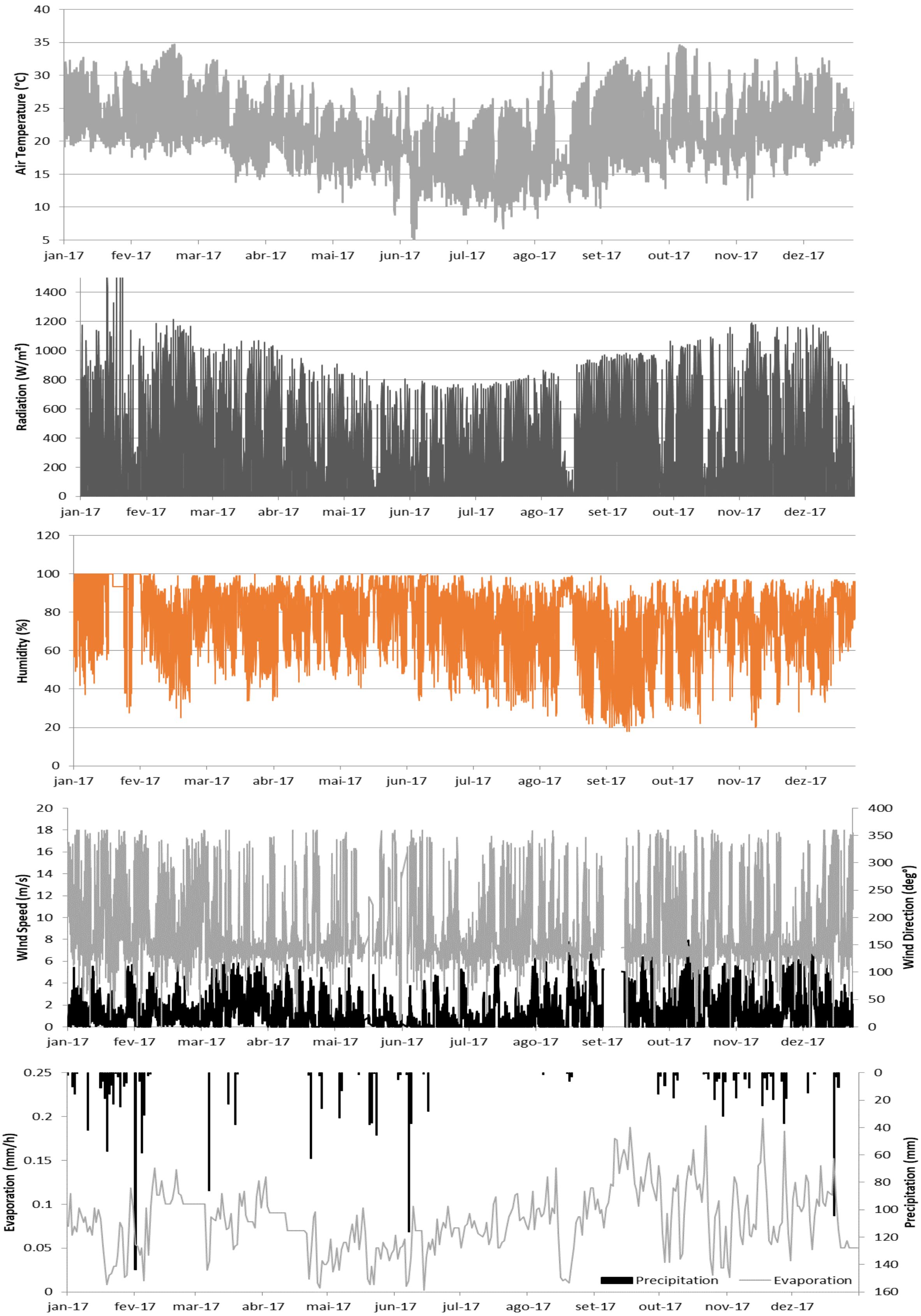


Source: Author.

**Figure 43. Meteorological data used as input on the Billings reservoir hydrodynamic model**

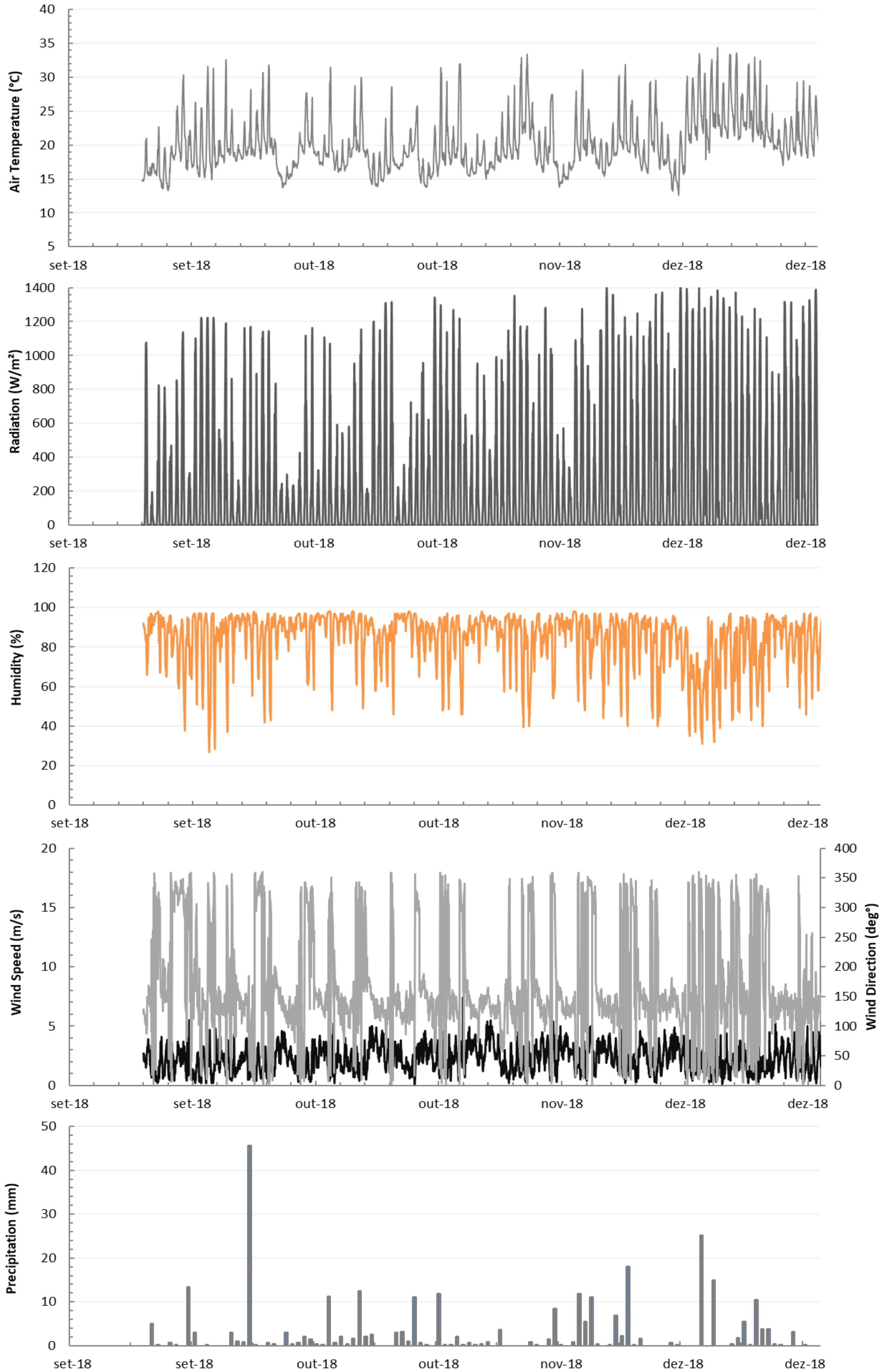


Source: Author.

### 2.3.2 Hydrodynamics

To characterize the hydrodynamic on the lakes the temperature profile was monitored, from a set of thermistors with a spacing of 1m between them. In the Hedberg lake, there were two monitoring points, one in the entry and the other in the lakes' deepest local, near to its centre (Figure 40). In the Billings reservoir, it was near to the Pedras Dam (begging of the reservoir - Figure 41), aiming to capture the influence of the pumping events.

The thermistors (4 to Hedberg lake and 5 to Billings reservoir) were fixed in a rope and a plummet with a float in the upper end (Figure 22). The time between measures was 1 min and the accuracy of the equipment is ±0.2°C. The Hedberg lake monitoring campaign was from April 2017 through September 2018, in Billings reservoir, it was from September 2018 through January 2019.

The collected shows that the Hedberg lake has a polymictic behaviour with several mixing events along the year, as well as the Billings reservoir, which stratifies and mix every day. The difference between the two environments is that the Hedberg lake can develop long stratified periods, with months without a mixing event (Feb - Apr Figure 44), while in Billings reservoir there’s a trend to the water column mixing (Sept – Nov Figure 45).

Based on the field experience, this is a consequence of the wind influence, which is greater in the Billings reservoir. Another factor that contributes to the reservoir mixing is the pumping events, as can be seen in Figure 46. From September through November, there were many pumping records, keeping the water column almost ever mixed. One event at the begging of December demonstrates its influence on the reservoir’ hydrodynamics, breaking the stratification.

**Figure 44. Data of the temperature profile monitored in Hedberg lake**

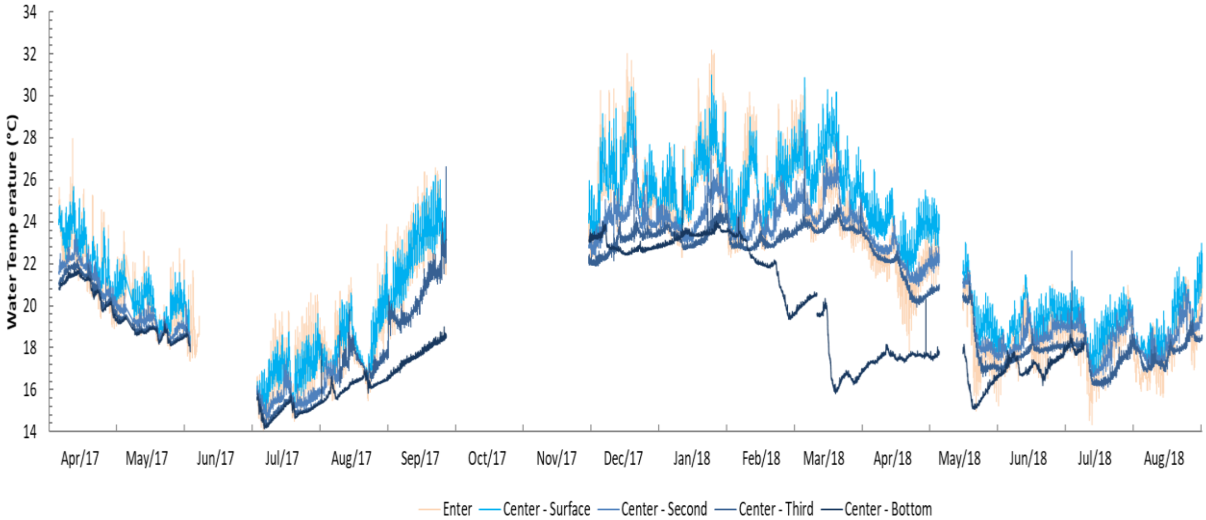


Source: Author.

**Figure 45. Data of the temperature profile monitored in Billings reservoir**

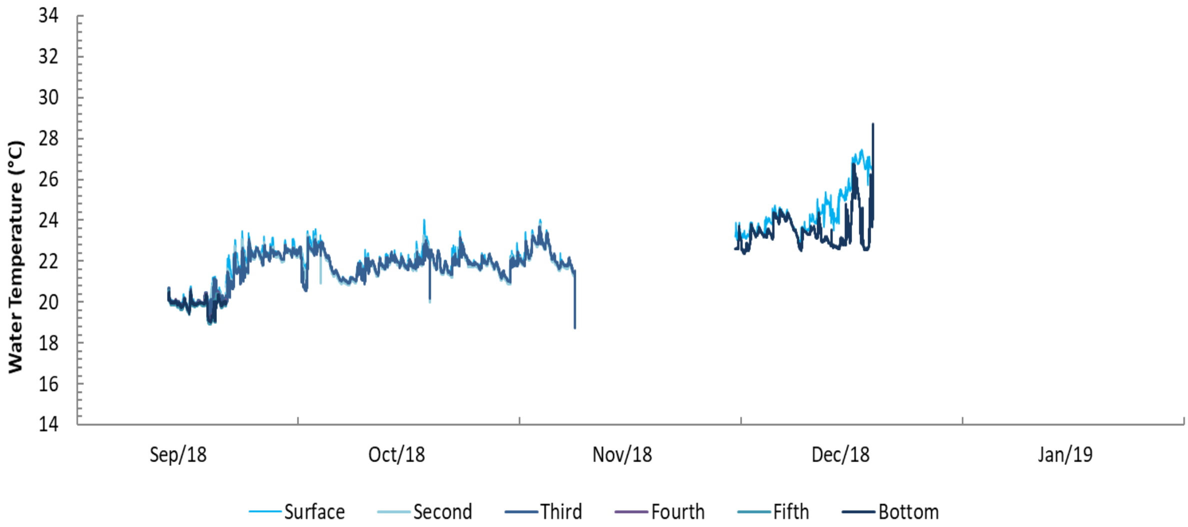


Source: Author.

**Figure 46. Data on the temperature profile monitored in Billings reservoir, along with the pumped flow**

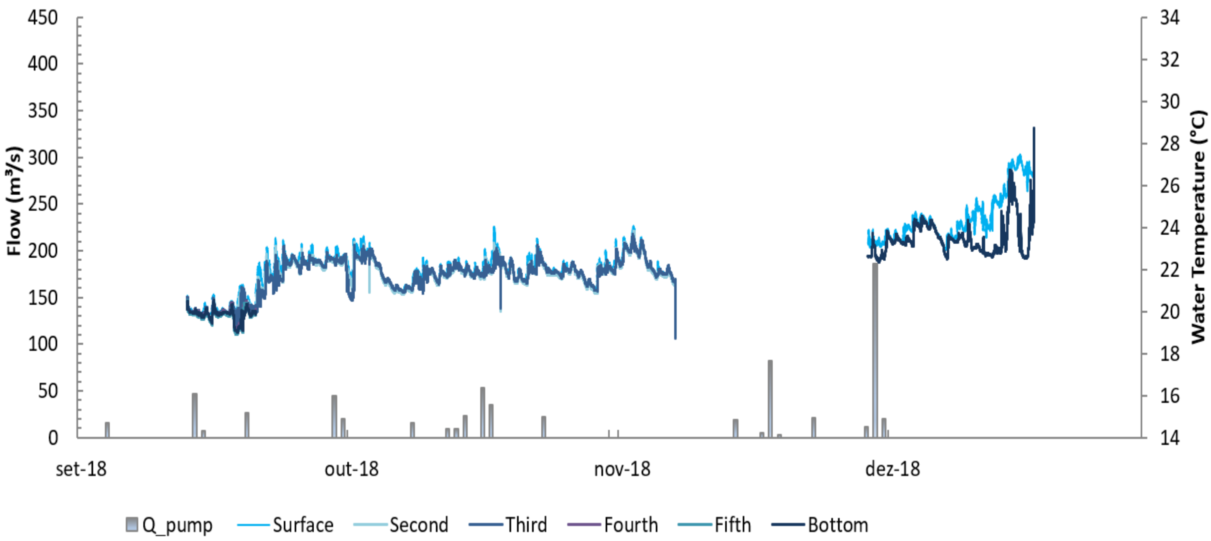


Source: Author.

### 2.3.3 Water Quality

The water quality monitoring counted with data from different variables to characterize nutrients, algal biomass, organic matter and gases in the study areas. The choose of the indicators considered the capacities of the university's laboratory and the data available on the government reports. The used variables were:

- Dissolved Oxygen;
- Biogeochemical Organic Matter;
- Nitrate;
- Nitrite
- Ammonia;
- Total Phosphorus;
- Soluble phosphorus
- Chlorophyll-a;
- Secchi depth.

The samples were collected at the same point in which the temperature profile was measured. The graphs from Figure 47 and Figure 48 reflects the indicators state along the monitored period and its accordance with the legislation (CONAMA, 2005). Both areas have problems with an excess Phosphorus, which associated with light penetration and Nitrogen forms available across the water column, facilitate the production of algal biomass.

Usually, a Phosphorus’ peak corresponds to a peak of Chlorophyll–a, like happen from May 2018 in Hedberg lake and from September through October 2018 in Billings reservoir. In the Billings reservoir, the situation is worrying, once the biomass stays almost the whole period above legal limits. This situation is not desirable for a water supply source and was also possible to observe in the field campaigns as illustrated in Figure 49.

Hedberg lake does not show problems with the other variables, under the legislation. Meanwhile, Billings reservoir has a serious problem with ammonia at the begging of the monitoring (Sep-Oct), but after this period the values come back to the normal range.

**Figure 47. Water Quality Data monitored in Hedberg lake.**

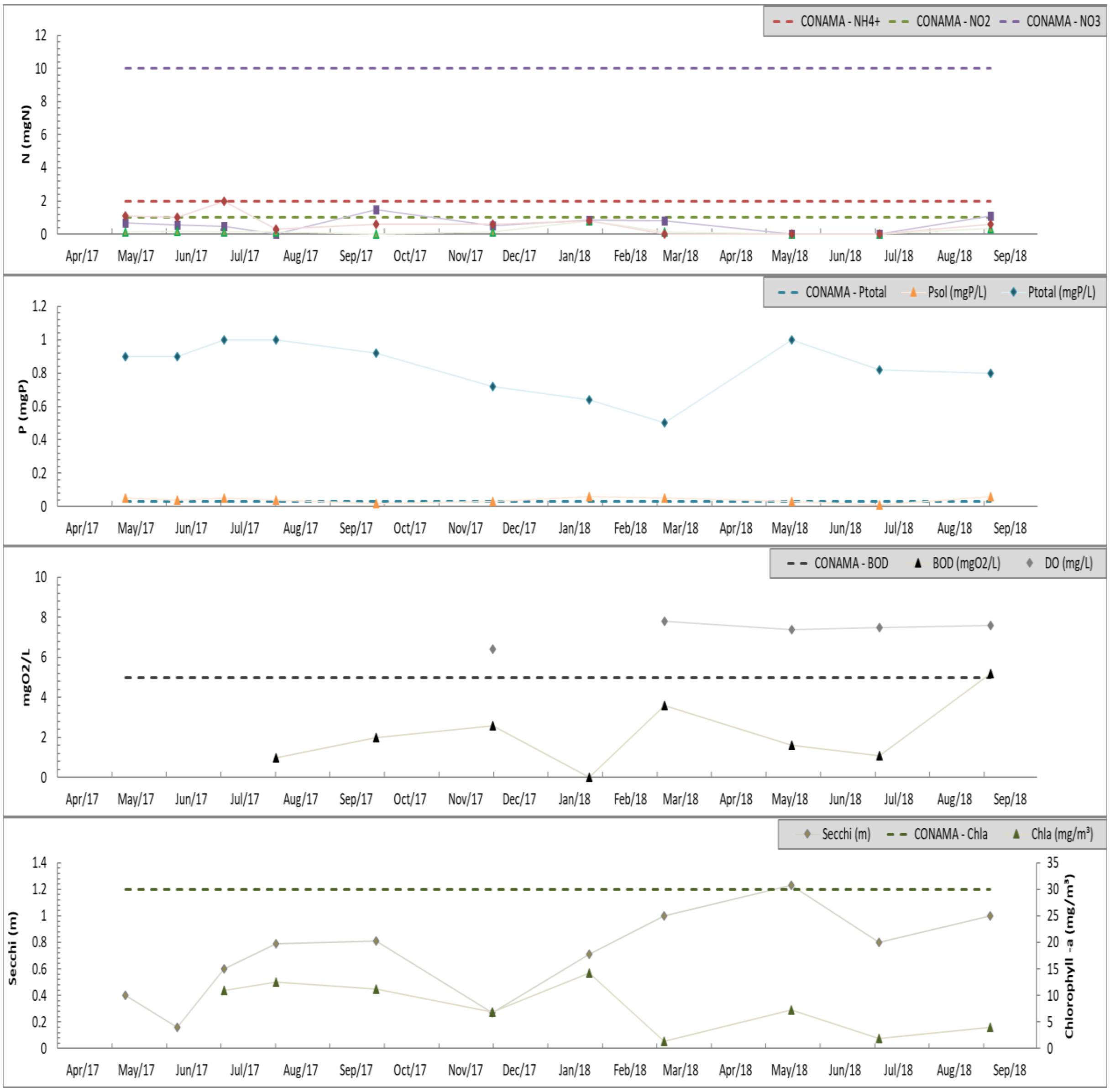


Source: Author.

**Figure 48. Water Quality Data monitored in Billings reservoir. For this area were used the CETESB data for Dissolved Oxygen and Biogeochemical Organic Matter**

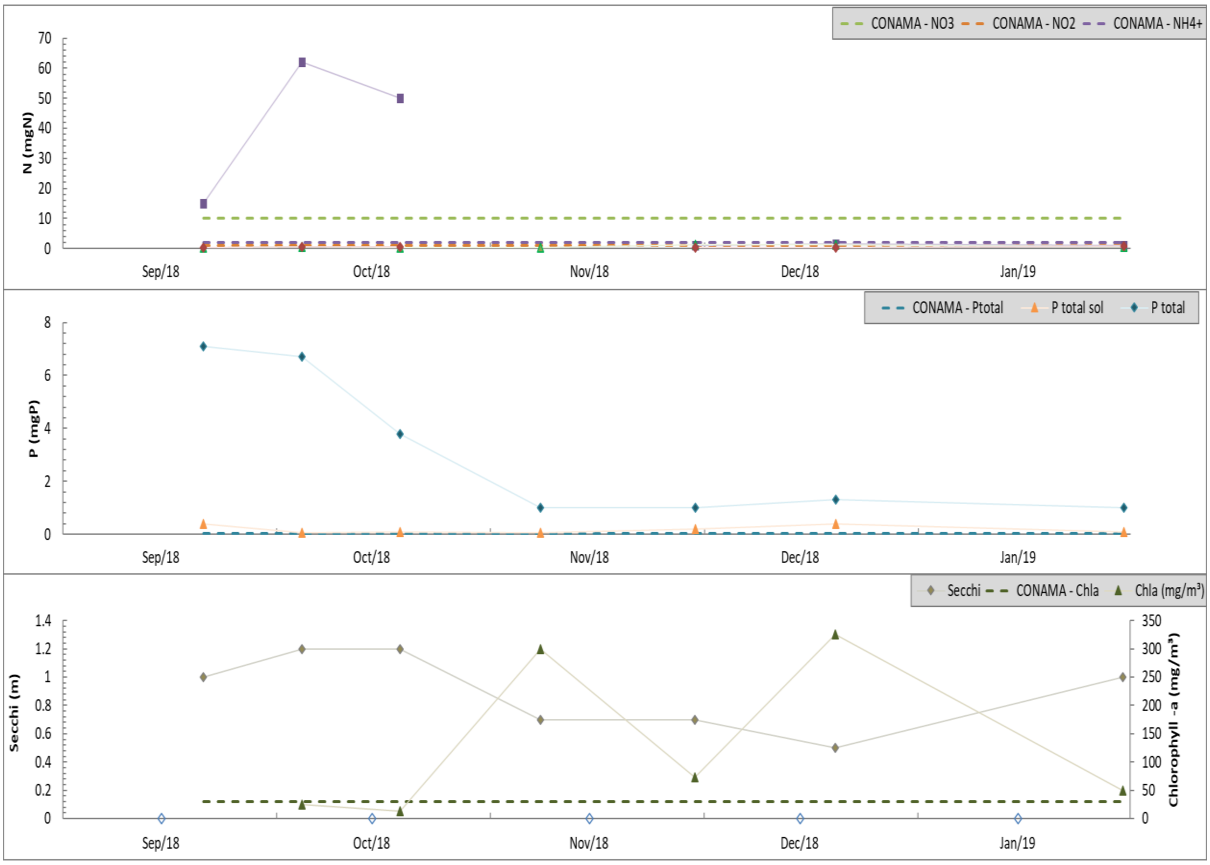


Source: Author.

**Figure 49. Register of algal biomass in Billings reservoir during October and November campaigns**


Source: Author.

### *2.3.4 Measuring vertical velocity*

The vertical velocity and its capacity to re-suspend bed material were studied by a monitoring system applied to the intervenient variables. A sensor was developed to prove this process existence, with the support of the CTH’s engineers.

It is an optical sensor that detects the relative turbidity on the water, based on the particles’ reflectance. It sends a light beam that reads the water clarity between measures interval (1min), according to the particles’ reflection. The optical sensor is composed of four luminosity sensors, positioned in 90° between each other in a dark structure, which stays near to the lake’s bottom (0.5 m).

Associated with the optical sensor are other equipment to acquire and store the measured data. The system (Figure 50) count with a solar panel, which is the energy supply, combined with the charge and current controller, and with the electronic components, which are responsible to manage the collected data, storing them in an SD card.

Measurements campaigns were performed from July through August 2018, for Hedberg lake and from 05 through 10 in October 2018 and from December 20’ through 10 in January for Billings reservoir. Figure 51 and Figure 52 expose the relative turbidity and climate variables data. It is important to highlight the turbidity's fluctuations, which are the ones that indicate particles move across the water column. The greater fluctuations occur associated with radiation reduction and the increase of precipitation and wind speed.

**Figure 50. Turbidity sensor**

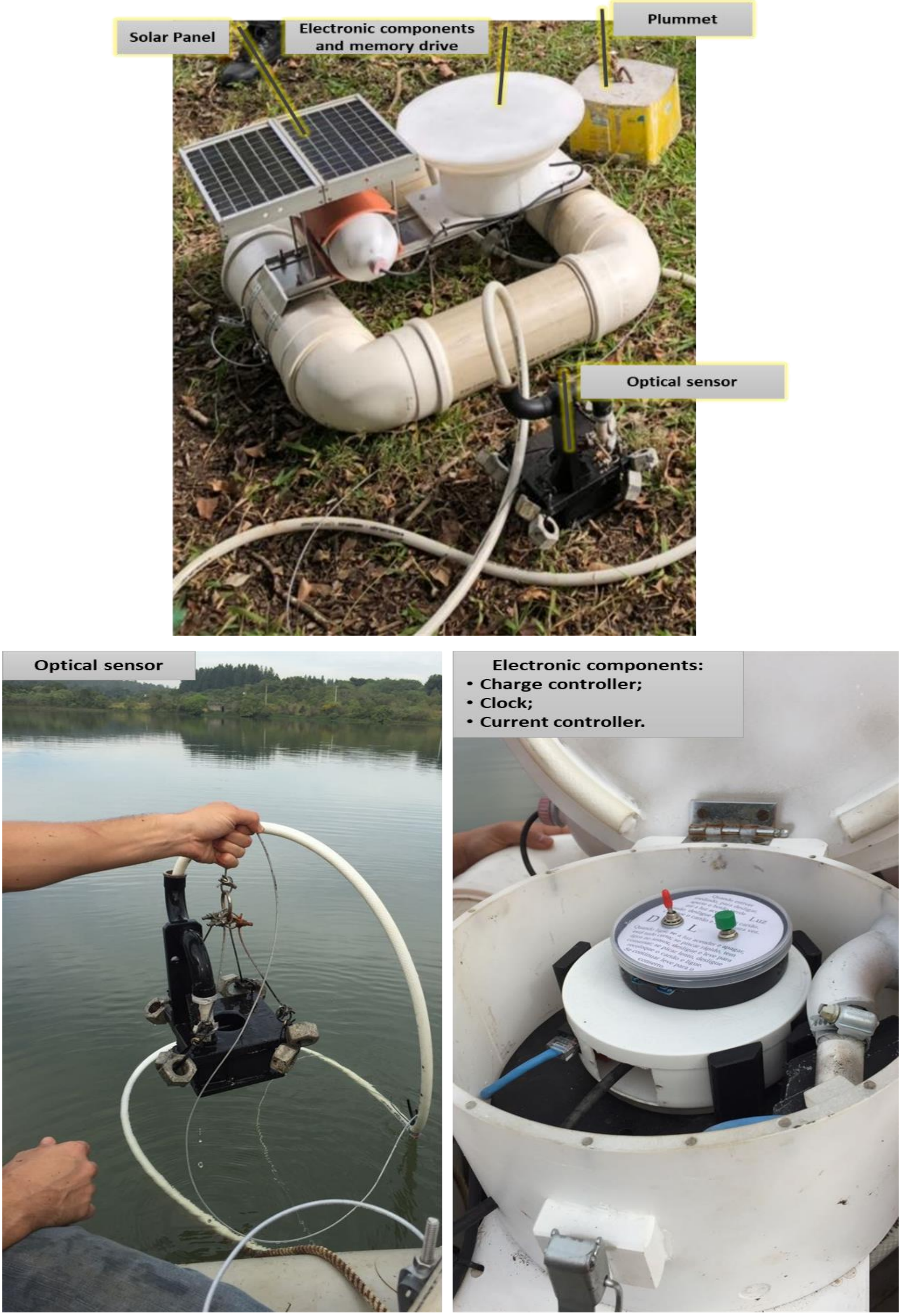


Source: Author.

**Figure 51. Data from relative turbidity and climate variables measured in Hedberg lake.**

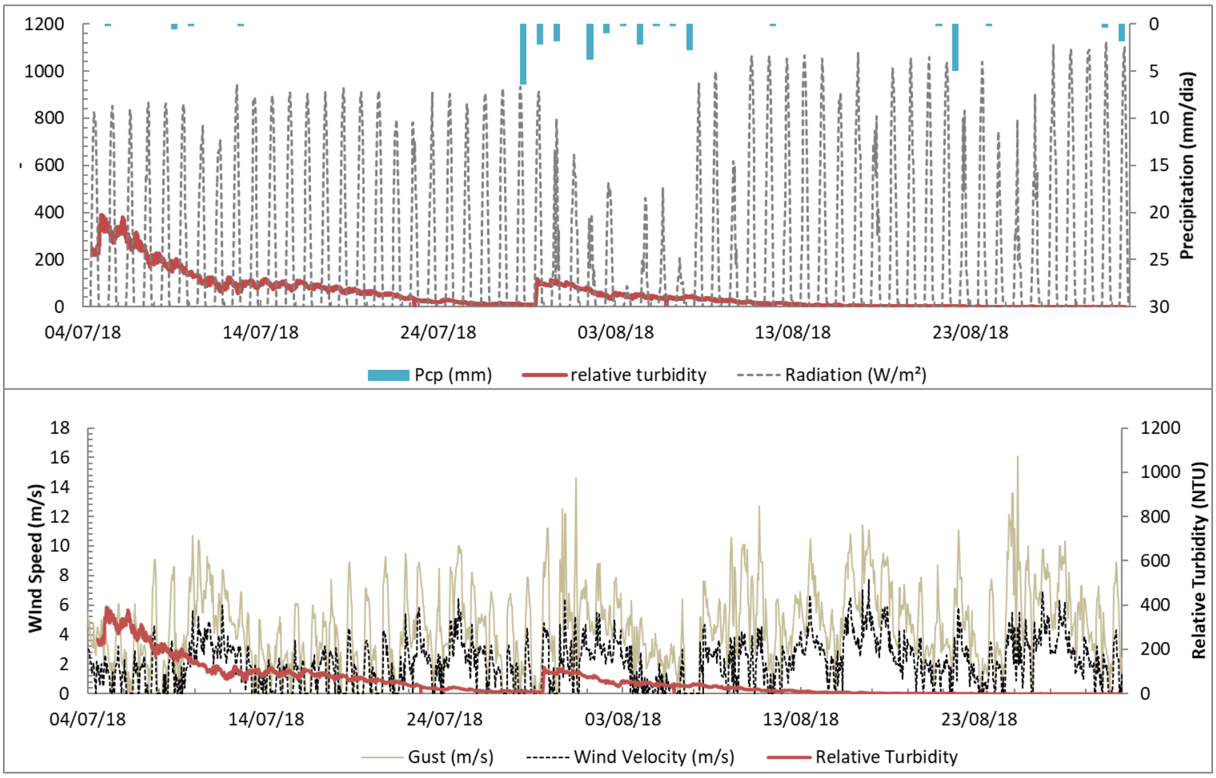


Source: Author.

**Figure 52. Data from relative turbidity and climate variables measured in Billings reservoir**

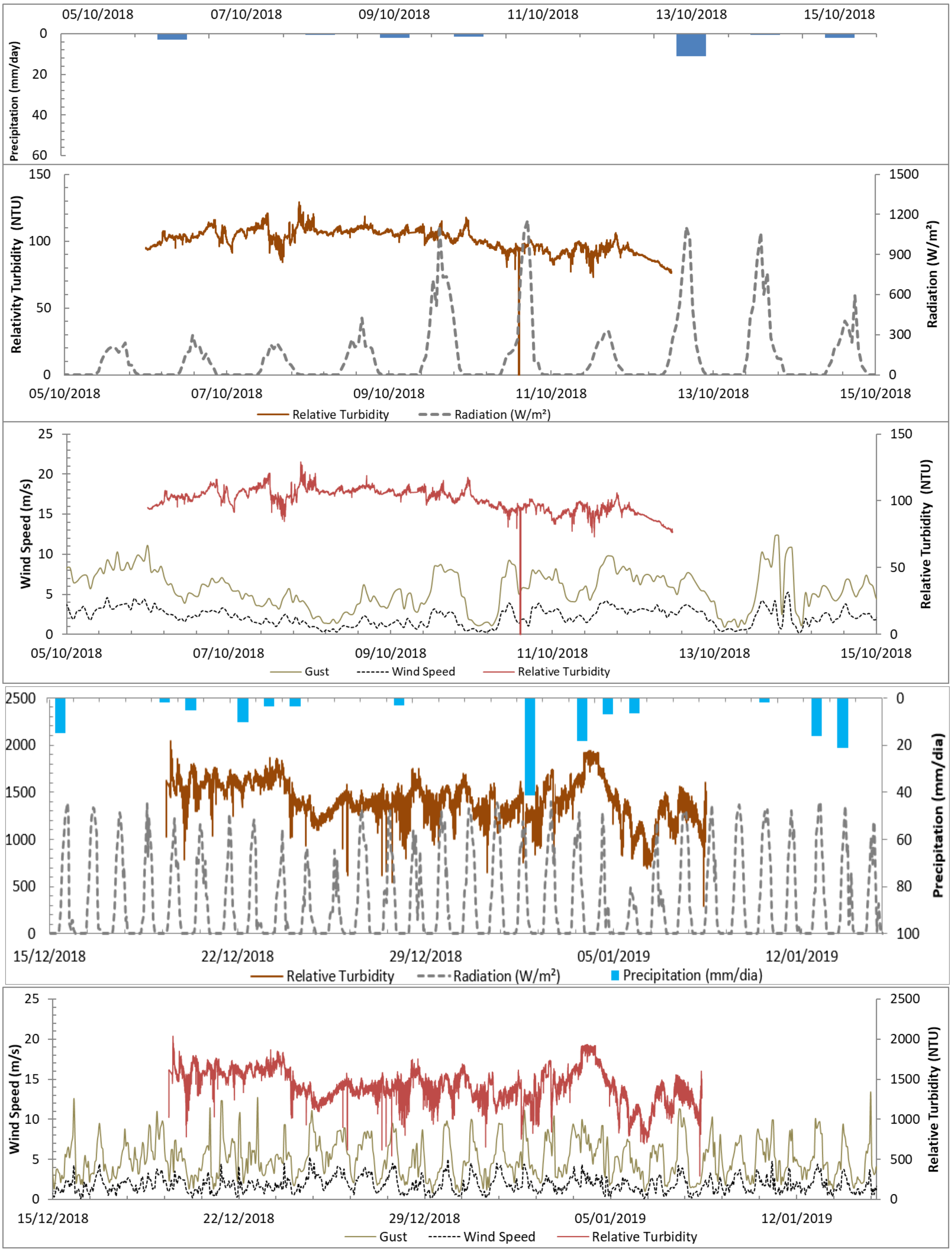


Source: Author.

# 3. Results and Discussions

## 3.1 Hedberg lake

### *3.1.1 Hydrodynamic Modelling*

The first step into the hydrodynamics representation in a mathematical model is to build the calculations grid. This net discretizes the study area so the model can perform the simulation based on finite differences. In the Hedberg lake case, an orthogonal grid with 13-meter cells was used to represent the spatial variations in the surface area, while the water column was described in 30 layers, with 0.2 m of thickness, in the z-model.

The boundary conditions were defined using the collected data. Physical and hydraulic parameters used were the lake's bathymetry, upstream input, and the spillway rating curve. In the heat model variables such as the radiation, wind's direction and velocity, air temperature, precipitation, humidity, and evaporation were used as models' driving forces. Those data were collected from the local and nearby weather stations, as explained in the Monitoring System section. The available variables and previous experiences (SOULIGNAC, VIÇON-LEITE, *et al.*, 2017), justified the chosen of Ocean as the heat model on the Delft3D.

The hydrodynamic model was calibrated and verified through the comparison of water temperature measured and simulated values. The period chosen for the calibration was from July - 07 until August - 19, and for the validation was September - 27 to October - 27 both from 2016.

Parameters must be set up in the model's calibration to adjust the simulated process to the local characteristics (Table 4). The graphics in Figure 53 represents simulation results compared to field measurements. As can be seen, the stratification and mixing events are simulated with consistency, as well as the oscillations in surface and bottom temperature, and the gradient between them.

The accuracy of the model was evaluated by applying the indices described in the previous chapter (Table 2). The evaluation showed good agreement between field measures and simulated results when compared with literature values, for example, a study that modelled 34 lakes has an NMAE mean of 0.11, a maximum of 0.25 and a minimum of 0.04 [1].

This elevated level of trustful is only possible because of the quality reached in the input data, which is an example of how the model trustful results depend on input data. The statistic evaluation results are an effect of the improvement in the input data with the high-frequency monitoring.

**Table 4. Parameters used in the calibration of the hydrodynamic model**

| *Parameters* | *Value* | *Parameters* | *Value* |
|---|---|---|---|
| Wind stress - Cd | 0.0001 [m $s^{-1}$] | Dalton number | 0.003 |
| Vertical Eddy Viscosity - VEV | 0 [m $s^{-1}$] | Stanton number | 0.007 |
| Vertical Eddy Diffusivity - VED | 0 [m $s^{-1}$] | | |
| Horizontal Eddy Viscosity - HEV | 0.1 [m $s^{-1}$] | Secchi Depth | 0.7 m |
| Horizontal Eddy Diffusivity - HED | 0.001 [m $s^{-1}$] | Manning | 0.02 |
| Cloud cover | 0% | Evaporation rate | given |

Source: Author.

**Figure 53. Graphs comparing field and model measures, in which (A) is calibration and (B) is validation**

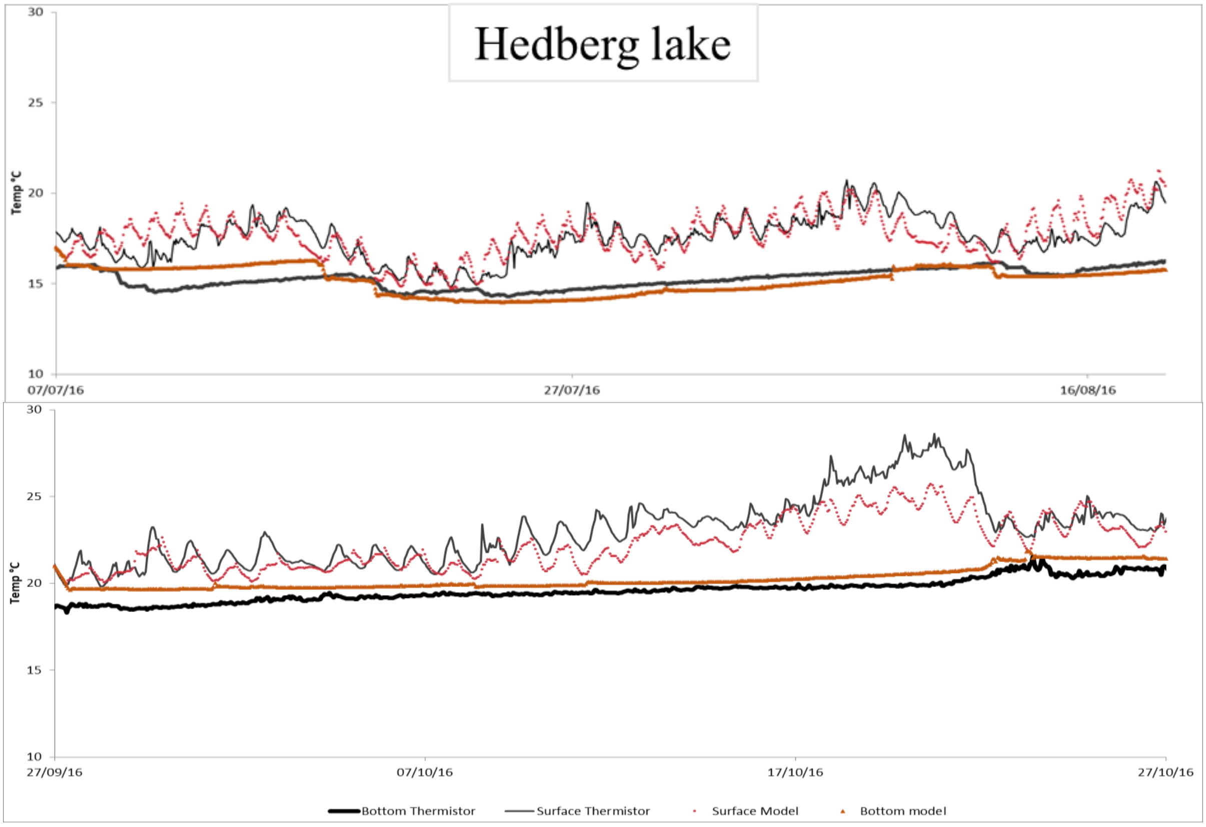


Source: Author.

**Table 5. Calibration and validation statistical indices founded for the simulations**

| Calibration indices | | Validation indices | |
|---|---|---|---|
| **MAE** | 0,07 bottom | **MAE** | 0,02 bottom |
| | 0,08 surface | | 0,34 surface |
| **Nash Sutcliffe** | 0,42 bottom | **Nash Sutcliffe** | 0,29 bottom |
| | 0,39 surface | | 0,62 surface |
| **RMSE** | 0,6 bottom | **RMSE** | 0,43 bottom |
| | 0,85 surface | | 0,86 surface |
| **NMAE** | 0.0044 bottom | **NMAE** | 0.28 bottom |
| | 0.0057 surface | | 0.32 surface |

Source: Author.

After the calibration and validation, was performed a simulation of an extended period (Apr – Set 2017), which includes drought (July and August) and flood events (May and June). The hydrodynamic behaviour (Figure 54) confirm the reservoir polymictic bias with several stratifications and mix events along the semester. On the warm periods, the stratification events have a higher amplitude between the epilimnion and hypolimnion layers, reaching almost 10 °C, while in the winter the difference stays close to 5°C.

This result shows how the external variables influence on the lake hydrodynamic behaviour. The balance between solar radiation and the wind energy commands the thermal stability of the lake, determining if it is stratified or mixed.

The external variables assessment demonstrates that the predominant wind direction is the same as the lake flow, which increases its influence. The combination of the decreasing radiation with the increasing wind velocity, raises the possibility of mixing events.

Hedberg lake has a polymictic characteristic, which means several mixing events throughout the year, and the model was successful in representing it. Because of its effects on the lake's thermal behaviour and consequently in its water quality, with a good simulation of the hydrodynamic behaviour was possible to implement the ecological module.

One example of this influence is demonstrated in Figure 55, with the temperature and density profile in a stratified and a mix situation. A stratified condition means separated layers across the water column, where the warm and so lighter water stays upper of the colder and heavier bottom layer, avoiding exchanges between them.

In the exposed example, a stratified condition implicates in a proximally 3.3°C and 1.3 kg m-³ difference between the lake's bottom and surface. On the other hand, the mixing event is characterized by having a minimum difference across the water column, with no layer segregation. This dynamic has a serious impact on water quality and was simulated in sequence.

**Figure 54. Temperature profile and water level results from the quasi-3D simulation of six months (April-September 2017)**

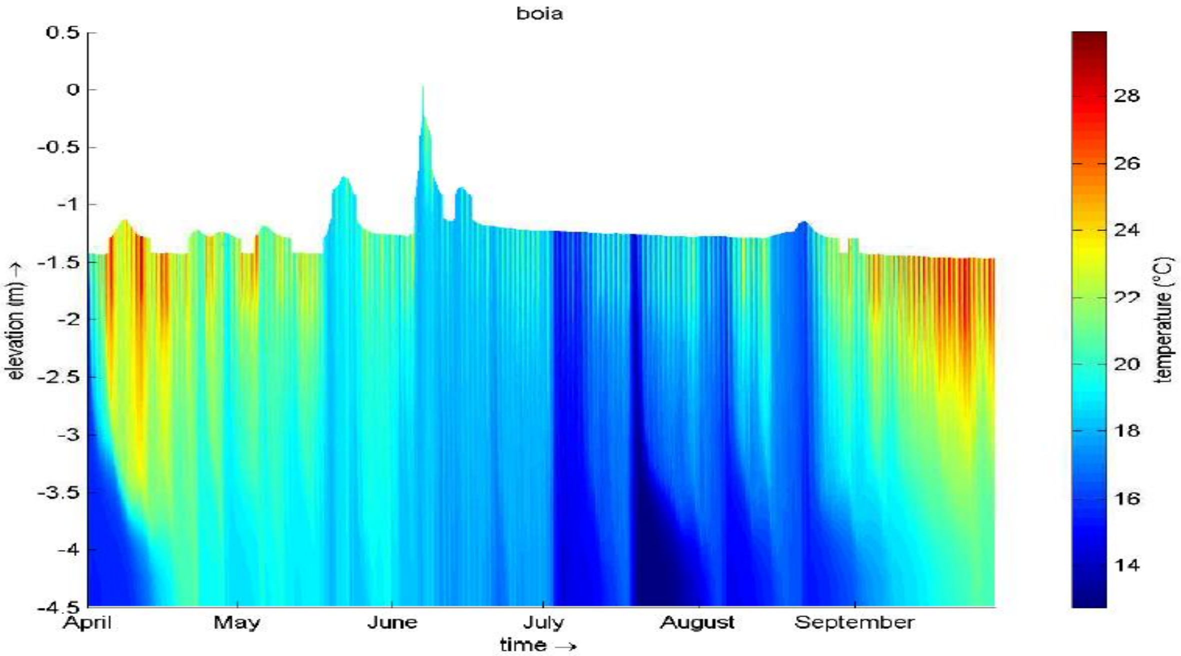


Source: Author.

**Figure 55. Temperature (left) and water density (right) profiles of mixed and stratified conditions**

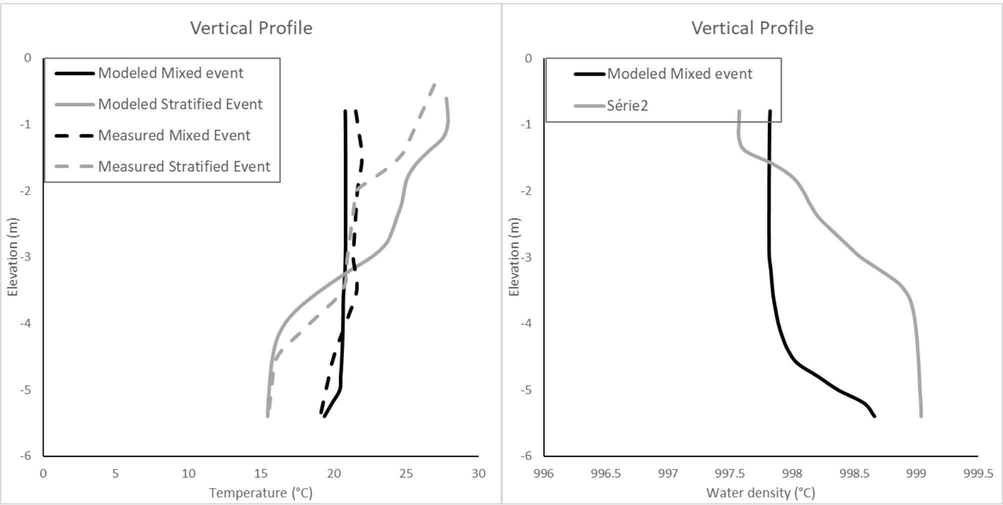


Source: Author.

### 3.1.2 Water Quality Modelling

Water quality models provide a wide view of the ecosystem, describing its components, interactions, and mass transport along the watercourse. In this work, the objective goes beyond demonstrate that lakes and reservoirs water quality can be well represented by 3D mathematical models, the goal is to evaluate the effect of the water column thermal behaviour on the water quality, especially in small and shallow lakes with faster responses to the external influences.

The month of July of 2017 was used to verify the model performance, crossing model results with field measures (Figure 56). The water quality measures are monthly; therefore, the model's purpose is to be able to reproduce the environmental bias, the low and high peaks of each component. The results show that the model can represent the behaviour of all control variables in the environmental, so the model is well-calibrated and validated.

To calibrate the inter-relationships on the lake's ecosystem parameters related to algal nitrogen and phosphorus consumption. BOD first order decay ($k_2$), oxygen production by algae, nitrification rate, salinity, wind speed, re-aeration coefficient ($k_1$), air temperature and wind speed height. The finals coefficient values are described on the Table 6.

**Table 6. Parameters used in the calibration of the water quality model.**

| *Parameters* | *Value* | *Parameters* | *Value* |
|---|---|---|---|
| N:C ratio Greens | 0.002 [gN $gC^{-1}$] | BOD decay rate | 0.03 [$d^{-1}$] |
| P:C ratio Greens | 0.001 [gP $gC^{-1}$] | Net primary production of Greens | Calculated by the model |
| Nitrification rate | 0.08 [$d^{-1}$] | | |
| Salinity | 0 [g/kg] | Air temperature | Given time series |
| Wind speed | Given time series | | |
| Minimum re-aeration coefficient | 0.8 [m $d^{-1}$] | Wind speed height | 10 [m] |

Source: Author.

**Figure 56. Hedberg lake water quality calibration results of Algae, Dissolved Oxygen, Biochemical Organic Demand and Nutrients**

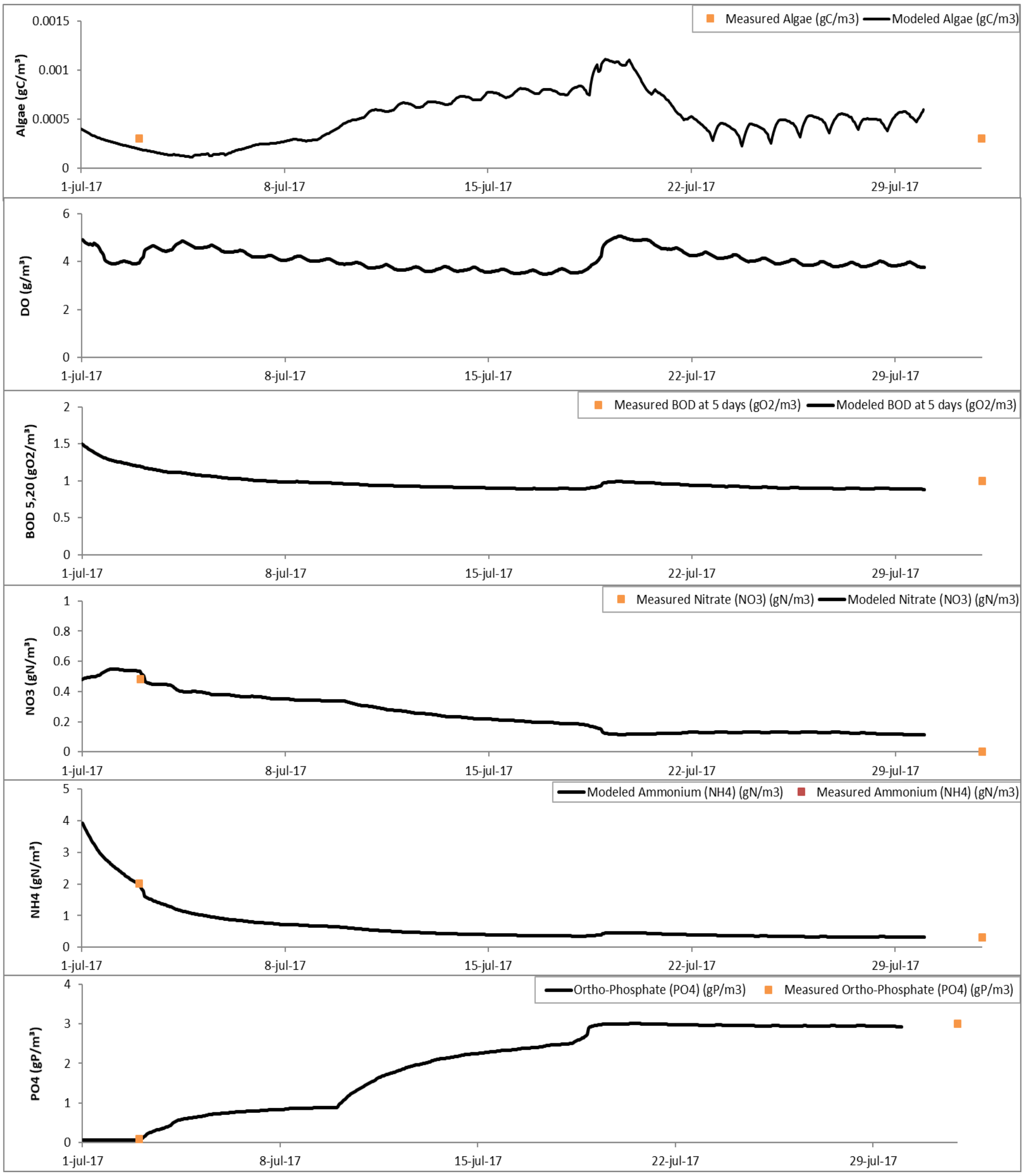


Source: Author.

The water quality simulation includes different hydrologic situations (droughts and floods) and typical hydrodynamic behaviour, with strong stratification moments and mixing events on the lake, which showed direct effects on its water quality (Figure 57). Using the algae mass as a proxy to the biological activity it can be noted that the mixing event causes a reduction in the biomass, while the stratification promotes its development. Thus, the algae maximum values

(0.001 gC $m^{-3}$ - using 1 gC: 30 gChl a [9-10] were registered in the stratification period, with propitious external conditions (high radiation and low wind speed) and available nutrients.

The nutrient consumption performed by the algae balances the NO3 and PO4 budget, as can be seen in the Figure 57, algae peaks provokes a nutrient decrease (July). The algae development also affects the DO concentration, as this organism can produce Oxygen, the algae peak is followed by higher DO concentrations.

The main addition to the organic matter concentration is the basin input, which enters the lake by the wash load and the river contribution. It is also affected by the algae behaviour, once at the end of its life cycle, they will contribute to the organic matter load. The low water velocity promotes the organic matter particle decay, accumulating it on the deeper layers. This material can be resuspended after strong mixing events.

Biochemical Organic Demand has an inverse relationship with Dissolved Oxygen, high values of BOD mean that the DO is being consumed in the organic matter transformation. As the bottom layers are accumulating organic matter, the oxygen demand increases, reducing the DO availability in these areas.

Exchanges between the epilimnion and the hypolimnion are needed to renew the DO on the deeper waters. This communication is blocked by the density difference in a stratified condition, which causes a DO vertical profile with high concentrations on the surface and very low at the bottom (Figure 58). The longer the reservoir stays stratified, the worse the water quality on the bottom gets. This explains why occurs the whole column shows bad water quality results after a mixing event (Figure 57: 20-may; 10-jun; 20-aug).

The oxygen depletion on the deeper layers is one of the major water quality problem. It makes possible to the anaerobic organisms to developing, resulting in greenhouse gases production (JI, 2008).

**Figure 57. Hedberg lake water quality simulation results**

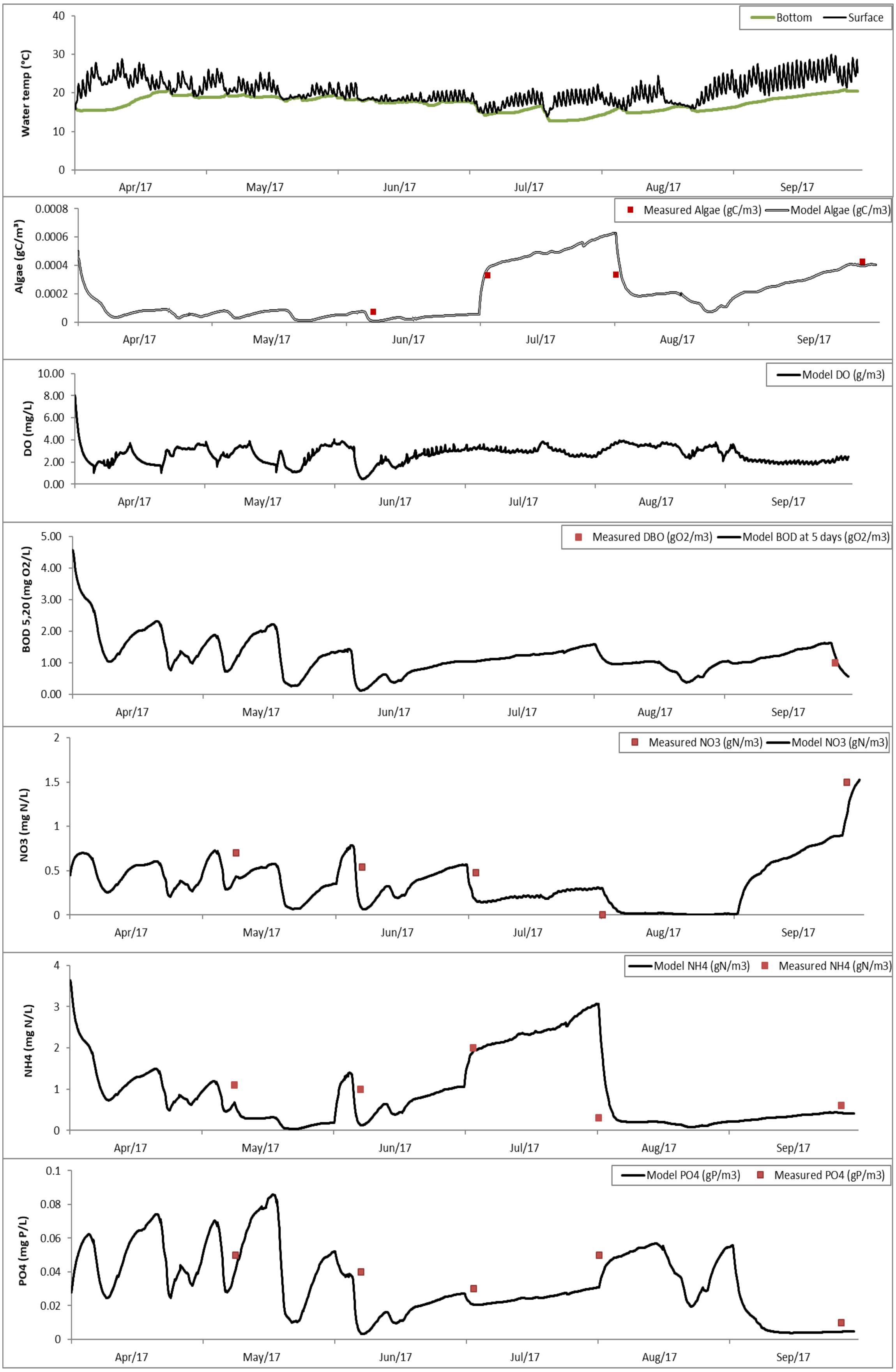


Source: Author.

**Figure 58. Hedberg lake water quality simulation results of the Dissolved Oxygen (DO) profile in stratified and mix condition. Each colour line means a different day of an event**

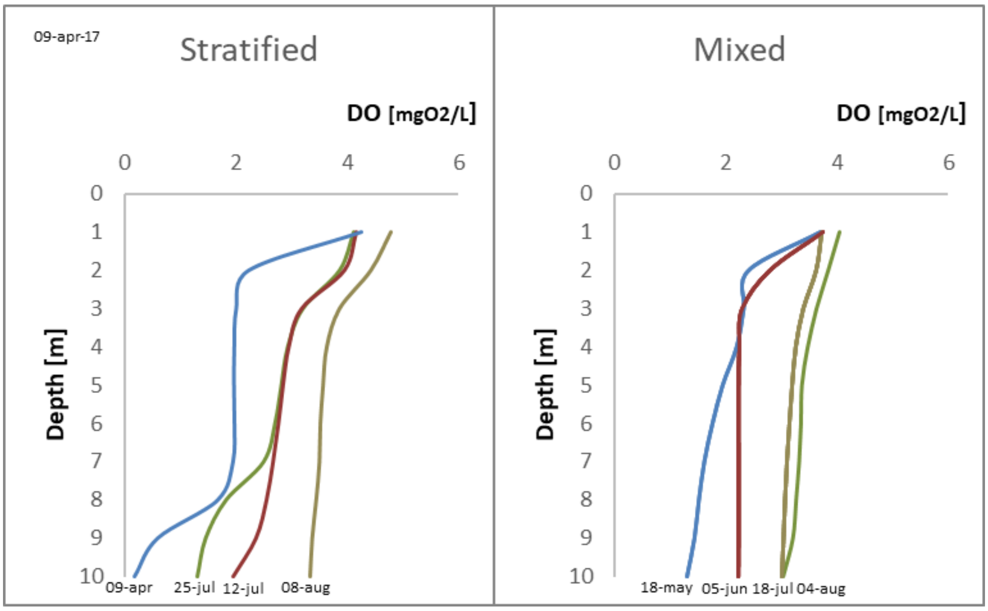


Source: Author.

## 3.2 Billings reservoir

### *3.2.1 Hydrodynamic modelling*

Billings' reservoir area was reproduced in the model by an orthogonal grid with 50 x 50 m cells and 11 layers with 1.68 m thickness. In this lake the σ-model was used, unlike in the Hedberg reservoir. This option aimed a better representation of the boundaries and morphology, since Billings is a large reservoir with significant morphometry differences along the reservoir.

Boundary conditions in this simulation had to describe the incoming flow from the affluent, the output flow created by the energy generation and the specific dynamics of this reservoir, which is the sporadic contribution from the pumped waters from the Pinheiros river. The pump and output flow data were provided by the reservoir operations, EMAE.

The natural flows enter the reservoir were estimated by the hydric balance of the Billings' system. From the alterations registered on the reservoir's water levels and its elevation x area x volume curve was possible to calculate the superficial flow on the contributing watersheds. This contribution associated with the flow regionalization equation proposed in Castro (2010) made possible to estimate each affluent input.

The heat flux data (relative humidity, air temperature, radiation, wind's direction, and speed) was obtained from the INMET São Paulo-SESC Interlagos-A771 station, located on the banks of the Cocaia Creek, as described in the item *2.3 - The monitoring system*. As in the Hedberg lake, the Ocean was used as the heat model in Delf3D.

The model's calibration and validation steps were executed based on this data set and the measures performed on the field (Sep through Dec 2018). The period used in calibration was from 14 through 24 September and the used values are shown in Table 7.

Figure 59 compares field measures with simulation results, in this is possible to note the model capacity to represent the reservoir hydrodynamic, matching the stratification and mixing events along the period. The model efficiency is identified by the index presented in Table 8, as Hedberg's model, the statistical evaluations showed indices values of a trustful representation of the system.

**Table 7. Parameters used in the calibration of the Billings' hydrodynamic model.**

| *Parameters* | *Value* | *Parameters* | *Value* |
|---|---|---|---|
| Wind stress - Cd | 0.001 [m $s^{-1}$] | Dalton number | 0.001 |
| Vertical Eddy Viscosity - VEV | 0.002 [m $s^{-1}$] | Stanton number | 0.005 |
| Vertical Eddy Diffusivity - VED | 0.0001 [m $s^{-1}$] | | |
| Horizontal Eddy Viscosity - HEV | 0.5 [m $s^{-1}$] | Secchi Depth | 0.7 m |
| Horizontal Eddy Diffusivity - HED | 0.5 [m $s^{-1}$] | Manning | 0.03 |
| Cloud cover | 0% | Evaporation rate | Calculated by the model |

Source: Author.

**Figure 59. The model calibration and validation results of the Billings reservoir**

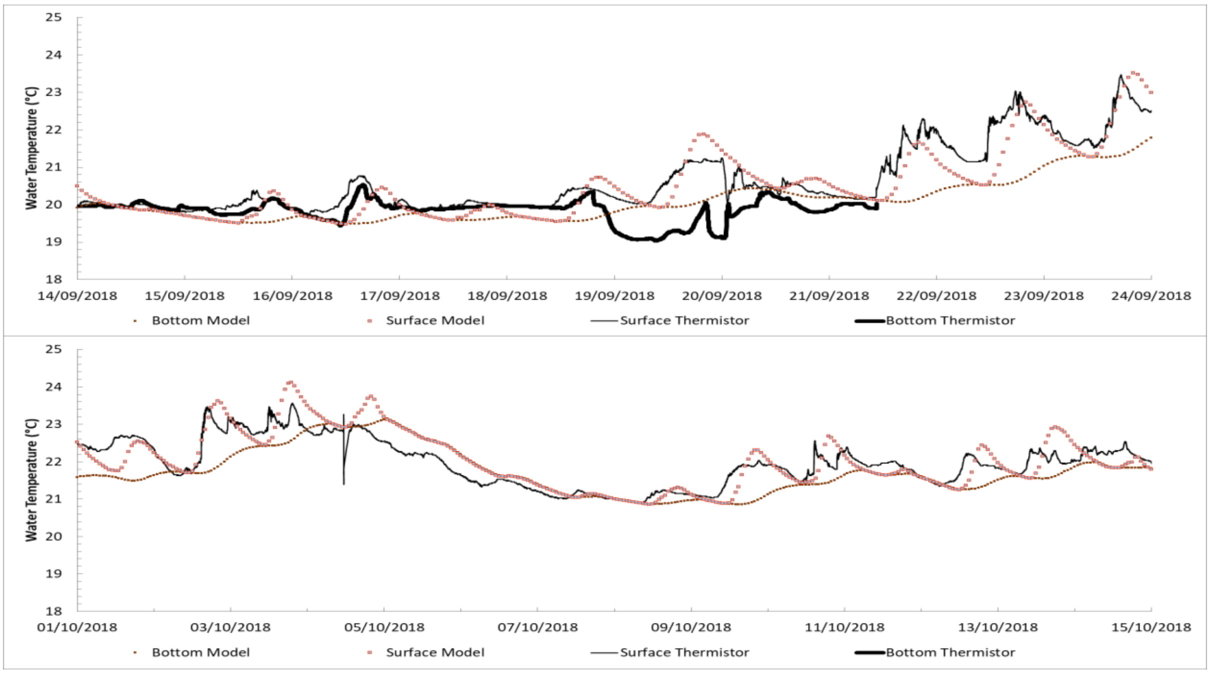


Source: Author.

**Table 8. Calibration and validation statistical indices founded for the Billings reservoir simulations**

| Calibration indices | | Validation indices | |
|---|---|---|---|
| **MAE** | 0,09 bottom | **MAE** | 0,15 bottom |
| | 0,15 surface | | 0,03 surface |
| **Nash Sutcliffe** | 0,66 bottom | **Nash Sutcliffe** | 0,38 bottom |
| | 0,76 surface | | 0,52 surface |
| **RMSE** | 0,48 bottom | **RMSE** | 0,45 bottom |
| | 0,48 surface | | 0,39 surface |
| **NMAE** | 0.01 bottom | **NMAE** | 0.005 bottom |
| | 0.0047 surface | | 0.0015 surface |

Source: Author.

The hydrodynamic behaviour of the reservoir was studied with the simulation of the whole monitored period (Figure 60). Even though Billings' reservoir is not shallow, it has plenty of movement on in the water column, mixing every night. This can be associated with the strong wind influence on the reservoir surface, which begins to blow more intensely every day near to the midday, cooling the reservoir upper layer and initiating the mixing process.

The Pinheiros' river waters pumped into the Billings reservoir can also produce a mixing in the water column. Those events can be noticed by the velocity increasing (Figure 69), especially at the begging of October and December. They maintain the water column mixed for more than a day.

Figure 62 demonstrates the simulation results for the temperature spatial variation. As can be expected the incoming points has the higher temperatures (26 – 30°C), due to the lower depths, while the reservoir's centre, with a maximum depth of 16m, has a mean temperature of 22°C.

**Figure 60. Simulated hydrodynamic behaviour of the Billings reservoir across the water column**

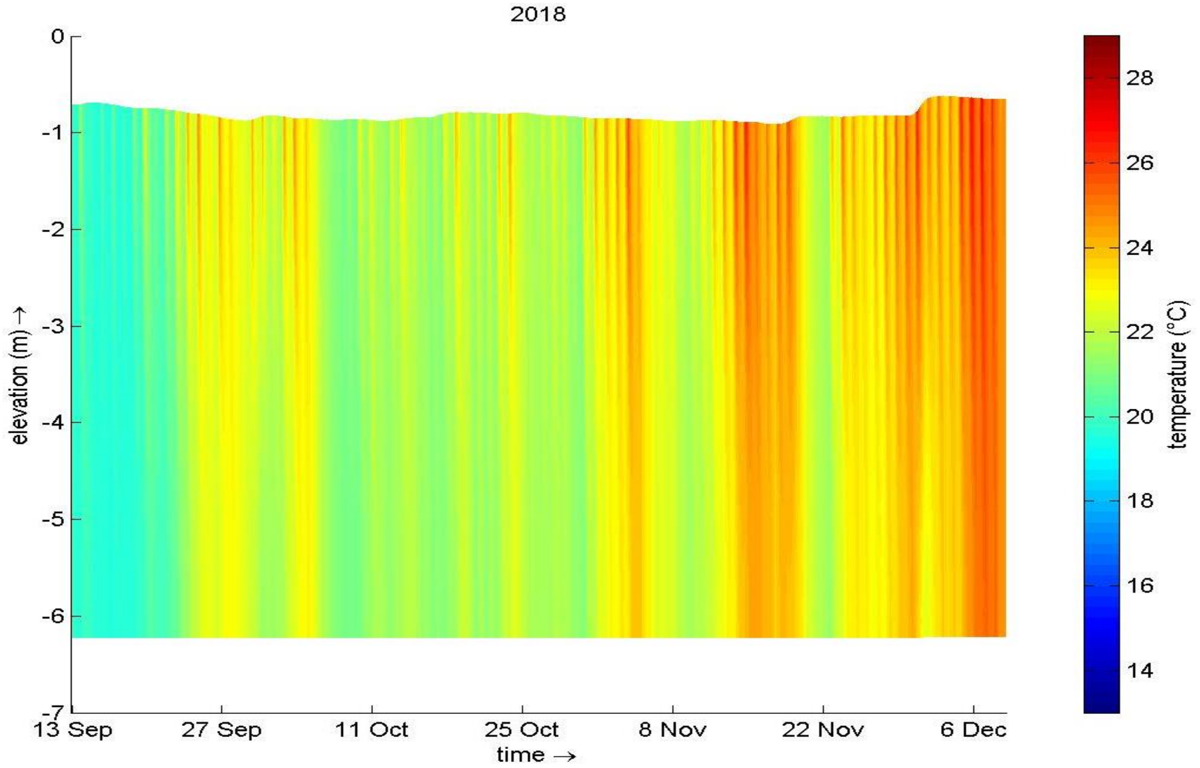


Source: Author.

**Figure 61. Simulated horizontal velocity behaviour of the Billings reservoir across the water column**

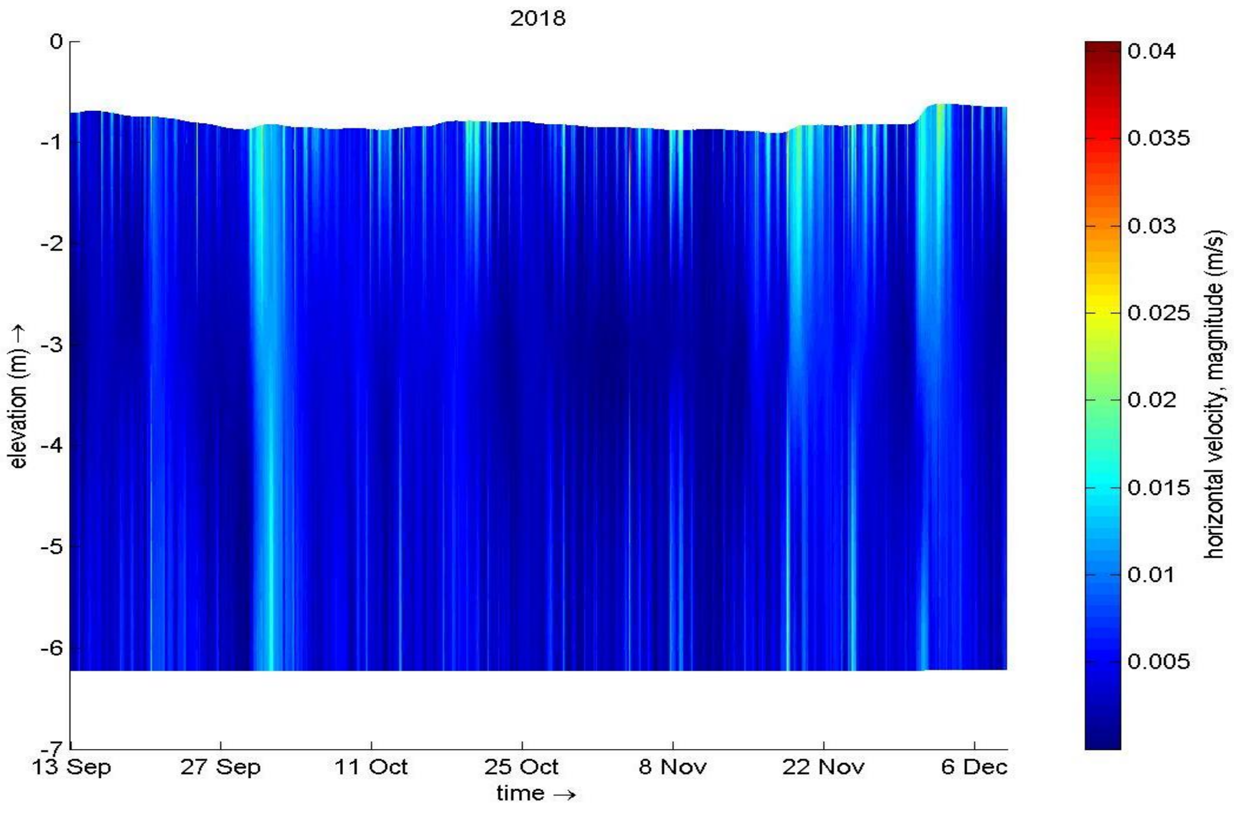


Source: Author.

**Figure 62. Simulated temperature spatial variation of the Billings reservoir**

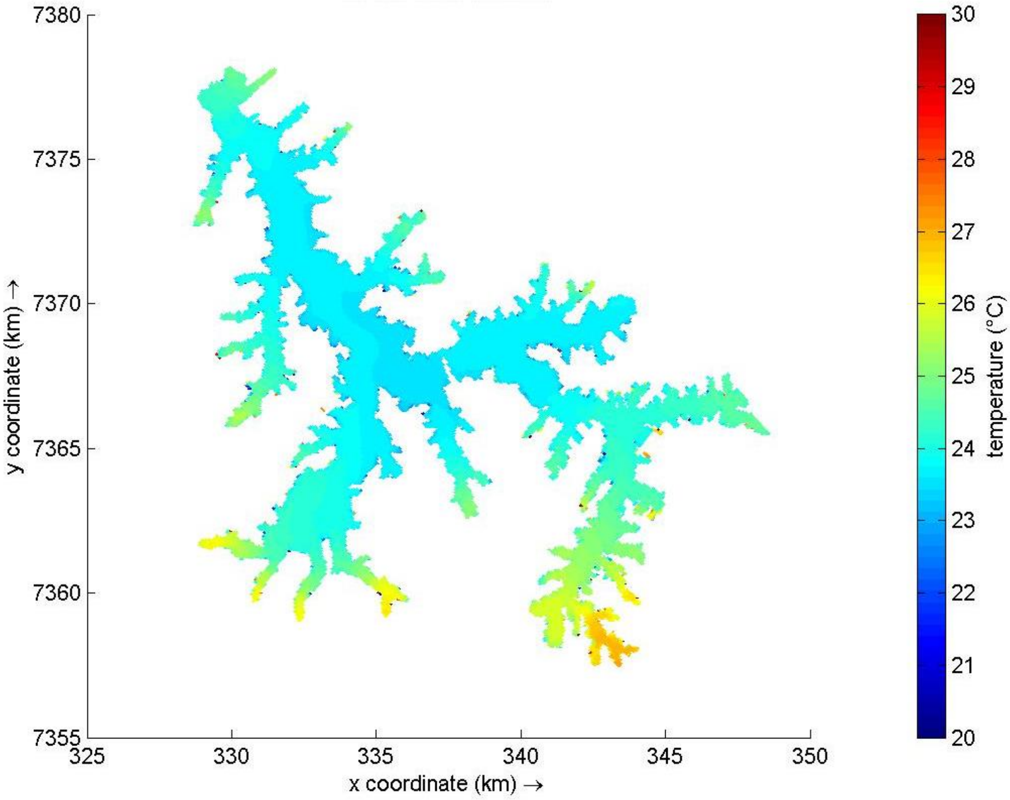


Source: Author.

### 3.2.2 *Water Quality Modelling*

The hydrodynamics results were used as input files in the water quality simulation, exporting the water temperature, horizontal and vertical velocities, and discharges, among other variables. The load time series entry was derived from the historical data of CETESB reports to points BITQ00100 and RGDE02200 and measured at the monitoring point of 2018 (Figure 63) (CETESB, 2017). The model's validation was made according to data from the CETESB's monitoring points (BILL02030; BILL02100; BILL02500).

**Figure 63. CETESB’s water quality monitoring points on Billings reservoir**


Source: Author.

The calibration of the water quality model was made by comparing field measurements to the simulation results at the same points (Figure 64), using the parameters described in In October end is demonstrated the dependence between nutrients, algae and DO. The nutrients greater availability, not only one, but of all three NO3, NH4, and PO4, allows algae development, which in turn produces greater DO levels.

Table 9. The simulation results show the hydrodynamics’ influence on its water quality, especially the pumping events generate greater water velocity and conducted the constituents along the reservoir’s central body. In the calibration period, an example of this effect is noted at the September end, in which water from the Pinheiros river is pumped to Billings reservoir, increasing horizontal and vertical velocity, perturbing the water column and increasing load entry and renewing nutrients on the lake.

In October end is demonstrated the dependence between nutrients, algae and DO. The nutrients greater availability, not only one, but of all three NO3, NH4, and PO4, allows algae development, which in turn produces greater DO levels.

**Table 9. Billing’s parameters used in the calibration of the water quality model.**

| *Parameters* | *Value* | *Parameters* | *Value* |
|---|---|---|---|
| N:C ratio Greens | 0.05 [gN $gC^{-1}$] | BOD decay rate | 0.008 [$d^{-1}$] |
| P:C ratio Greens | 0.009 [gP $gC^{-1}$] | Net primary production of Greens | Calculated by the model |
| Nitrification rate | 0.01 [$d^{-1}$] | | |
| Salinity | 0.1 [g/kg] | Air temperature | Given time series |
| Minimum re-aeration coefficient | 0.4 [m $d^{-1}$] | Wind speed | Given time series |

Source: Author.

**Figure 64. Water quality calibration results in the measuring point on Billings reservoir**

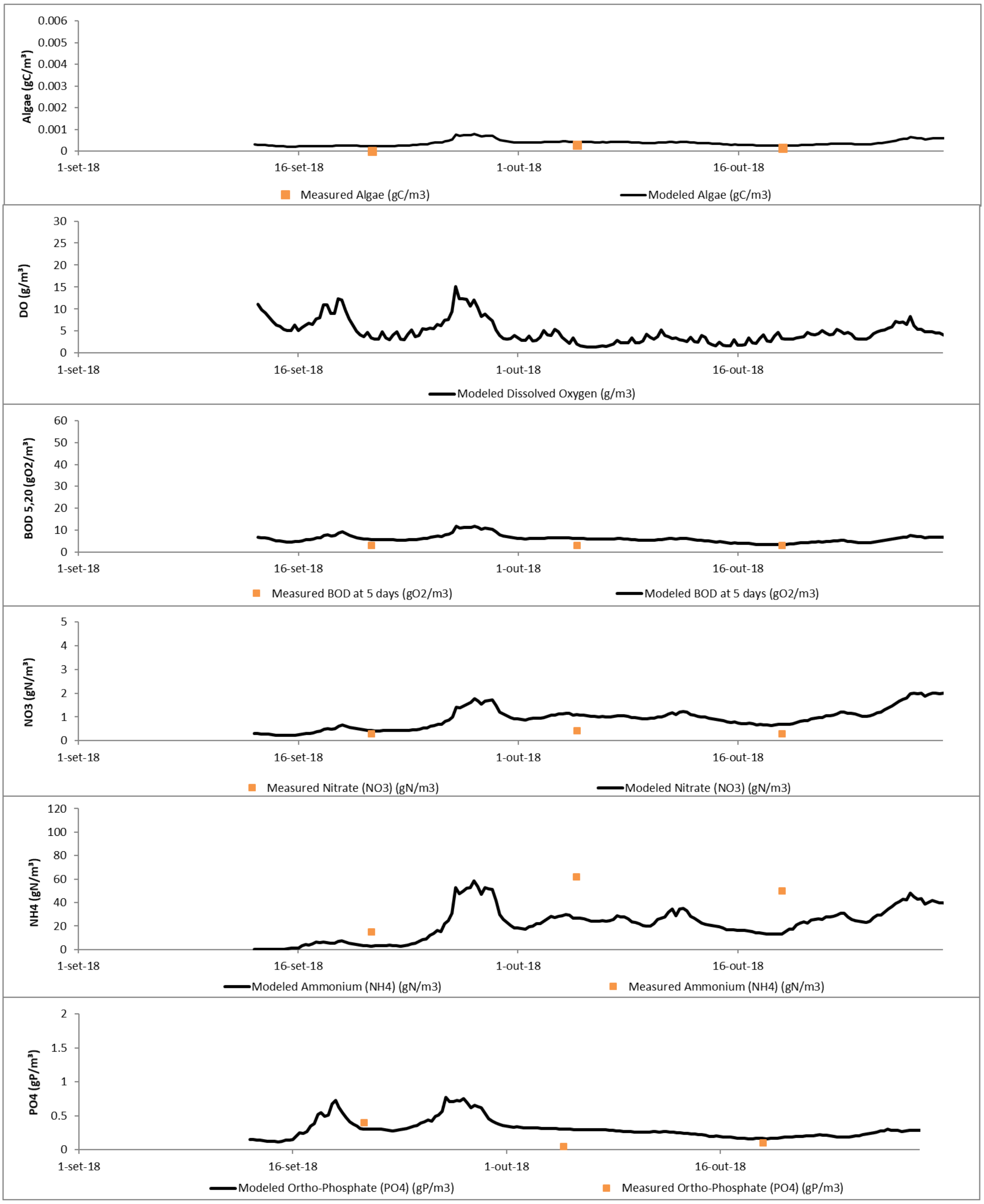


Source: Author.

An extended period was simulated after calibration (Figure 65), allowing to correlate different hydrodynamic conditions with the reservoir's water quality. On the first and eight December are found the greater constituents peaks, but each one has a completely different hydrodynamic condition. In the first moment, the reservoir mixing, and consequent quality deterioration are correlated with the greater pumping event of the period (185 $m^3 s^{-1}$), while in the next, the vertical inversion is the driving force.

The constituents' behaviour inside the reservoir is observed with the results of the monitoring points situated at the main body. The model performed good results, all inside the range of CETESB historic data (Appendix A).

In general, the water quality improves in the direction of the outlet, with the constituents' sedimentation promoted by the lentic environment. All variables values decrease downstream, allowing DO recuperation.

According to the levels established in CONAMA 357/2005, the main problems found on the Billings reservoir are with BOD and PO4. They're identified in the BILL2030 and BILL2100 monitoring points, while in the BILL2500 only PO4 is not compliant with the legislation. This is an effect of the anthropic occupation in the reservoir's surrounding areas.

**Figure 65. Water quality simulations results in the measuring point on Billings reservoir**

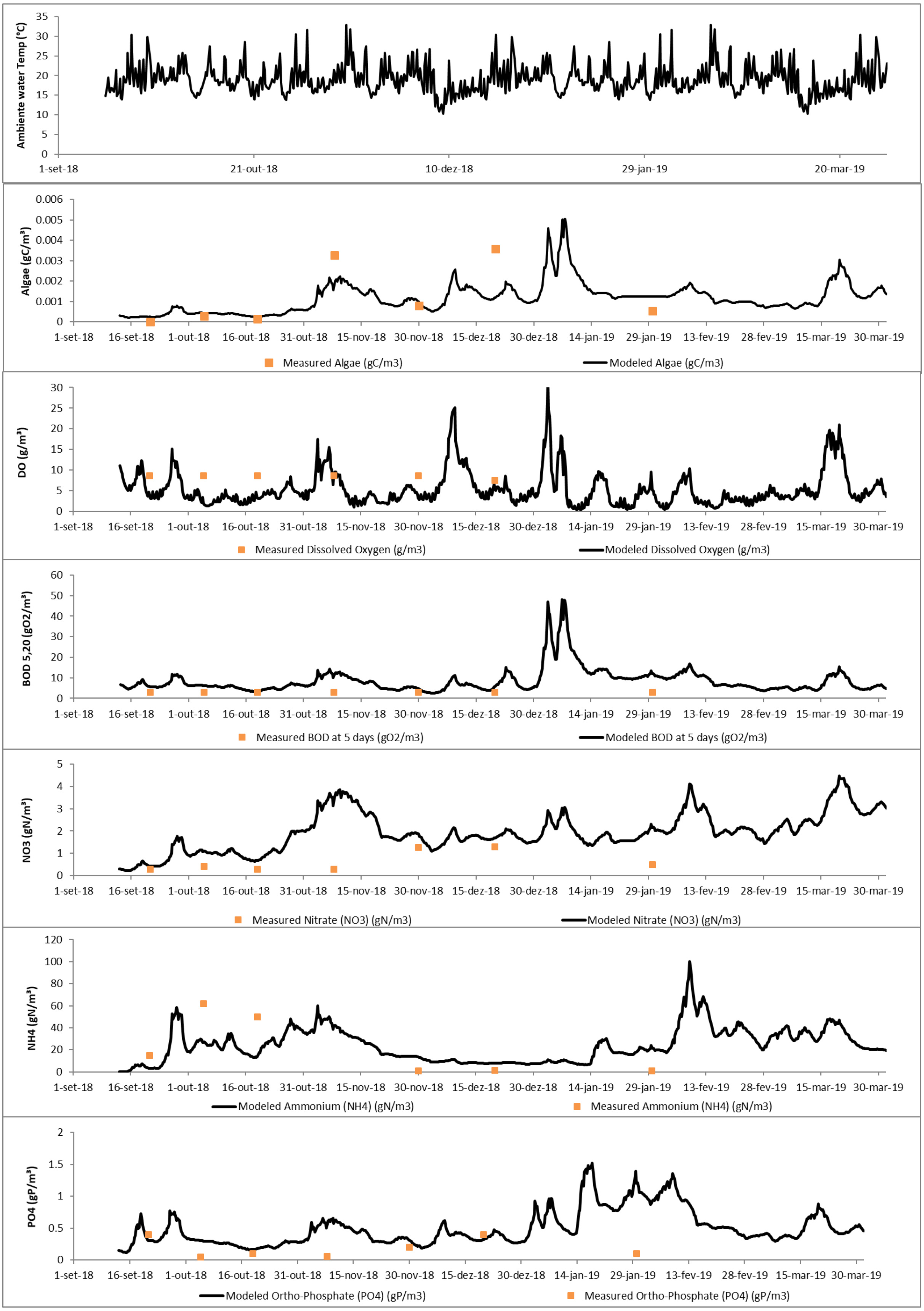


Source: Author.

**Figure 66. Water quality simulations results on the Billings reservoir's monitoring points**

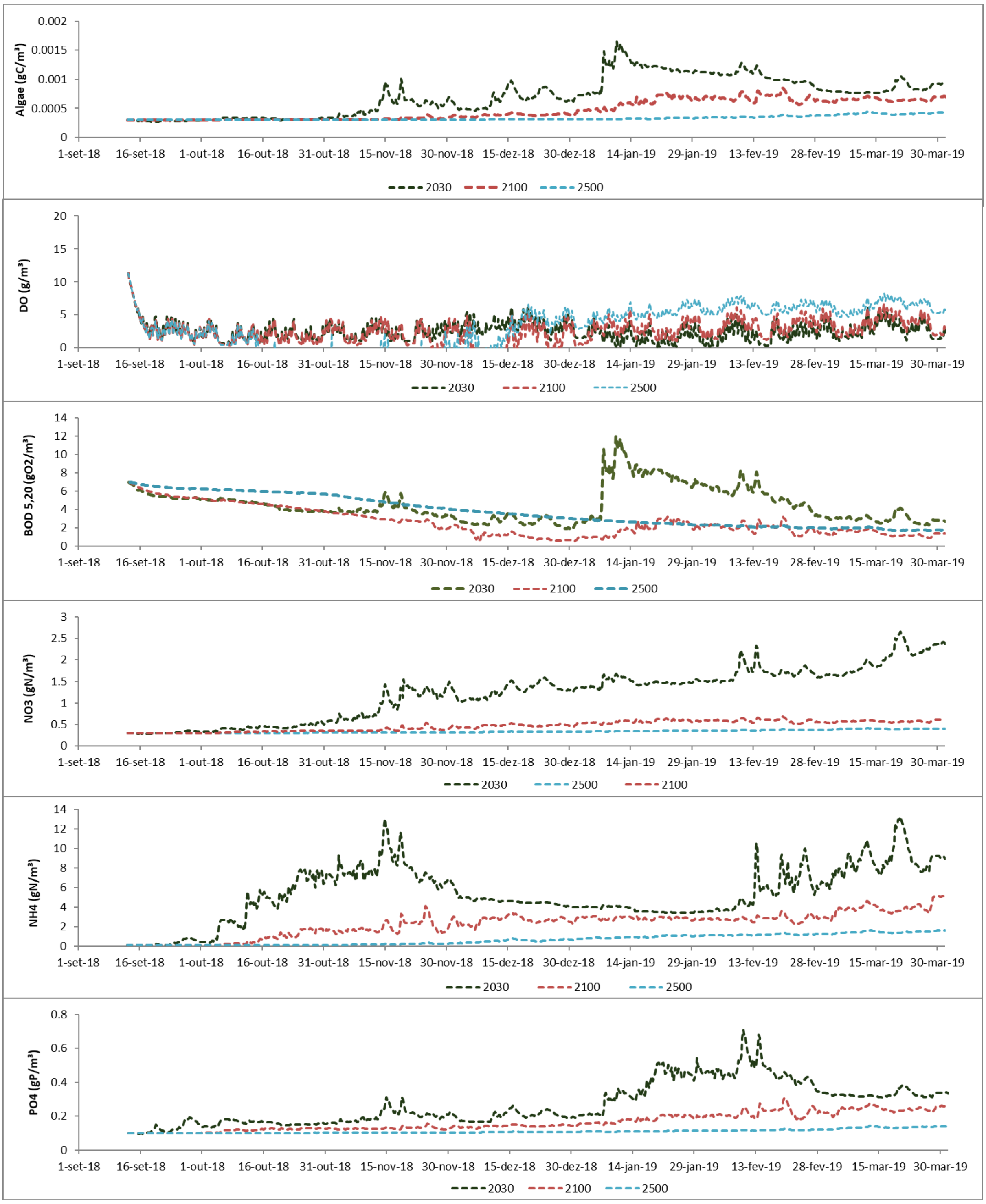


Source: Author.

## 3.3 Bed Material Resuspension

One of the graters effects of the stratification is the mass transport limitation across the water column, this includes the nutrients dispersion and gas exchanges. Over time, this impossibility of nutrients recharge makes them unavailable in the upper layers, affecting the biota development. That's why the mixing events are important to the ecosystem balance (JALIL, LI, *et al.*, 2017) (MATISOFF, WATSON, *et al.*, 2017).

However, not only the nutrients are adsorbed with bed material, but also the pollutants, which can be harmful to the water quality (ELC¸I, 2008) (SOMLYÓDY e KONCSOS, 1991). Especially in polymictic lakes, it is necessary to understand the characteristics of the mixing events, as their frequency and capacity to resuspend bed material. Chapter II studied the atmospheric conditions to a mixing event occur and presented a tool able to forecast those events, making possible to operate the reservoir according to the intention to encourage or prevent the mixing.

In this item, the aim is to investigate, using field measurements, the mixing events' capacity to resuspend bed material. It is discussed in the literature that mixing events produce vertical velocities in the water column, and so can resuspend bed material, but this was never measured and correlated with the temperature profile in a study area (KULLEMBERG, 1976) (LUETTICH-JR, HARLEMAN e SOMLYÓDY, 1990) (BAILEY e HAMILTON, 1997) (LOU, SCHWAB, *et al.*, 2000) (CHUNG, BOMBARDELLI e SCHLADOW, 2009) (CÓZAR, GÁLVEZ, *et al.*, 2005) (JALIL, LI, *et al.*, 2017) (JIN e SUN, 2007) (MATISOFF, WATSON, *et al.*, 2017).

The field measures, made with the sensor described on item 2.3.4 of this chapter, describe the variations on the water turbidity due to mixing events. The next topic demonstrates the results of the vertical velocity quasi-3D simulation, associated with those measures, evaluating the model's capacity to represent it and if the created vertical velocities are great enough to resuspend bed material.

### *3.2.1 Results*

Hedberg lake was the first analysed, crossing the turbidity data with the water temperature measured, to observe its behaviour on to the mixing moments. The turbidity data in Figure 67 shows a peak at the end of July, which is the same time that the mixing event begins to happen.

After a long period of a stratified and stable water column, with a decreasing in turbidity measures, it rises rapidly, when the temperature profile begins to homogenize.

Beholding the major mixing event on the Hedberg lake, Figure 68 shows the wind speed measures higher variance, combined with the posterior decrease of the solar radiation, provide the condition to the accumulated energy of the stratification transforms itself in vertical velocity and re-suspend bed material. This goes according to the conclusions in Chapter II.

In Hedberg lake's mixing events, the turbidity peak represents a difference of ~ 100 units, meanwhile, in the Billings reservoir, the values are smaller (Figure 69). The main reason for this situation is that along the monitored period there was no stratification significant event, with no energy accumulation on the water column, restraining the energy release to creates the upward vertical velocity. The realized pumping in October helped to maintain the reservoir mixed.

Even so, is possible to notice differences in turbidity measures between a period of a complete mix (06 – 09 Oct) and a period with stratification (10 – 11 Oct). The turbidity showed more variation between measures when a mixed water column occurs, but the beginning of stabilizing triggers a sedimentation, reducing the activity across the column.

**Figure 67. Time series of Hedberg's turbidity and water temperature measures**

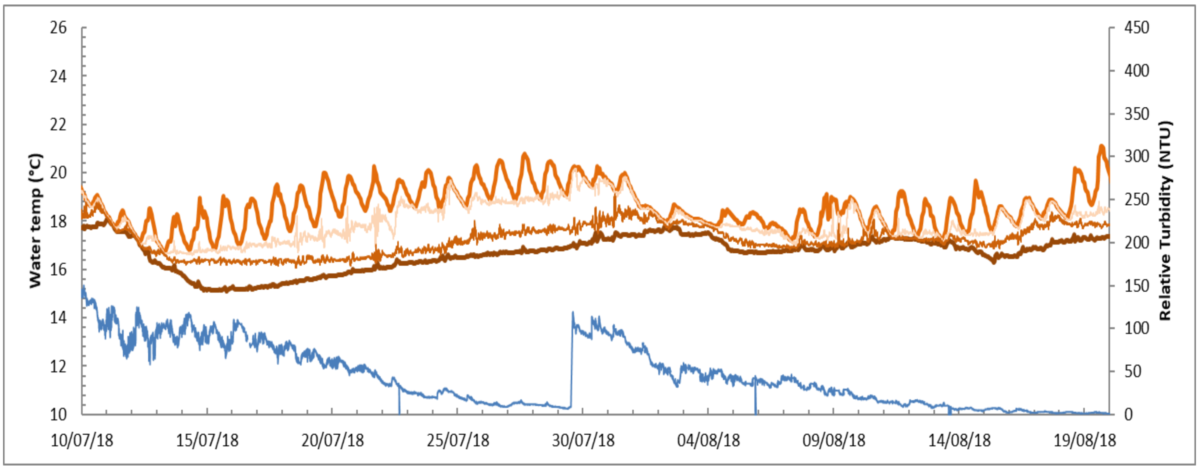


Source: Author.

**Figure 68. Hedberg's turbidity behaviour detail during turnover moments**

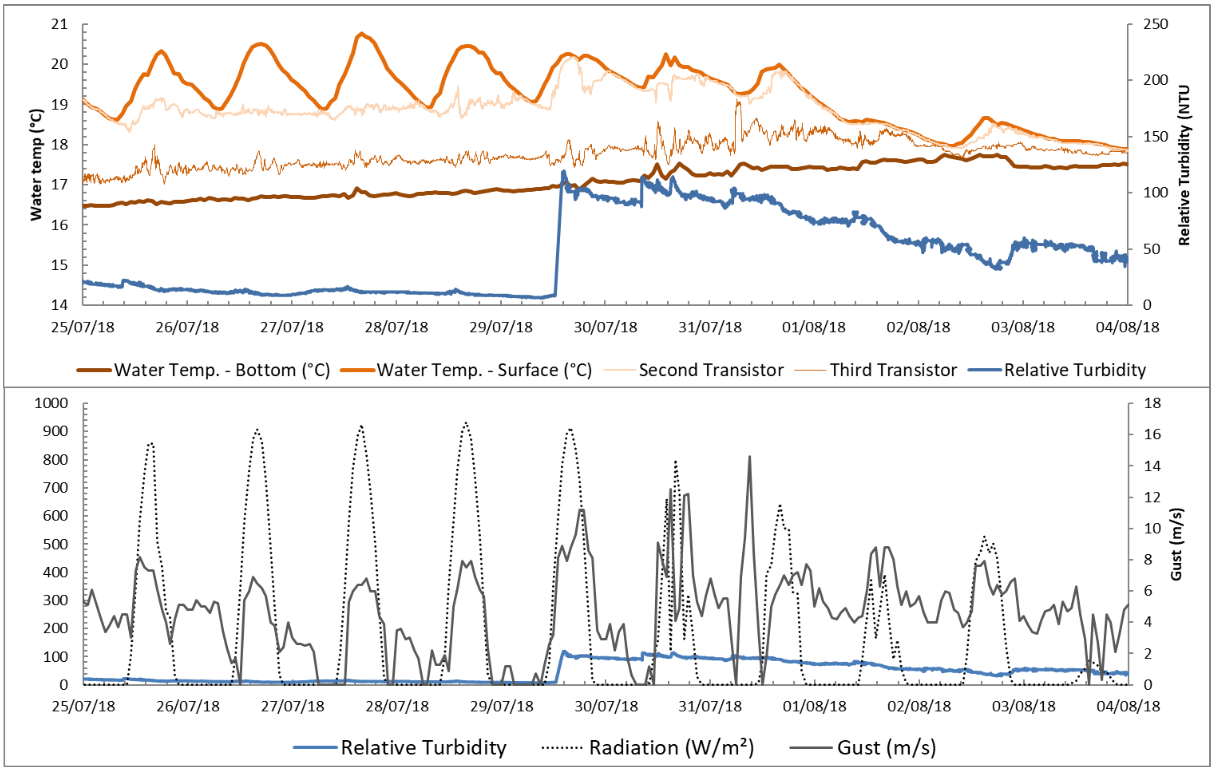


Source: Author.

**Figure 69. Billings' turbidity and water temperature measures**

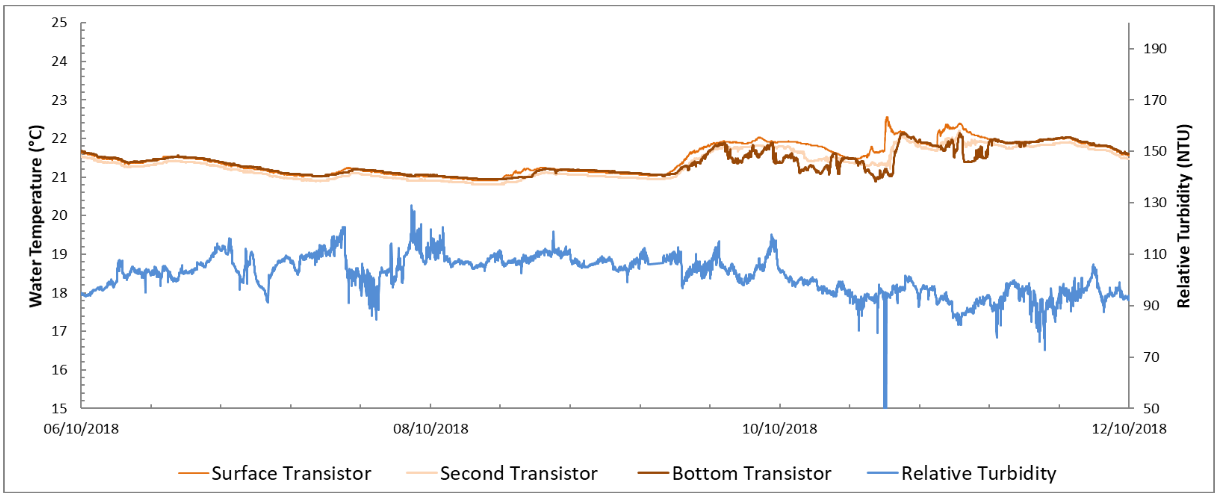


Source: Author.

**Figure 70. Billings' turbidity and climate variables behaviour**

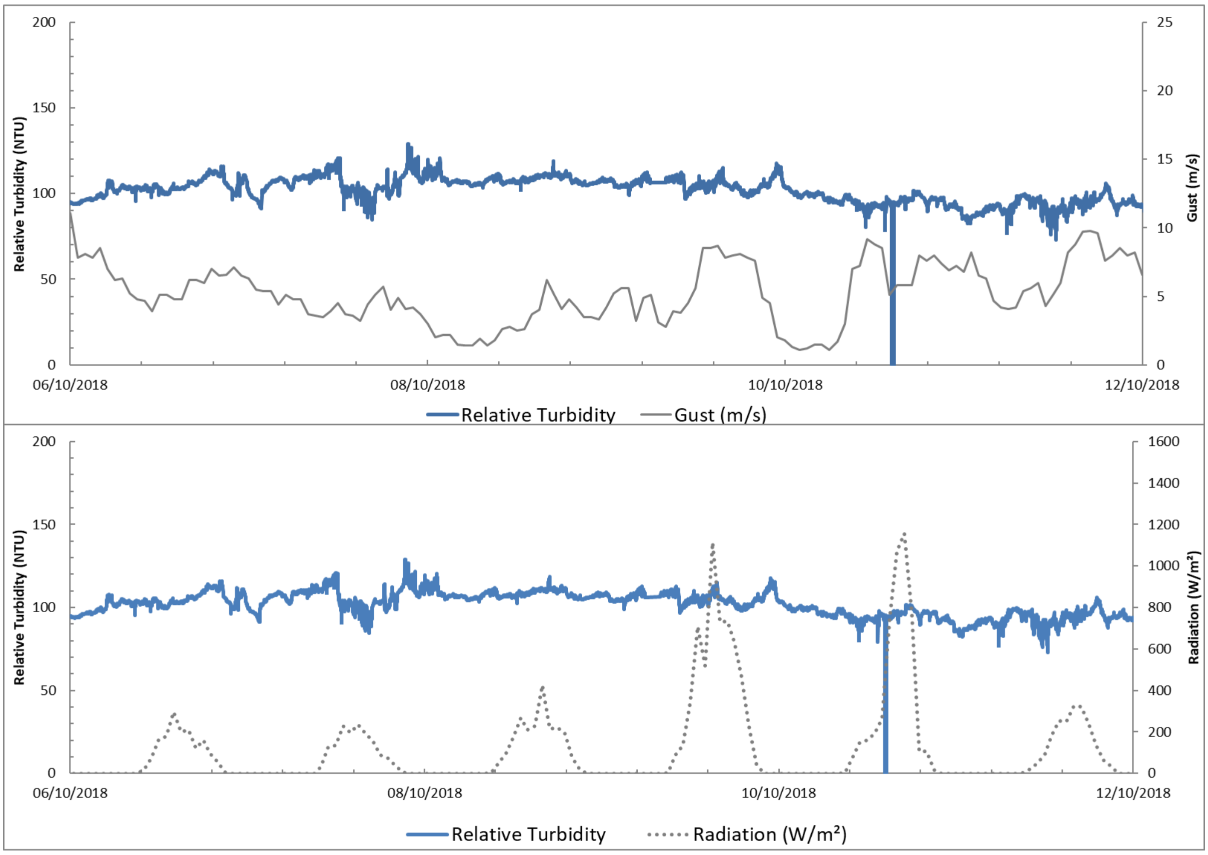


Source: Author.

After observing the correlation between the mixing events and the increase of water turbidity, was evaluated the 3D model capacity to representing this phenomenon. It was represented by the vertical velocity in the simulation, a reflection of the mixing events.

Vertical velocities simulation for Hedberg lake (Figure 71 and Figure 72) had peaks of $6x10^{-4}$ m $s^{-1}$, along with and several events between $4x10^{-4}$ and $2x10^{-4}$ $m.s^{-1}$, while Billings' peaks were of $2x10^{-4}$ $m.s^{-1}$. This is a response from a powerful stratification period in Hedberg lake, creating greater vertical velocities.

Those values founded for modelled vertical velocities indicates that mixing events are capable of re-suspend bed material. This affirmation is confirmed by studies, such as (LUETTICH-JR., HARLEMAN, *et al.*, 1993) (JALIL, LI, *et al.*, 2017), which say that velocities of4x10-4 m $s^{-1}$ begin the movement of the bed material.

**Figure 71. Hedberg's modelled vertical velocity**

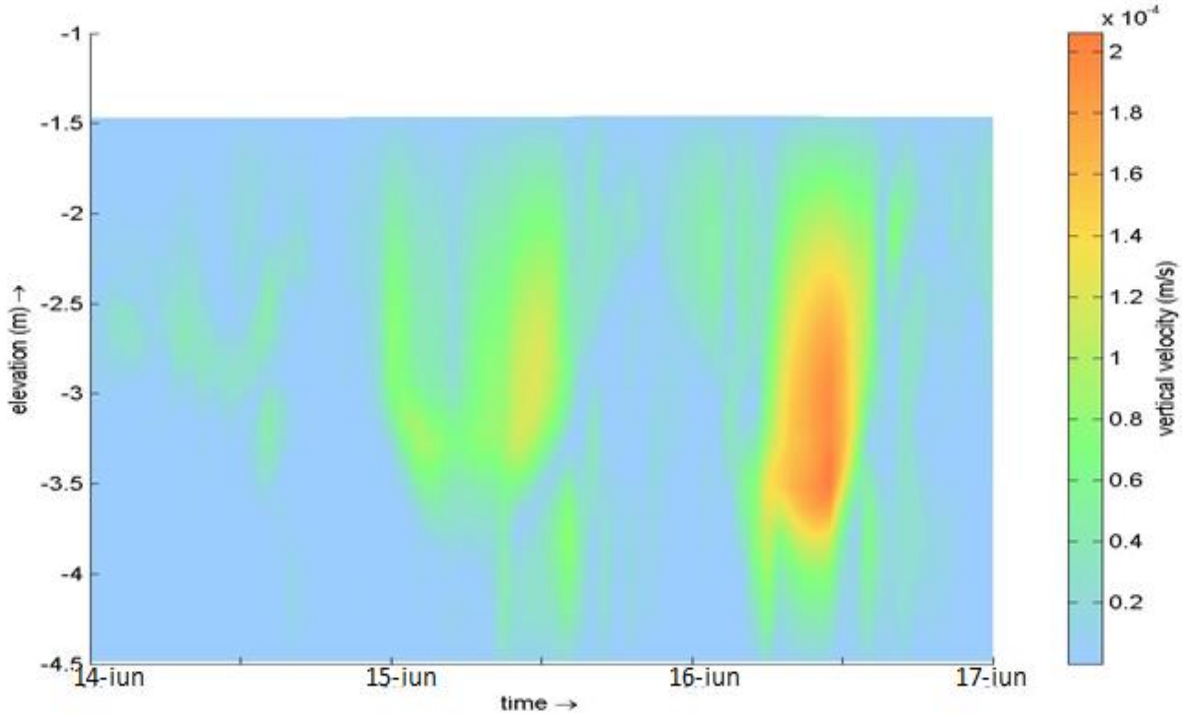


Source: Author.

**Figure 72. Hedberg's turbidity measures related to the modelled vertical velocity and water temperature profile**

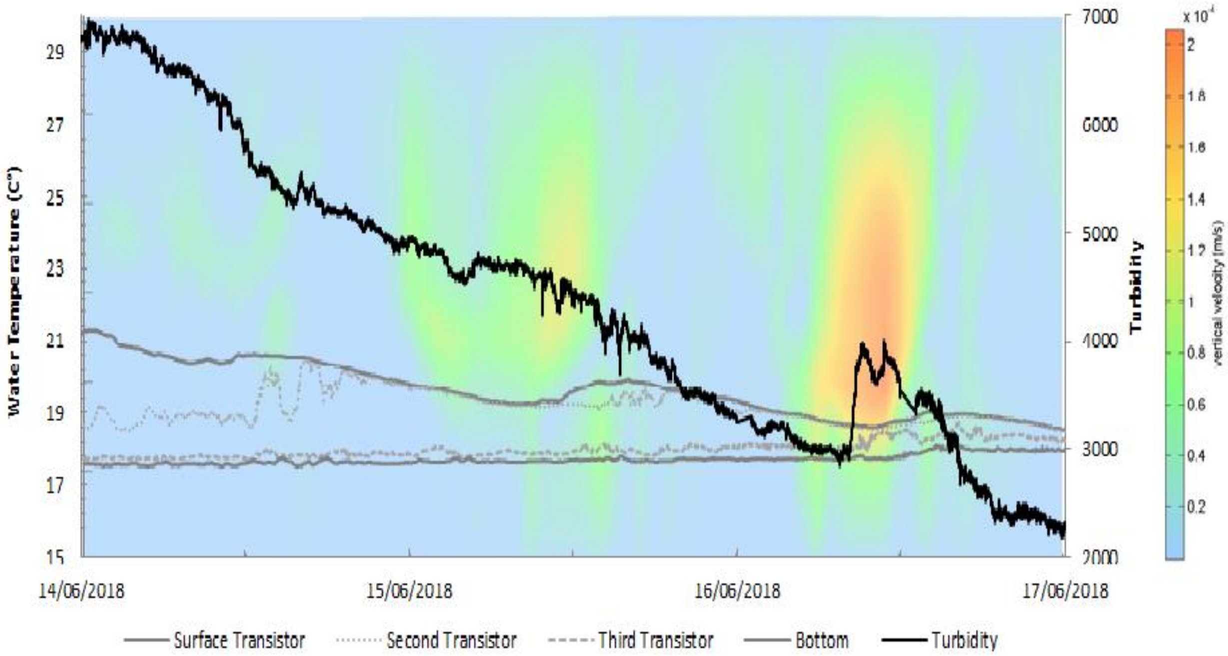


Source: Author.

**Figure 73. Billings' modelled vertical velocity**

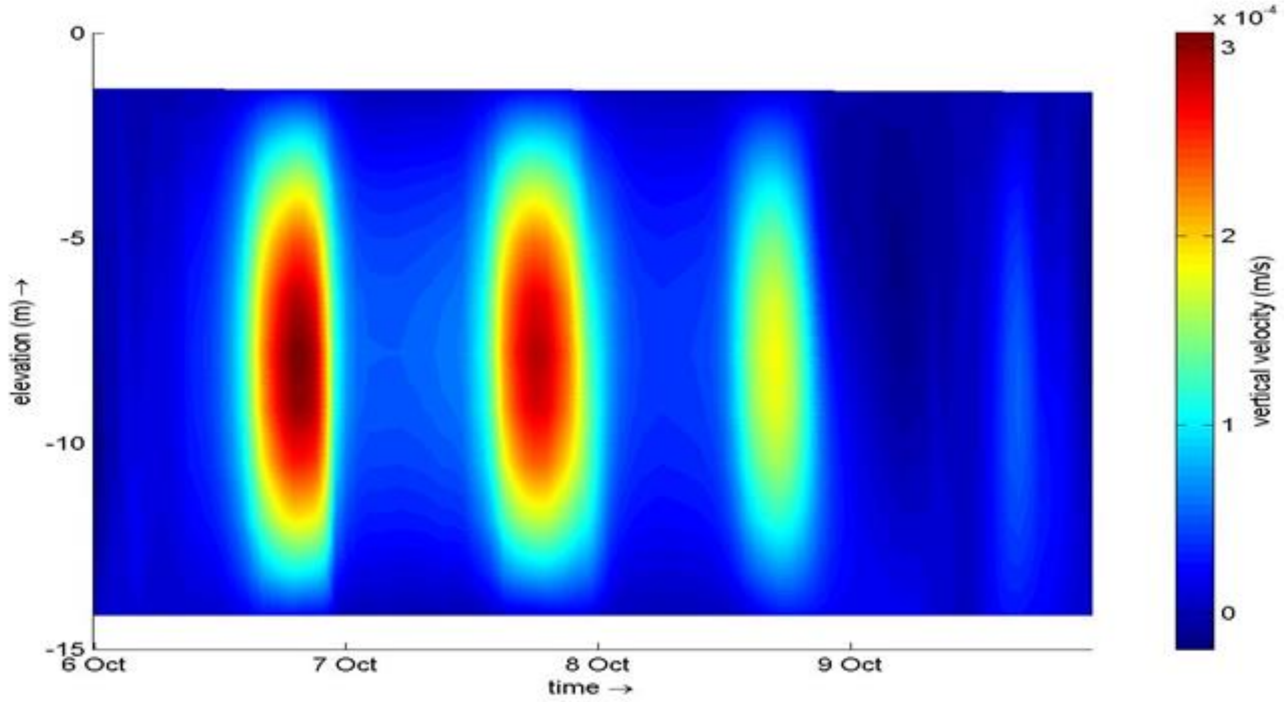


Source: Author.

**Figure 74. Billings' turbidity measures related to the modelled vertical velocity and water temperature profile**

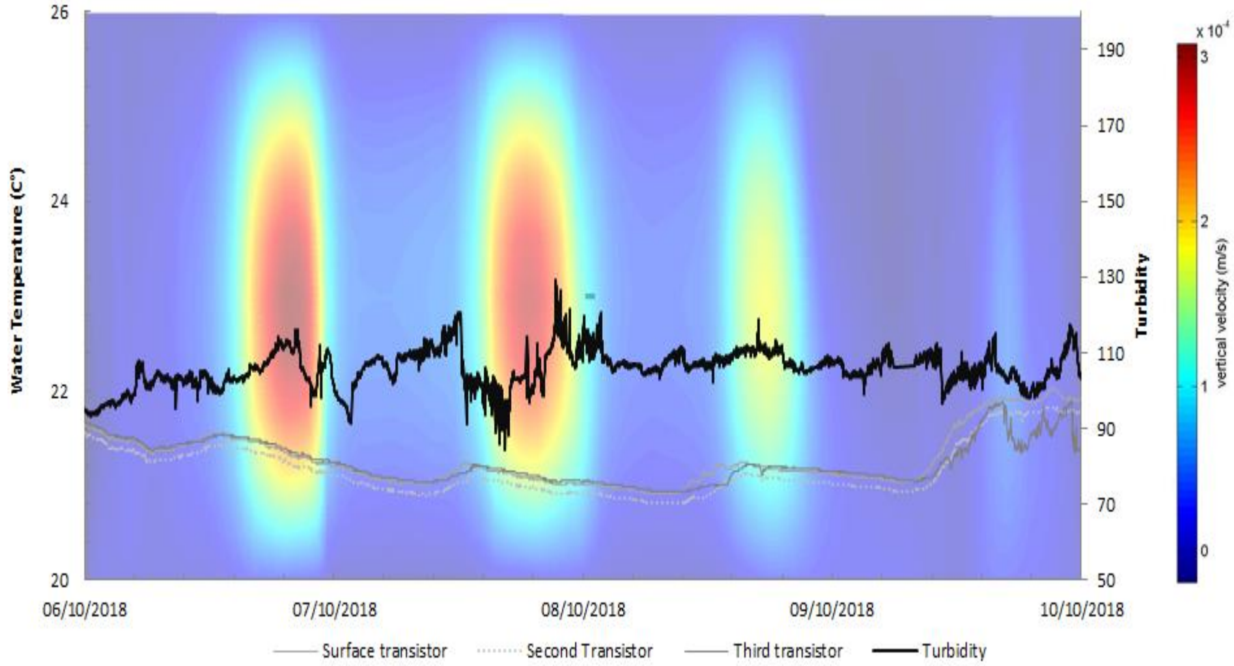


Source: Author.

## 4. Conclusion

This chapter demonstrated the performance of a numerical tool to simulate the hydrodynamic and water quality behaviour under stratifying and mixing conditions. The quasi-3D model, coupled with appropriate boundary conditions and input data, showed good results, representing accurately the temperature along the water column in tropical lakes.

The consequences of the thermal behaviour over the water quality were also investigated with the model. A gain of this tool was to be able to reproduce the reservoir spatial variability and vertical profiles.

The studied lakes have a polymictic behaviour, with several events of mixing along the simulated period. This hydrodynamic particularity perturbs the water quality each time the column overturn, which is an example of how the lake's thermal condition can determine its water quality.

To the algae component, stratified periods mean better conditions to its development, due to turbidity reduction and light penetration increase. Apart from that, the mixing event is also important for the algae, it represents the nutrients recycled and renew.

The simulations also showed the reflection of the hydrodynamic behaviour on the dissolved oxygen. Long periods of stratification are problematic to the water quality, once they drop dissolved oxygen levels down at the deeper layers, enabling anaerobic organisms to develop and increasing greenhouse gas generation.

Hence, the influence of the temperature gradient on the lakes' hydrodynamics and water quality is verified, as well as the importance of improving monitoring techniques. The use of high-frequency monitoring showed its importance in provide accurate models' results.

An “intense” lake's mixing regime has higher vertical velocities, which re-feed the water column frequently with constituents and nutrients, adsorbed on the sediments. This movement was also investigated in this chapter, by the proposition of a turbidity sensor and the relation of its data and the mixing events.

The results showed turbidity peaks of variation at the same time as the mixing events occurred, and the more intense and lasting was the previous stratification period, the higher is the upward velocity generated. The next step was to evaluate the hydrodynamic quasi-3D model capacity to represent the vertical velocities.

The simulations results confirm the field observations and the calculated peaks of vertical velocities matching with the mixing events. The peaks vary between $6x10^{-4}$ m $s^{-1}$ and $2x10^{-4}$ m $s^{-1}$, which according to literature is enough to move bed materials. This means that mixing events can bring on the surface bottom material.

Be capable of understanding, forecast and prevent re-suspension episodes on polluted environmental can be crucial to maintain the water quality on reservoirs that are used as a water source for cities, avoiding algae blooming harmful events. In this field lies the main contribution of this study, which proves that water column mixing events are correlated with the increase of the water turbidity, indicating that the vertical velocity created by this phenomenon is can re-suspend bed material.

# *CHAPTER IV - Evaluation of Management Tools to Forecast Lakes' Thermal Condition*

## 1. Introduction

Inland waters have a key role in climate change studies, especially shallow waters bodies, due to its faster response to climate variability. The climate and its variables are key factors to lakes management, changes in it may have drastic effects on their hydrodynamics (HÖLBIG, MAZZONETTO, *et al.*, 2018) (KIRILLIN; SHATWELL, 2016) (AMORIM et al., 2017).

The previous chapters presented two different tools used to represent lakes' hydrodynamic and the influence of the atmospheric forces on it. The forces presented on the heat budget depend directly on climate, which raises the question of how climate changes affect a lake's ecosystem.

Alterations in atmospheric variables, especially in radiation and wind speed amplitudes, can affect a lake's mixing regime. An increase in the number of mixing events can provoke harmful events, such as algal blooms depending on the environment condition. On the other hand, the drastic reduction in the number of mixing events can compromise the oxygen distribution in the water column, cause the depletion of the nutrients in the water, affecting lakes' biota (KIRILLIN G. , 2010) (KIRILLIN & SHATWELL, 2016)(AMORIM et al., 2017)(MARTINS, 2017) (BRUCE et al., 2018).

In this context, this chapter aimed to test the stability limit curve and the quasi-3D model to forecast the climate change influence on a lakes' mixing regime, using data from climate models.

## 2. Methods and Materials

This chapter presents the comparison of the use of the thermal limit curve, which was proposed by the author in Chapter II, and the well know quasi-3D mathematical model to represent a lake's hydrodynamics and evaluate the influence of climate changes on it.

To perform climate change simulations data from the PROJETA was applied. This project assessed climate change over South America based on the Eta Regional Climate Model simulations, which is forced by two global climate models the HadGEM2-ES and the MIROC5 (HÖLBIG, MAZZONETTO, *et al.*, 2018).

The PROJETA data is divided into two scenarios, the first one is called here, the pessimistic scenario; it considers the predicition of the climate variables as calculated in the RPC 8.5 model. The optmistic scenario uses the RPC 4.5 model. The main difference between these two scenarios is green house gas prodution, which is greater in the pessimistic scenario (HÖLBIG, MAZZONETTO, *et al.*, 2018). In this research, the climate model used was the HadGEM2-ES, most used in similar studies (KIRILLIN, 2010) (MACKAY, NEALE, *et al.*, 2009).

The thermal stability proxies (***log*** $\boldsymbol{S^*/Rad}$ and ***log*** $\boldsymbol{W^*/S^*}$) were calculated using the information, as described in Table 10. The quasi-3D model simulations used the calibrated and validated model, developed in Chapter IV, applying the PROJETA data as input, also as presented in Table 10. The lakes utilized as study areas were the same as the ones in Chapter IV, which are Hedberg lake and Billings reservoir.

**Table 10. Input data used in climate change simulations and their sources**

| DATA | SOURCE |
|---|---|
| Climate variables (evaporation, radiation, precipitation, humidity, air temperature, wind speed and direction) | PROJETA |
| Input flow | Calculated from PROJETA pluviometry data |
| Water temperature | Calculated from PROJETA air temperature data |
| Output flow | Calculated from the spillway rating curve |

Source: Author.

To permorf the mathematical simulations the  hydrodynamic model from chapter III was used. The model configuration include the data from PROJETA (wind speed, air temperature, humidity, air pressure, radiation, water level, and water temperature) associated with the rating curve of the spillway and the morphometry data of the lakes composed the data to represent the lakes' characteristics, boundary conditions, and atmospheric forces (Figure 75. and Figure 76. ).

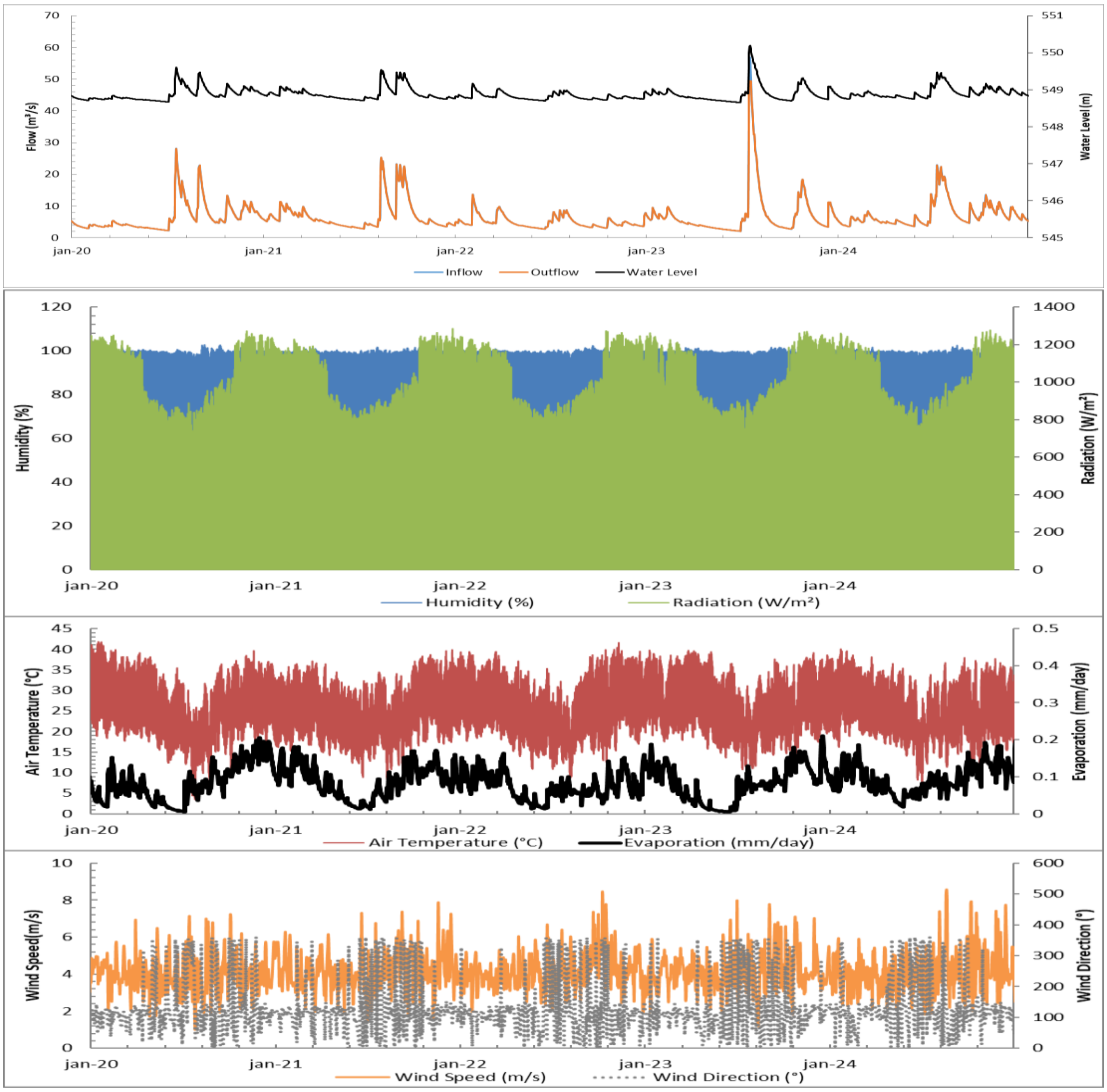


**Figure 75. Data from PROJETA, which was used on the simulation of Hedberg Lake.**

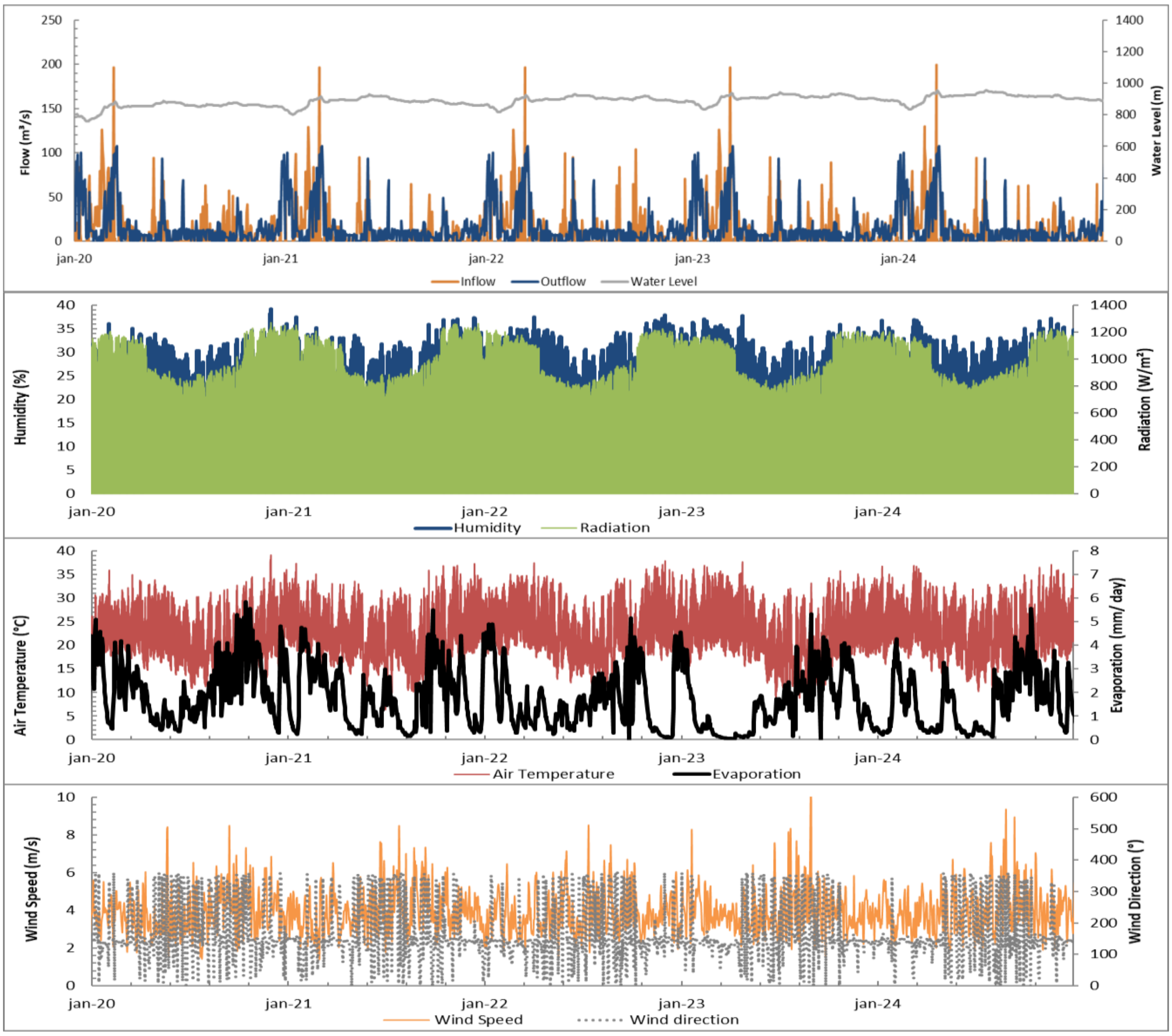


**Figure 76. Data from PROJETA, which was used on the simulation of Billings Reservoir.**

# 3. Results and Discussions

## 3.1 Forecasting a lake's thermal condition using the thermal stability curve

The meteorological data provided by the climate model PROJETA was plotted in the thermal stability limit curve (Figure 77). As expected, the tool continues to produce solid results, with the events of water column overturn being explained by the proposed proxies.

This application confirms the utility of the curve for reservoir management and water quality maintenance. Unlike the indices presented in the literature (i.e., LN, W, Ri, etc.), the thermal stability curve gives reservoirs operators the ability to forecast the instability moments and prevent harmful consequences that compromise the reservoirs' uses.

Along with that, it is possible to relate different types of water bodies on the same basis and with a comparable number. In comparison with the mathematical model, this tool can forecast the thermal condition of the water column faster and with fewer input data than the simulations (only water temperature, radiation and wind speed are required). This situation makes the management process easier and more efficient.

Researches with data from global climate model are to notice trends and not the specific values, due to the models' accuracy is not enough that objective. In this application is possible to note the effects of the climate change scenarios in this first five years ahead.

The main noted effect was the expansion of the stratification events (Figure 78), currently in the range of ***log W*/S****<-1.9 and ***log S*/Rad*** >-3.7, while in those scenarios they occupy a larger interval (***log W*/S****<-1.1 and ***log S*/Rad*** >-4). Those effects are not major but indicate the trend to the next years of heating up the mean temperature of the lakes and promoting the stratification. This result is according with other researches performed in the climate change theme, as: Woolway, Dokulil, *et al.* (2017); Lewis-Jr., Mccutchan-Jr. and Roberson (2019); Woolway and Merchant (2019).

**Figure 77. Proxies of climate change simulation results for pessimistic and optimistic scenarios**

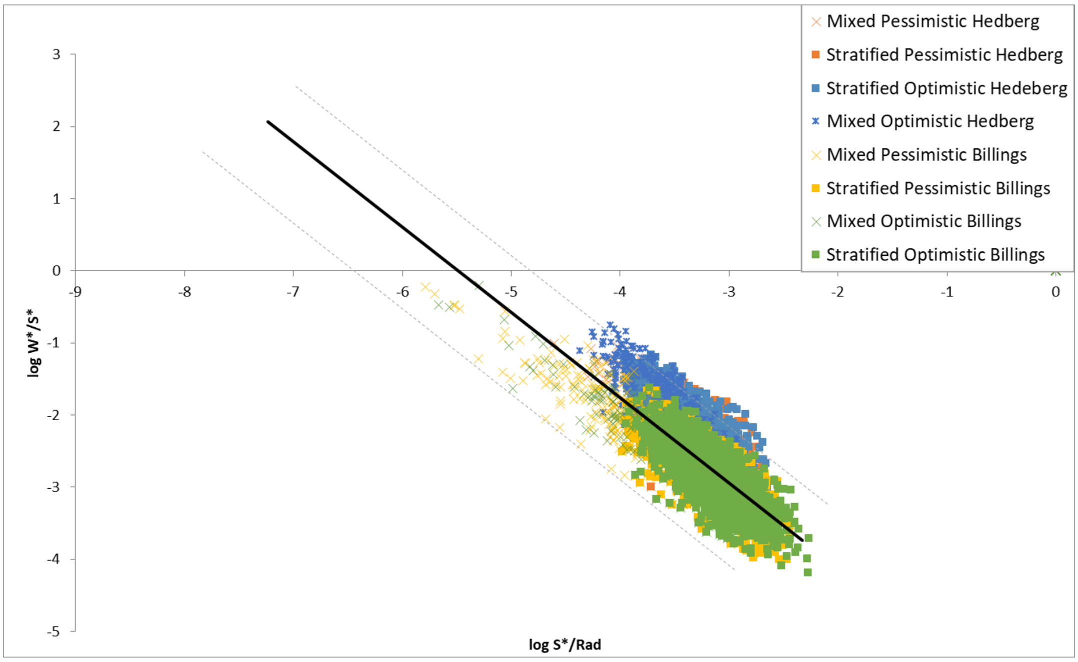


Source: Author; Data from VIÇON-LEITE, et al., (2014); Soulignac, Viçon-Leite, et al (2017).

**Figure 78. Thermal Stability curve comparation between actual scenario and climate change simulations**

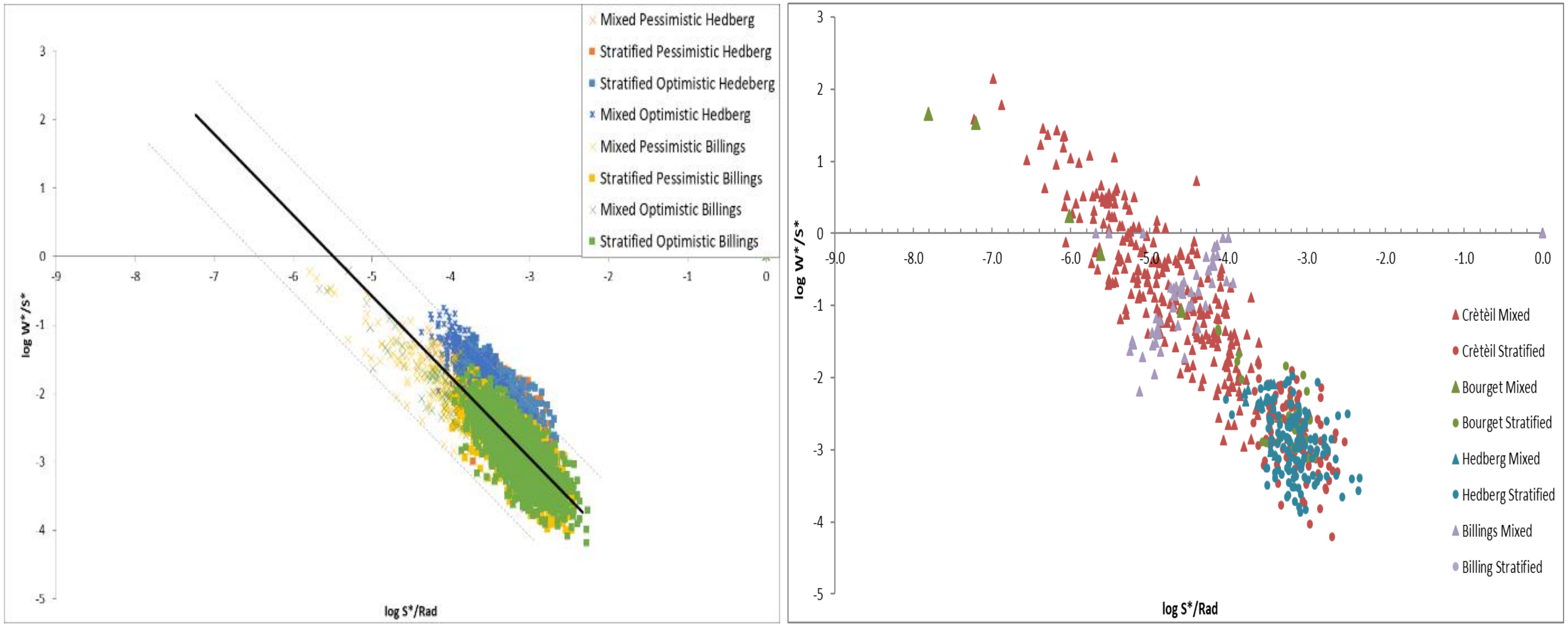


Source: Author; Data from VIÇON-LEITE, et al., (2014); Soulignac, Viçon-Leite, et al (2017)

Assuming the model's capacity to represent a lake's mixing regime, climate change scenarios were simulated with the aim of showing how external variables influence lake hydrodynamic behaviour. The optimistic and pessimistic scenarios (from Figure 79 trough Figure 82) were used to represent hydrodynamic trends for Hedberg lake and Billings reservoir over the next five years (2020 to 2025).

Over time, the lakes' mean temperature increases in both scenarios, making the cold season shorter. The changes in the atmospheric variables reflect directly on the lake mixing regime, altering the number of mixing events. To evaluate that through simulation results, the number of mixing events was counted, in which the lake was considered mixed when the difference between the bottom and the surface is less than 1 °C.

The scenarios results showed fewer mixing events than the current situation, this is an effect of the elevation of the water column temperature. The pessimistic scenario forecast more mixing events than the optimistic scenario (136 more for Hedberg lake and 725 more for the Billings reservoir), when comparing the scenarios between each other. This situation is noted because of the heating of the deeper layer, which favours the lake's turnover.

A mixing regime with more powerful stratification periods enhances dissolved oxygen depletion in the deeper layers. This condition makes the mixing events more harmful for the water quality, once that each time the water column overturns, the deeper layers, with a higher load of organic matter and lower levels of dissolved oxygen, will be brought to the surface, impairing the water quality throughout the whole water column.

**Figure 79. Climate change simulations for the optimistic scenario in Hedberg lake**

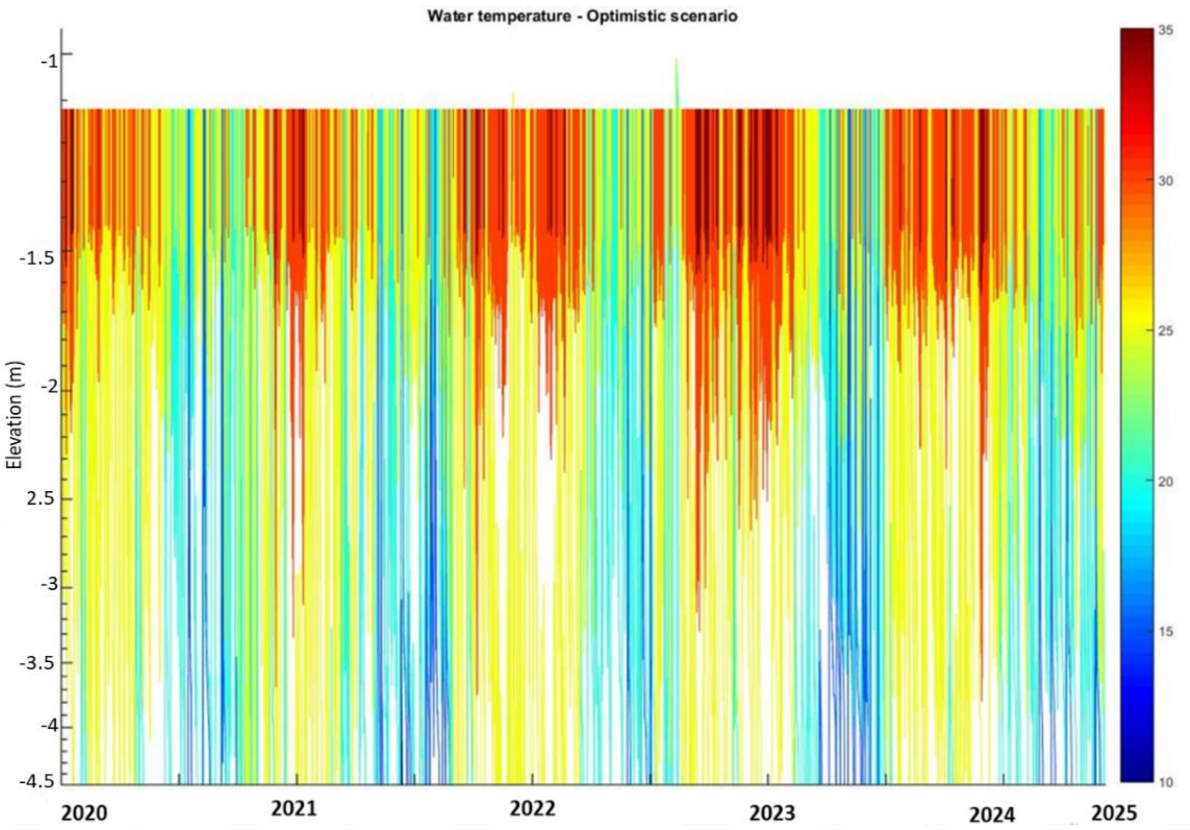


Source: Author.

**Figure 80. Climate change simulations for the pessimistic scenario in Hedberg lake**

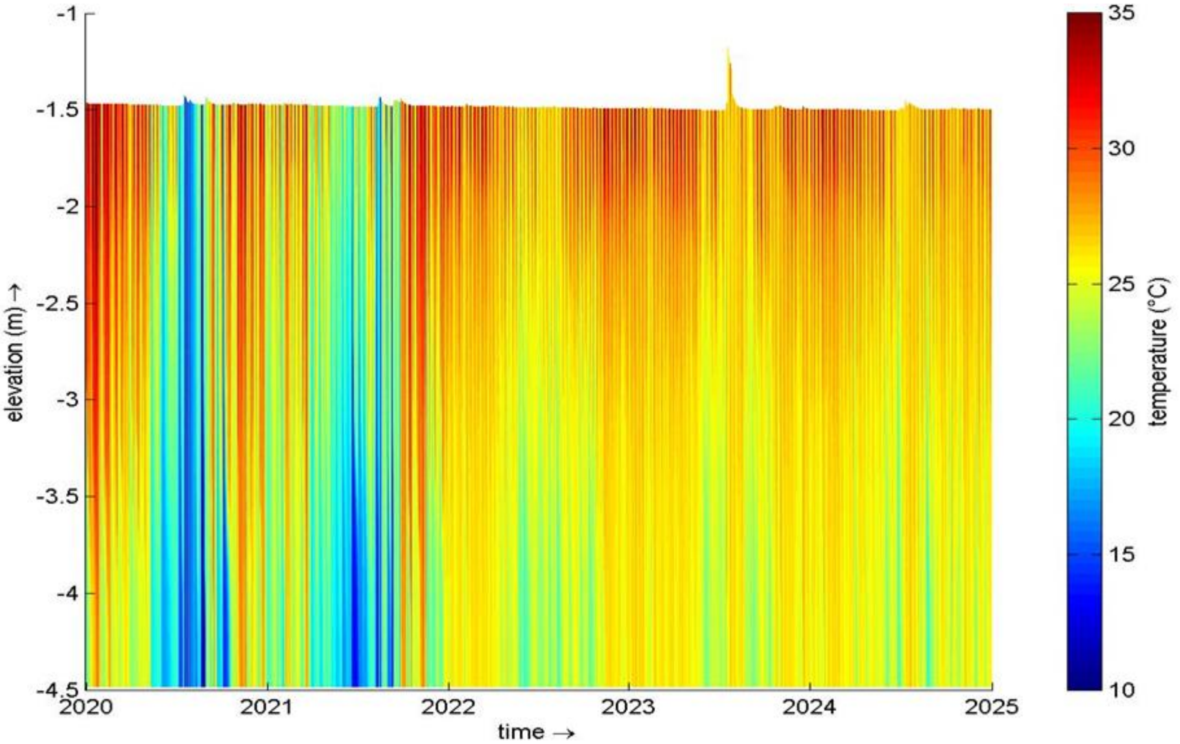


Source: Author.

**Figure 81. Climate changes simulations for the optimistic scenario to Billings reservoir**

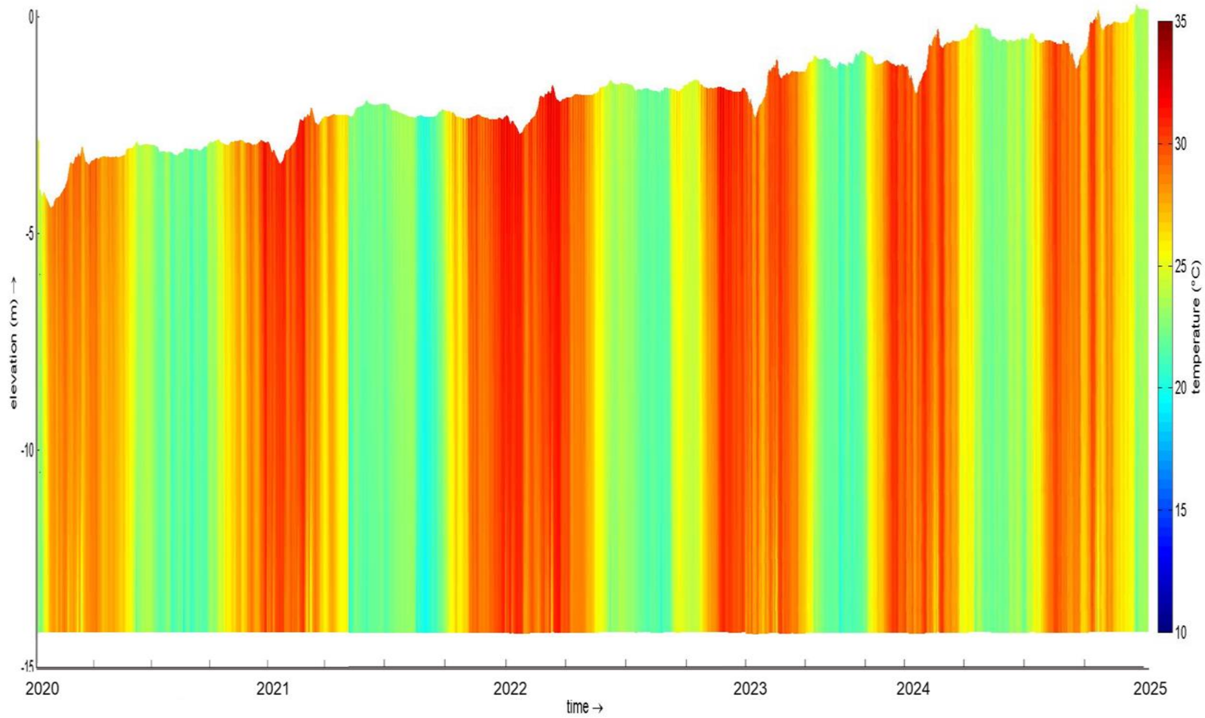


Source: Author.

**Figure 82. Climate changes simulations for the pessimistic scenario to Billings reservoir**

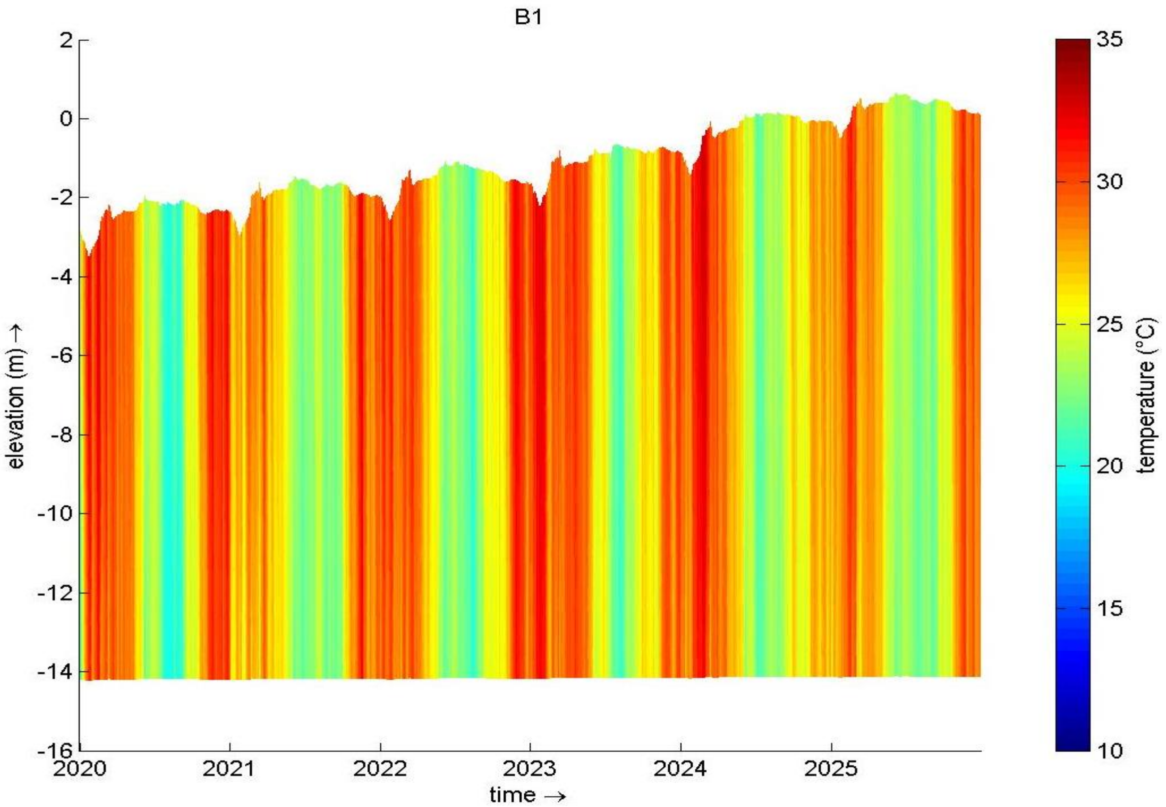


Source: Author.

## 4. Conclusion

In the context of climate changes and water scarcity worldwide, the development of tools to better understand, maintain and improve water quality in lakes and reservoirs becomes an essential ally to environmental research and limnology.

The applications performed in this chapter tested the stability limit curve and the quasi-3D model to forecast the climate change influence on a lakes' mixing regime, using data from climate models. Both methods maintained the good performance showed in the previous chapters, representing lakes hydrodynamics accurately.

The climate change simulations showed the driving forces' strong influence on the lake's mixing regime and a warming of the lakes, reducing the period of the colder season and promoting the stratification. The mixing events number is an interesting proxy to analyse this influence. It was greater in the pessimistic scenarios but still less than in the current situation. This means long periods of stratification, which can cause dissolved oxygen depletion in the deeper layers.

Those effects will influence directly the lakes' water quality, reducing the exchanges between layers, promoting the anoxia problems on the bottom and, consequently, turning the mixing event problematic to the environment.

The pessimistic scenarios have mixing events with greater amplitude, which results from a powerful stratification in previous periods. This situation creates higher vertical velocities, resuspending more organic load and dropping dissolved oxygen levels along the water column.

The application of the equation presented on the chapter II to the global climate model showed it suitability into forecast the lakes' thermal condition trough the proxies ***log W*/S**** and ***log S*/Rad***, with the results fitting the same equation. The thermal stability curve enables to forecast the instability moments and prevent harmful consequences that compromise the reservoirs' uses.

The curve has the advantage of faster response and minor need for data input, on the other hand, the quasi-3D models are capable of more detailed results. Possibly in the lakes' management, it would be more indicated the use of those two methods together, using the curve to analyse faster the period's trend and be able to delimitate the exact period which needs more detailed studies.

# *CHAPTER V - Comments and Referrals for Upcoming Papers*

# 1. Summary Comments and recommendations

Lakes have a unique hydrodynamic, provoked by its lentic characteristics, which is strongly influenced by atmospheric variables. The major effect of this influence is the water column vertical stratification, in which the upper layers stay warmer than the deeper ones, changing its density.

This condition is break when the wind stress is big enough to perturb this stability and turn over the water column, mixing it. A consequence of this movement is the generation of vertical velocities coming from the bottom to the lake’s surface. This dynamic affects all the interactions on the environment, including gases and nutrients distribution, so its water quality.

Lakes have many important uses to the human way of life and development in actual society, such as water guaranty, water supply, hydropower generation, irrigation, flood contain or landscape component, in many cases, they have multiple uses.

It is necessary to understand lakes' hydrodynamics and water quality, due to its intense relationship with society’s development. Limnology field studies are evolving to improve the management of the reservoirs, but still has gaps to fill. These are mostly concentrated in representing the algal role in the ecosystem by coupled models, and the interaction between sediments, hydrodynamics and water quality.

In this context, this research proposed a functional relationship between atmospheric forces and lakes’ thermal conditions, along with a quasi-3D model to represent its hydrodynamics, water quality and capacity to resuspend sediment. Those methods were applied as management tools, representing the climate change effects on lakes’ mixing regime.

First was established a tool to interpret lakes’ thermal behaviour and the limits of regime change, contemplating the driving forces acting on the environments. Beside the morphometry characteristics, the meteorological aspects were considered, such as: incoming radiation and variation of wind speed.

The lakes’ energy balance was studied and the correlation between atmospheric driving forces and the responses on the water mixing regime was demonstred by two proxies ***log W*/S**** and ***log S*/Rad***.

This curve allows the knowledge of the lakes thermal condition only with wind speed, radiation and water temperature data, which are easily and common monitored variables. It can be associated weather forecast and applied to predict inversion moments in the water column, which are very important in reservoir operations and water quality management. This is a new contribution in the field, once that once was impossible to do with previous lake indices (Lake Number, Richardson Number, Wedderburn Number).

Lakes' hydrodynamics continued to be studied with the implementation of the quasi-3D model. This work, based on previous experiences, was able to demonstrate this tool capacity to represent accurately the change in the lakes' thermal regime. A gain of this type of tool was to be able to reproduce the reservoir spatial variability and vertical profiles.

Those two tools were applied into a forecast of the effects of the climate change on the lakes' mixing regime. Data from the climate global model were used as input data to simulate the next five years of hydrodynamics.

Both methods maintained accurate performance in representing lakes hydrodynamics, although, their advantages and limitations became highlighted. The curve has the advantage of faster response and minor need for data input. On the other hand, the quasi-3D models give more detailed results, such as vertical profiles, but for that consume much processing time.

The methods showed the relation between the alteration on the climate, represented by the driving forces, and the lakes' thermal behaviour. A major consequence was its warming, which reduces colder season duration and promotes the stratification.

Those effects influence the water quality by the impairing of the exchanges between layers. As a result, the DO levels drop on the deeper waters, turning the mixing event problematic to the environment.

The crossing of the quasi-3D model simulations and the turbidity field measurements showed the extension of the climate change alterations. With the model calibrated and a turbidity sensor on the field was showed that exists a relationship of the hydrodynamic movements and the bed material re-suspension on the lakes.

It was proved that the upward movement, created by the mixing events, generates vertical velocities peaks big enough to move bed materials, so giving it the capacity to re-solubilize constituents that were trapped on the bottom.

Those relations make the tool even more important because it shows that lakes' hydrodynamics affects the water quality also in other aspects, beyond the ones already known, such as the water turbidity. The linking between climate change impacts and the state of the water quality is showed with the content of this research, such as the importance of capacity to forecast and know the lake's thermal condition.

These two methods should be applied together to better lakes' management. The curve can be used to faster analysis of the data trend, allowing the delimitation of the exact period which needs detailed studies, which can be performed by the models.

The contributions produced by this thesis allow the filling some of the knowledge gaps discussed in the introduction. The future researches can focus on the equipment' development, providing more quantity and quality of data, and improving the coupling of ecological and hydrodynamic models. A specific matter of interesting should be the implementation of mathematical modelling to simulate the effects of sediment resuspension on water quality.

## 2. Scientific Contributions

During the doctorate period, scientific papers were produced and published, they are listed below:

a. Title: Assessments of lake indicators through a comparison between tropical and temperate shallow lakes;

Event: 20th Workshop on Physical Processes in Natural Waters, Hyytiälä, Finland, 21-25 August 2017

b. Title: Hydrodynamic and Ecological 3D Modelling in Tropical Lakes;

Event: 61st Annual Conference on Great Lakes Research to be held June 18-22, 2018, at the University of Toronto - Scarborough

c. Title: Modelling vertical velocity in lakes

Event: IAHR 09/2019.

d. Title: Forecasting water column thermal condition based on atmospheric driving forces and applying to climate changes scenarios.

Event: SBRH 11/2019.

e. Title: 3D Modelling and forecasting the effects on lake's water column thermal condition for different scenarios of climate change

Journal: Revista Brasileira de Recursos Hídricos - RBRH

Status: Waiting for the review analysis.

f. Title: Development of a method to forecast water column thermal condition based on atmospheric driving forces.

Journal: Journal of Applied Water Engineering and Research -JAWER

Status: Waiting for analysis.

g. Title: Hydrodynamic and ecological 3D modelling in tropical lakes

Journal: Environmental Modelling and Assessments

Status: Waiting for analysis.

# 3. Bibliography

AMBROSETTI, W.; BARBANTI, L. Temperature, heat content, mixing and stability in Lake Orta: a pluriannual investigation. **Journal of Limnology**, v. 60, n. 1, p. 60-68, 2001.

AMORIM, L. F. et al. **Assessments of lake indices through a comparison between tropical and subtropical shallow lakes.** PPNW 2017. Finland, 21-25 August.: [s.n.]. August 2017.

ANA. **Conjuntura de Recursos Hídricos do Brasil- informe anual**. Brasília. 2018.

BAILEY, M. C.; HAMILTON, D. P. Wind induced sediment resuspension: a lake-wide model. **Ecological Modelling**, v. 99, p. 217-228, 1997. ISSN 0304-3800:Y7.

BONNET, M.-P.; POULIN, M.; DEVAUX, J. Numerical modeling of thermal stratification in a lake reservoir. Methodology and case study. **Aquatic Sciences**, Basel, v. 62, p. 105-124, 2000.

BROOKS, B. W. et al. Are Harmful Algal Blooms Becoming the Greatest Inland Water Quality Threat to Public Health and Aquatic Ecosystems? **Environmental Toxicology and Chemistry**, v. 35, n. 1, p. 6-13, January 2016.

BRUCE, L. C. et al. A multi-lake comparative analysis of the General Lake Model (GLM): Stress-testing across a global observatory network. **Environmental Modelling & Software**, v. 102, p. 274 – 291., 2018. ISSN doi.org/10.1016/j.envsoft.2017.11.016.

CASTRO, M. M. D. **MODELAÇÃO MATEMÁTICA DE LAGOS E RESERVATÓRIOS:** Caso do Reservatório Billings. São Paulo: Master Thesis - USP, 2010.

CASTRO, M. M.; MARTINS, J. R. S.; MARTINS, R. H. O. **Modelação matemática do reservatório Billings:** Calibração de um modelo bidimensional horizontal. XVIII Simpósio Brasileiro de Recursos Hídricos. Campo Grande: ABRH. 2009.

CASULLI, V.; CHENG, R. T. Semi-implicit finite difference methods for three-dimensional shallow water flow. **International Journal for Numerical Methods in Fluids**, v. 15, n. 6, p. 629-648, sep 1992.

CASULLI, V.; STELLING, G. S. NUMERICAL SIMULATION OF 3D QUASI-HYDROSTATIC, FREE-SURFACE FLOWS. **JOURNAL OF HYDRAULIC ENGINEERING**, v. 124, n. 7, p. 678-686, jul 1998.

CBH-AT. **Relatório de caracterização geral.**. São Paulo. 2014.

CETESB. **Relatório de Qualidade das Águas Interiores no estado de São Paulo**. Companhia Ambiental do Estado de São Paulo. São Paulo, p. 303. 2017. ( ISSN 0103-4103).

CHAI, T.; DRAXLER, R. R. Root mean square error (RMSE) or mean absolute error (MAE)? – Arguments against avoiding RMSE in the literature. **Geoscientific Model Development**, jul. 2014. 1247–1250.

CHAPRA, S. C. **Surface Water-Quality Modeling**. [S.l.]: Waveland Press, 2008.

CHIN, D. A. **WATER-QUALITY ENGINEERING in Natural Systems**. Miami: John Wiley & Sons, Inc, 2006. ISBN ISBN-13: 978-0-471-71830-7.

CHUNG, E. G.; BOMBARDELLI, F. A.; SCHLADOW, S. G. Sediment resuspension in a shallow lake. **Water Resources Research**, p. W05422: 1-18, 2009.

CONAMA. **Resolução 357**. Brasília. 2005.

CÓZAR, A. et al. Sediment resuspension by wind in a shallow lake of Esteros del Iber´a (Argentina): a model based on turbidimetry. **Ecological Modelling**, v. 186, p. 63-76, 2005. ISSN 0304-3800.

CUYPERS, Y. et al. Impact of internal waves on the spatial distribution of Planktothrix rubescens (cyanobacteria) in an alpine lake. **The ISME Journal**, maio 2011. 580-589.

CUYPERS, Y. et al. Impact of internal waves on the spatial distribution of Planktothrix rubescens (cyanobacteria) in an alpine lake. **The ISME Journal**, maio 2011. 580-589.

DELTARES. **3D/2D modelling suite for integral water solutions - Delft3D - FLOW - User Manual.** Delf. 2014.

EE MODELING SYSTEM. Stratified Lakes. **EE Modeling System**, may 2017. Disponivel em: <https://www.eemodelingsystem.com/solution-type/applications/stratified-lakes>.

ELC¸I, S. Effects of thermal stratification and mixing on a reservoir water quality. **Limnology**, set. 2008. 135–142.

ESTADÃO. Guarapiranga e Billings liberam 60 bilhões de litros de água. **ABCdoABC**, 19 jan. 2016. Disponivel em: <https://www.abcdoabc.com.br/brasil-mundo/noticia/guarapiranga-billings-liberam-60-bilhoes-litros-agua-35522>. Acesso em: 10 maio 2019.

FCTH. **FCTH. Relatório 1 - Avaliação da qualidade das águas do sistema Pinheiros-Billings.**. São Paulo. 2008.

FEE, E. E. A. Effects of lake size, water clarity, and climatic variability on mixing depths in Canadian Shield lake. **Limnol. Oceanogr.**, 41(5) 1996. 912-920.

FRANZEN, M.; CYBIS, L. F.; MERTEN, G. H. Circulação da Água Hipolimnética no Reservatório Divisa do Sistema Salto (RS). **RBRH – Revista Brasileira de Recursos Hídricos**, Out/Dez 2011. 16(4): 41-48.

FUSP. **PLANO DA BACIA DO ALTO TIETÊ – RELATÓRIO FINAL**. São Paulo. 2009.

HENDERSON-SELLERS, B. Calculating the Surface Energy Balance for lake and reservoir modeling: a review. **Reviwes of geophysics**, 1986. 625-649.

HODGES, B. R. et al. **Modeling the Hydrodynamics of Stratified Lakes**. Hydroinformatics 2000 conference. Iowa: Iowa Institute of Hydraulic Research. 2000. p. 1-14.

HÖLBIG, C. A. et al. PROJETA platform: accessing high resolution climate change projections over Central and South America using the Eta model. **Agrometeoros**, Paço Fundo, v. 26, n. 1, p. 71-81, jun 2018.

IBAMA. **Ipanema National Forest Management Plan**. MMA/ICMBio. Brasília, p. 99. 2012.

ICMBIO. **Operative Plan for the Prevention and Combating of Forest Fires: Ipanema National Forest.**. MMA/ICMBio/IBAMA/PREVFOGO. Iperó, p. 36. 2008.

IDSO, S. B. On the concept of lake stability, v. 18, p. 681-683, mar 1973.

IMBERGER, J. **Physical Process in lakes and Oceans**. Washington: (Vol. I) American Geophysical Union., 1998.

JALIL, A. et al. Wind-induced flow velocity effects on nutrient concentrations at Eastern Bay of Lake Taihu, China. **Environ Sci Pollut Res**, v. 14, p. 17900–17911, June 2017.

JESUS, J. A. O. **Use of a 3D Mathematical Model in Water Quality Management – Billings Reservoir´s case.** University of Sao Paulo. [S.l.], p. 142. 2006.

JI, Z.-G. **Hydrodynamics and Water Quality:** Modeling Rivers, Lakes, and Estuaries. [S.l.]: John Wiley & Sons, Inc., 2008.

JIN, K.-R.; SUN, D. Sediment Resuspension and Hydrodynamics in Lake Okeechobee during the Late Summer. **JOURNAL OF ENGINEERING MECHANICS**, v. 133, n. 8, p. 899-910, August 2007.

KIRILLIN, G. Modeling the impact of global warming on water temperature and seasonal mixing regimes in small temperate lakes. **Boreal Environment Research**, 15 2010. 279–293.

KIRILLIN, G.; SHATWELL, T. Generalized scaling of seasonal thermal stratification in lakes. **Earth-Science Reviews**, 16 2016. 179-190.

KULLEMBERG, G. E. On vertical mixing and the energy transfer from the wind to the water.. **Tellus**, 1976. 159-165.

LEENDERTSE, J. J. Aspects Of A Computational Model For Long-Period Water-Wave Propagation. **Rand Corp Santa Monica Calif.**, 1967. ISSN Rm-5294-Pr.

LEWIS-JR., W. M.; MCCUTCHAN-JR., J. H.; ROBERSON, J. Effects of Climatic Change on Temperature and Thermal Structure of a Mountain Reservoir. **Water Resources Research**, n. 55, 12 mar 2019. 1988-1999.

LIU, H. et al. An integrated system dynamics model developed for managing lake water quality at the watershed scale. **Journal of Environmental Management**, v. 155, p. 11-23, 2015. ISSN 0301-4797.

LOU, J. et al. A model of sediment resuspension and transport dynamics in southern Lake Michigan. **JOURNAL OF GEOPHYSICAL RESEARCH**, v. 105, n. C3, p. 6591-6610, March 2000. ISSN 0148-0227/00/1999J C900325.

LUETTICH-JR, R. A.; HARLEMAN, D. R. F.; SOMLYÓDY, L. WIND-INDUCED SEDIMENT RESUSPENSION AND ITS IMPACT ON ALGAL GROWTH FOR LAKE BALATON. **Liminology and Oceanography**, v. 35, n. 5, p. 1050-1067, 1990.

LUETTICH-JR., R. A. et al. **WIND-INDUCED SEDIMENT RESUSPENSION AND ITS IMPACT ON ALGAL GROWTH FOR LAKE BALATON**. Laxenburg, Austria: INTERNATIONAL INSTITUTE FOR APPLIED SYSTEMS ANALYSIS, 1993.

MACINTYRE, S.; MELACK, J. M. Mixing Dynamics in Lakes Across Climatic Zones. **Elsevier**, p. 603-612, 2009.

MACKAY, M. D. et al. Modeling lakes and reservoirs in the climate system. **Limnology and Oceanography**, 56(6, part 2) 2009. 2315–2329.

MARTINS, J. R. S. **HIDRODINÂMICA APLICADA À MODELAGEM DE QUALIDADE DAS ÁGUAS SUPERFICIAIS:** Revisão de processos e métodos. Tese de livre docência. ed. São Paulo: USP, 2017.

MARTINS, J. R. S. et al. UNDERSTANDING HYDRODYNAMICS OF A URBAN RESERVOIR IN SAO PAULO - BRAZIL WITH DELFT 3D MODEL , 2014. 1-4.

MATISOFF, G. et al. Sediment and nutrient distribution and resuspension in Lake Winnipeg. **Science of the Total Environment**, v. 575, p. 173-186, 2017. ISSN 0048-9697.

MCCUEN, R. H.; KNIGHT, Z.; CUTTER, A. G. Evaluation of the Nash–Sutcliffe Efficiency Index. **Journal of hydrologic engineering** , 11(6) 2006. 597-602.

PEETERS, F. et al. Turbulent mixing and phytoplankton spring bloom development in a deep lake. **Limnology and Oceanography**, v. 52, n. 1, p. 286–298, 2007.

PIVELI, R. P.; KATO, M. T. **Qualidade das Águas e Poluição:** Aspectos Físicos- Químicos. São Paulo: ABES, 2006.

READ, E. K. et al. The importance of lake-specific characteristics for water qualityacross the continental United States. **Ecological Applications**, v. 25, n. 4, p. 943-955, June 2015.

READ, J. S. et al. Derivation of lake mixing and stratification indices from high-resolution lake buoy data. **Environmental Modelling & Software**, 26 2011. 1325-1336.

READ, J. S. et al. Derivation of lake mixing and stratification indices from high-resolution lake buoy data. **Environmental Modelling & Software**, 26, 2011. 1325-1336.

READ, J. S. et al. Simulating 2368 temperate lakes reveals weak coherence in stratification phenology. **Ecological Modelling**, 291 2014. 142–150.

ROBERTSON, D. M.; IMBERGER, J. Lake Number, a Quantitative Indicator of Mixing Used to Estimate Changes in Dissolved Oxygen. **Internationale Revue der gesamten Hydrobiologie und Hydrographie**, 1994. 159-176.

SADEGHIAN, A. et al. Improving in-lake water quality modeling using variable chlorophyll-a/algal biomass ratios. **Environmental Modelling & Software**, v. 101, p. 73-85, 2018. ISSN 1364-8152.

SHERRY, J. E.; JUSTUS, C. G. A SIMPLE HOURLY CLEAR-SKY SOLAR RADIATION MODEL BASED ON METEOROLOGICAL PARAMETERS. **Solar Energy**, 30, n. 5, 1983. 425-431.

SMITH, W. S.; BIAGIONI, R. C.; HALCSIK, L. Fish Fauna Of Floresta Nacional De Ipanema, São Paulo State, Brazil.. **Biota Neotropica**, 13, 2013. 175-181.

SOMLYÓDY, L.; KONCSOS, L. Influence of sediment resuspension on the light conditions and algal growth in Lake Balaton. **Ecological Modelling**, Amsterdam, v. 57, p. 173-192, 1991.

SOULIGNAC, F. et al. Performance assessment of a 3d hydrodynamic model using high temporal resolution measurements in a shallow urban lake. **Environmental modeling and assessment**, p. 22:4, 2017.

SOULIGNAC, F. et al. Performance assessment of a 3d hydrodynamic model using high temporal resolution measurements in a shallow urban lake. **Environmental modeling and assessment**, p. 22:4, 2017.

SPERLING, M. V. **Estudos de modelagem da qualidade da água de rios**. Belo Horizonte: UFMG, 2007.

SPIGEL, R.; IMBERGER, J. The classification of the mixed-layer dynamics in lakes of small to medium size. **Journal of Physical Oceanography**, out. 1980. 1104-1121.

STELLING, G. S. On The Construction Of Computational Methods For Shallow Water Flow Problems. **Doctoral Thesis**, Tudelft, 1983.

TELEDYNE RD INSTRUMENTS. **Acoustic Doppler Current Profiler Principles of Operation**. California. 2011.

TENNEKES, H. Similarity Relations, Scaling Laws And Spectral Dynamics.. **Royal Netherlands Meteorological Institute, De Bilt**, The Netherlands., 1984.

VINÇON-LEITE, B. et al. Long-term temperature evolution in a deep sub-alpine lake, Lake Bourget, France: how a one-dimensional model improves its trend assessment. **Hydrobiologia**, v. 731, p. 49-64, 2014. ISSN ISSN 0018-8158.

WANG, D. et al. A cloud model-based approach for water quality assessment. **Environmental Research**, v. 148, p. 24-35, 2016. ISSN 0301-4797.

WENGRAT, S.; BICUDO, D. D. Spatial evaluation of water quality in an urban reservoir: Billings Complex, southeastern Brazil. **Acta Limnologica Brasiliensia**, 2011. 200-216.

WOOLWAY, R. I. et al. Warming of Central European lakes and their response to the 1980s climate regime shift. **Climatic Change**, n. 142, 2017. 505-520.

WOOLWAY, R. I.; MERCHANT, C. J. Worldwide alteration of lake mixing regimes in response to climate change. **Nature Geoscience**, n. 12, 2019. 271-176.

WU, T.-F. et al. Modeling of turbidity dynamics caused by wind-induced waves and current in the Taihu Lake. **International Journal of Sediment Research**, v. 28, n. 2, p. 139-148, 2013.

WÜEST, A.; LORKE, A. Small-Scale hydrodynamics in lakes. **Annual review os fluid mechanics**, n. 35, p. 373-412, 2003.

# 1. Appendix A

The next figures show the historic results on the CETESB monitoring points.

- BILL 2030

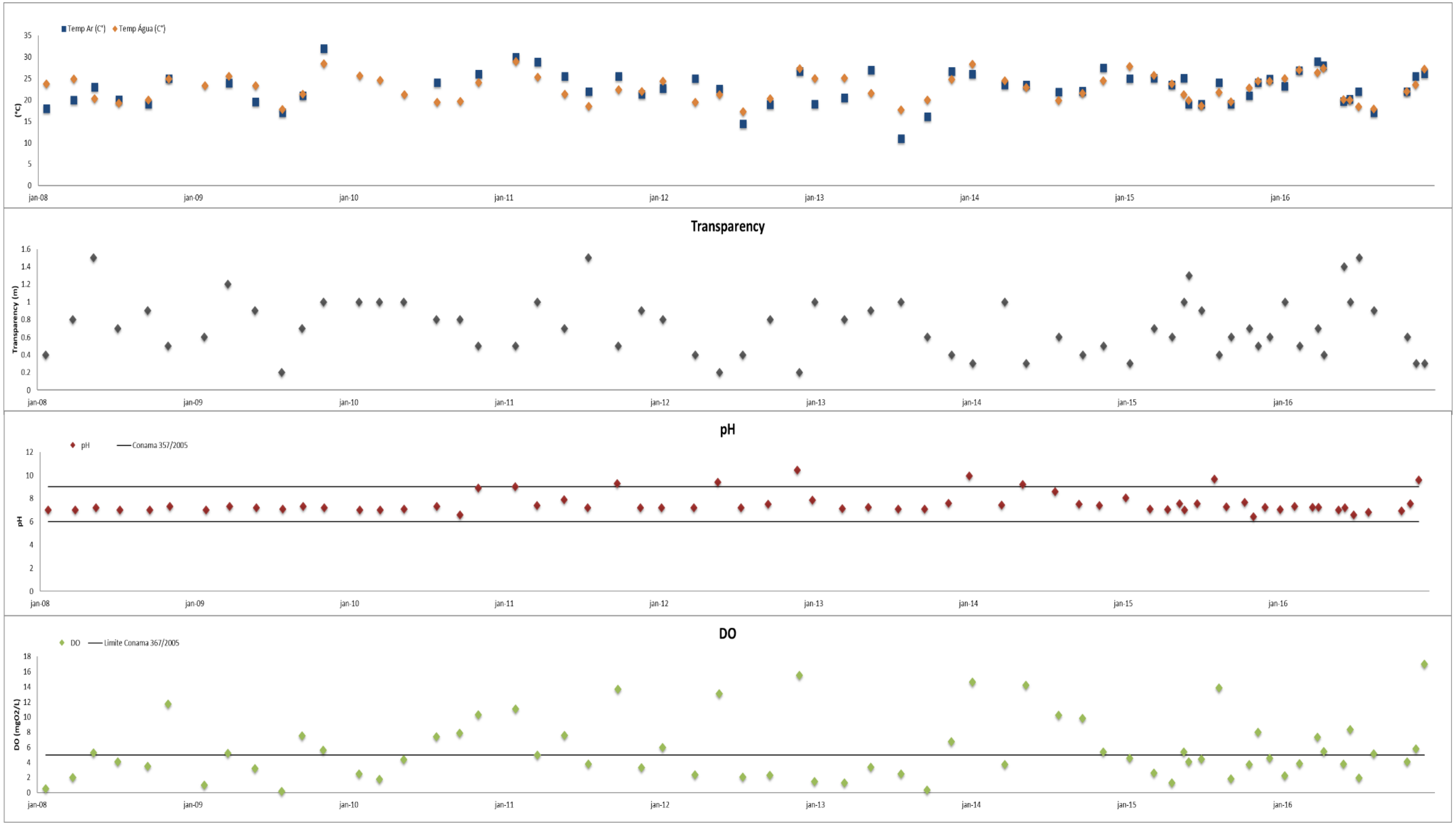

Temp Ar (C°)
Temp Água (C°)
(°C)
Transparency
Transparency (m)
pH
pH
Conama 357/2005
DO
DO
Limite Conama 367/2005
DO (mgO2/L)
jan-08
jan-09
jan-10
jan-11
jan-12
jan-13
jan-14
jan-15
jan-16

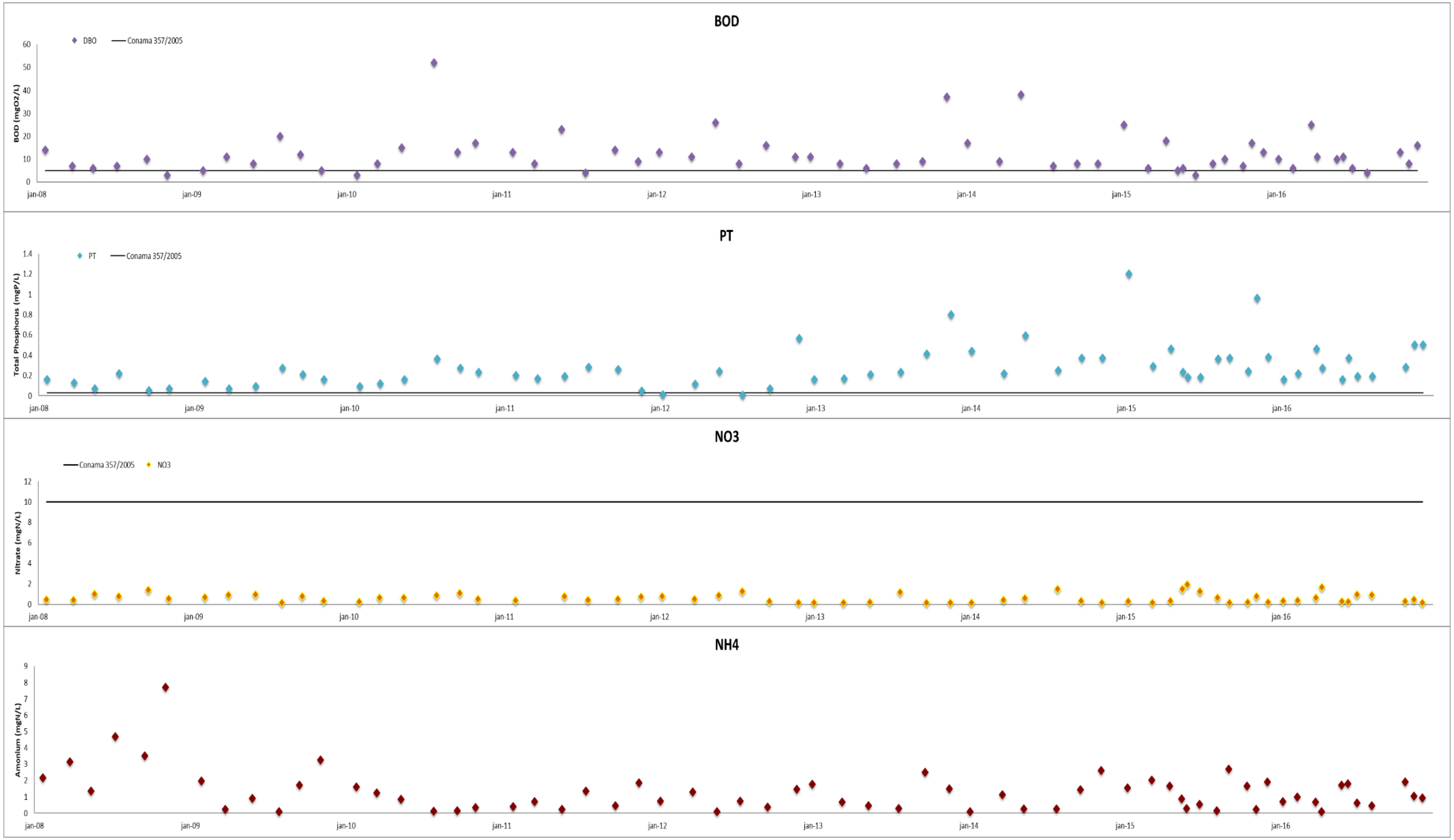

BOD
DBO
Conama 357/2005
BOD (mgO2/L)
60
50
40
30
20
10
0
jan-08
jan-09
jan-10
jan-11
jan-12
jan-13
jan-14
jan-15
jan-16
PT
PT
Conama 357/2005
Total Phosphorus (mgP/L)
1.4
1.2
1
0.8
0.6
0.4
0.2
0
NO3
Conama 357/2005
NO3
Nitrate (mgN/L)
12
10
8
6
4
2
0
NH4
Amonium (mgN/L)
9
8
7
6
5
4
3
2
1
0

- BILL2100

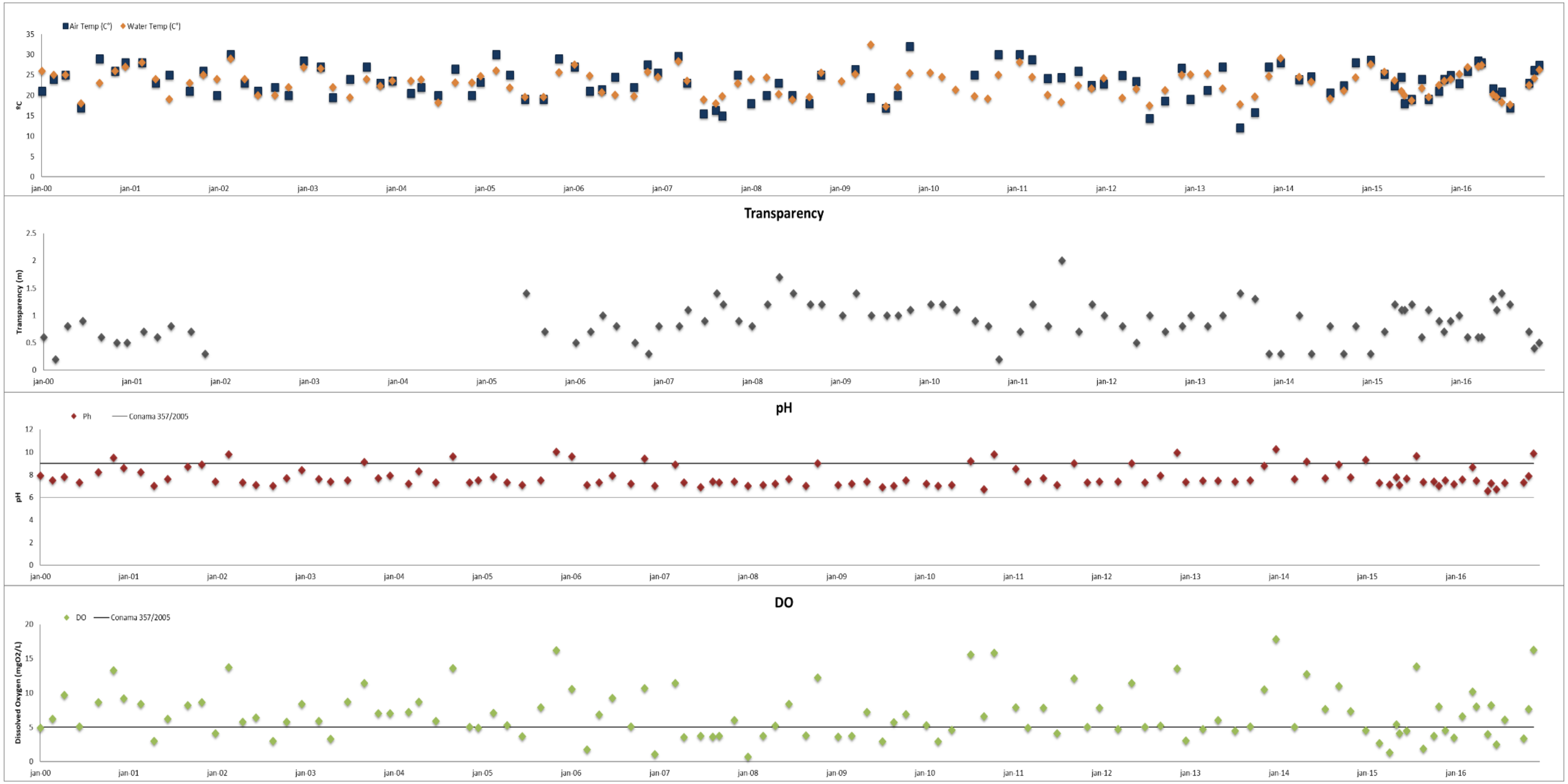

Air Temp (C°)
Water Temp (C°)
°C
Transparency
Transparency (m)
pH
Ph
Conama 357/2005
DO
DO
Conama 357/2005
Dissolved Oxygen (mgO2/L)
jan-00
jan-01
jan-02
jan-03
jan-04
jan-05
jan-06
jan-07
jan-08
jan-09
jan-10
jan-11
jan-12
jan-13
jan-14
jan-15
jan-16

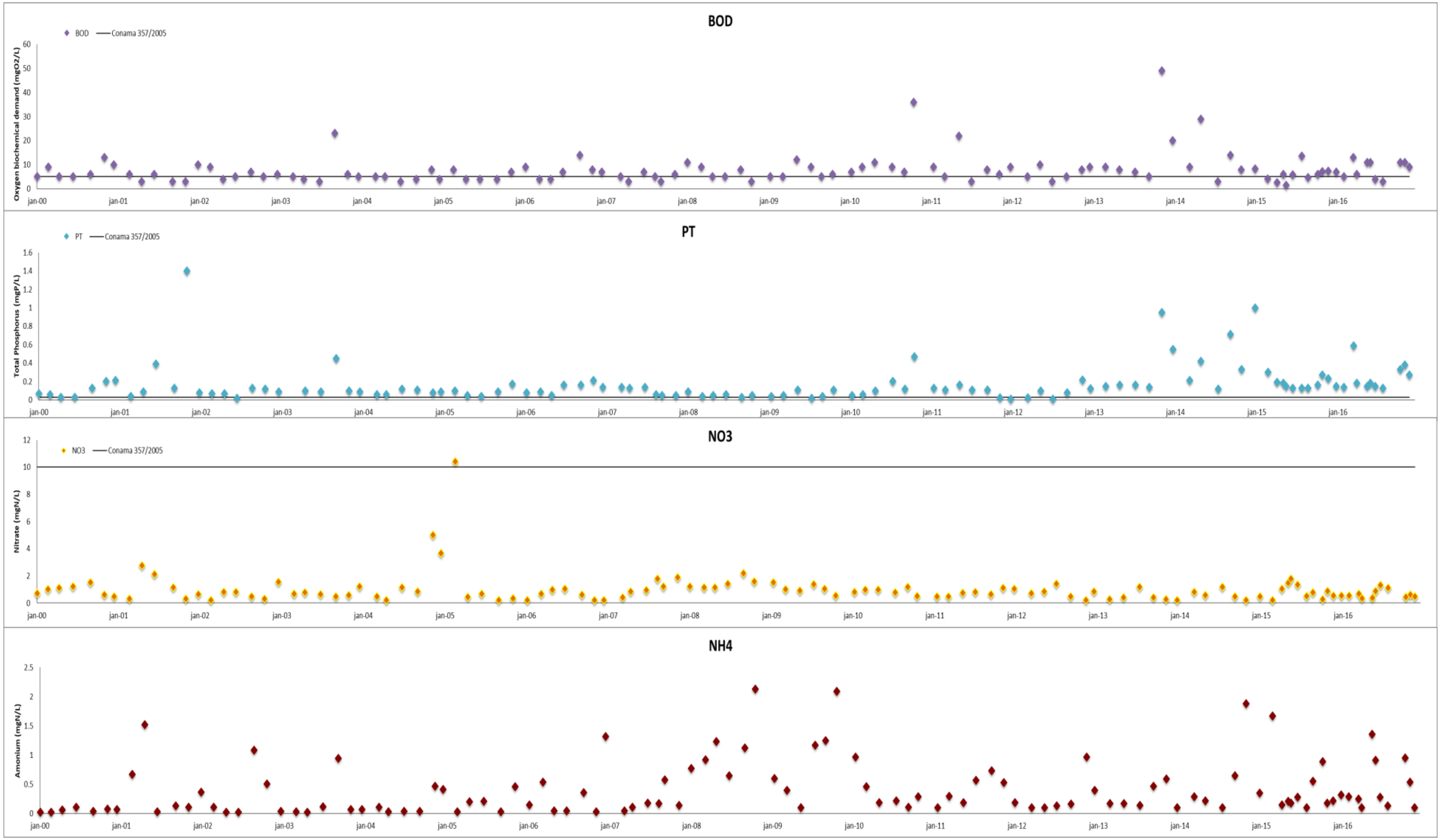
BOD
BOD
Conama 357/2005
Oxygen biochemical demand (mgO2/L)
PT
PT
Conama 357/2005
Total Phosphorus (mgP/L)
NO3
NO3
Conama 357/2005
Nitrate (mgN/L)
NH4
Amonium (mgN/L)
jan-00
jan-01
jan-02
jan-03
jan-04
jan-05
jan-06
jan-07
jan-08
jan-09
jan-10
jan-11
jan-12
jan-13
jan-14
jan-15
jan-16

- BILL2500

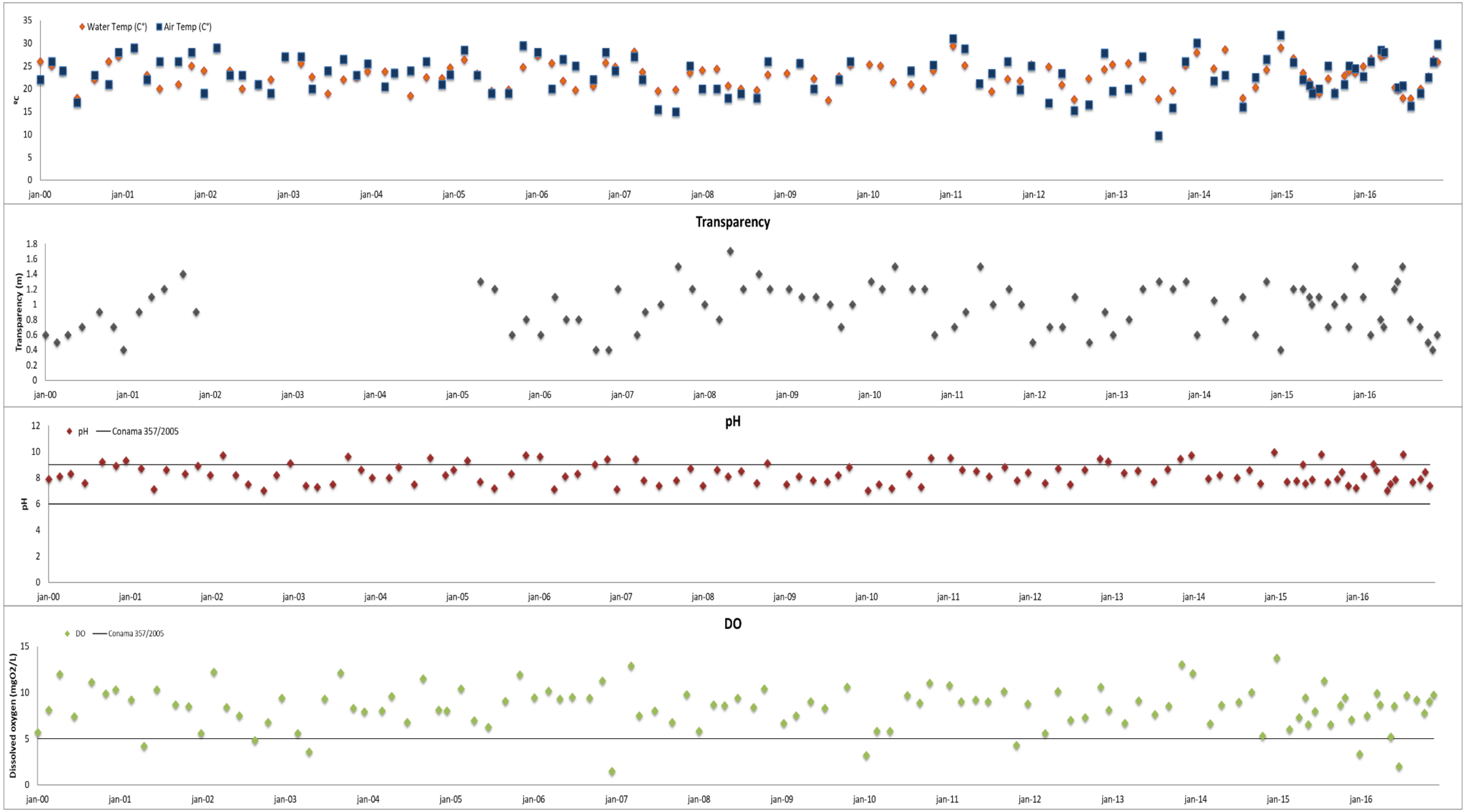
Water Temp (C°)
Air Temp (C°)
°C
Transparency
Transparency (m)
pH
pH
Conama 357/2005
DO
DO
Conama 357/2005
Dissolved oxygen (mgO2/L)
jan-00
jan-01
jan-02
jan-03
jan-04
jan-05
jan-06
jan-07
jan-08
jan-09
jan-10
jan-11
jan-12
jan-13
jan-14
jan-15
jan-16


BOD
BOD
Conama 357/2005
Biochemical oxygen demand (mgO2/L)
PT
PT
Conama 357/2005
Total Phosphorus (mgP/L)
NO3
Conama 357/2005
Nitrate
Nitrate (mgN/L)
NH4
Amonium (mgN/L)
jan-00 jan-01 jan-02 jan-03 jan-04 jan-05 jan-06 jan-07 jan-08 jan-09 jan-10 jan-11 jan-12 jan-13 jan-14 jan-15 jan-16